BEHAVIOR AND FUNCTIONAL MORPHOLOGY OF RESPIRATION IN THE BASKET STAR, *GORGONOCEPHALUS EUCNEMIS* AND TWO BRITTLE STARS IN THE GENUS *OPHIOTHRIX*.

by

MACKENNA A. H. HAINEY

A THESIS

Presented to the Department of Biology
and the Graduate School of the University of Oregon
in partial fulfillment of the requirements
for the degree of
Master of Science

September 2018

THESIS APPROVAL PAGE

Student: MacKenna A. H. Hainey

Title: Behavior and Functional Morphology of Respiration in the Basket Star, *Gorgonocephalus eucnemis* and Two Brittle Stars in the Genus *Ophiothrix*

This thesis has been accepted and approved in partial fulfillment of the requirements for the Master of Science degree in the Department of Biology by:

Richard B. Emlet	Advisor
Alan L. Shanks	Member
Maya Watts	Member

and

Janet Woodruff-Borden Vice Provost and Dean of the Graduate School
Original approval signatures are on file with the University of Oregon Graduate School.

Degree awarded September 2018

THESIS ABSTRACT

MacKenna A. H. Hainey

Master of Science

Department of Biology

September 2018

Title: Behavior and Functional Morphology of Respiration in the Basket Star, Gorgonocephalus eucnemis and Two Brittle Stars in the Genus Ophiothrix

Gorgonocephalus eucnemis, Ophiothrix suensonii and *Ophiothrix spiculata* are aerobic Echinoderms. Previous observations on the anatomy of these two genera state five pairs of radial shields and genital plates are responsible for regulating the position of the roof of the body disc and the flushing of water in and out of the bursae. Rates of bursal ventilation increase by an average 60-64% when the ophiuroid is exposed to an increase in food or a decrease in dissolved oxygen in *Gorgonocephalus*. When exposed to hypoxic oxygen concentrations *O. suensonii* and *O. spiculata* increased bursal-ventilation rates by (means of) 35% and 28%. Measurements of DO from inside and outside the bursae show that DO is being absorbed during bursal-ventilations. These findings suggest bursal ventilation is a means of respiration and increased rates of bursal-ventilation may help meet increased oxygen demands during feeding and some periods of hypoxia.

This dissertation includes unpublished, co-authored material.

CURRICULUM VITAE

NAME OF AUTHOR: MacKenna A. H. Hainey

GRADUATE AND UNDERGRADUATE SCHOOLS ATTENDED:

University of Oregon, Eugene
Umpqua Community College, Roseburg

DEGREES AWARDED:

Master of Science, Biology, 2018

Bachelor of Science with Departmental Honors, Marine Biology, 2016
University of Oregon

AREAS OF SPECIAL INTEREST:

Invertebrate Zoology
Organismal Biology
Functional Morphology
Paleobiology
Marine Biology

PROFESSIONAL EXPERIENCE:

Marine Science Exploration Leader, AmeriCorps – Charleston Marine Life Center, 2018

Application developer, Oregon Sea Grant, 2018

Coastal Master Naturalist Program Assistant, Oregon Sea Grant, 2018 Graduate

Teaching Fellow, University of Oregon, 2016-2018

R.E.U. Graduate Assistant, University of Oregon, 2017

Graduate Research Assistant, University of Oregon, 2017]

National Science Foundation International Research Experience for Students, Lough Hyne, Ireland, 2017

Research Intern, South Slough National Estuarine Research Reserve, 2015-2016

Undergraduate Research Assistant, University of Oregon, 2015 -2016

Dean's List, University of Oregon, 2015-2016

Golden Key International Honor Society, University of Oregon, 2015

GRANTS, AWARDS, AND HONORS:

Ford Scholars Recipient, The Ford Family Foundation, 2011-2015

Williams Fund scholarship, University of Oregon, 2015, 2017

Paul and Helen Weiser Memorial Scholarship, 2018

[Ford Graduate Scholars Recipient, The Ford Family Foundation, 2016-2018

PUBLICATIONS:

Adult and juvenile *Gorgonocephalus eucnemis.* Photograph. Oregon Quarterly Magazine, Spring 2018. University of Oregon, pp. 16-17.

ACKNOWLEDGMENTS

I wish to express sincere appreciation to my committee members, Drs. Richard Emlet, Alan Shanks, and Maya Watts. I consider myself very fortunate that our paths crossed during the middle of my undergraduate program. Through their teaching and advising they rekindled and reinforced the love I have for science, helping me find my niche along the way. An additional thank you to Richard, who provided me with research opportunities early on, sparked my initial interest in echinoderms and helped me refine my broad interests in invertebrate organismal biology, provided intellectual challenges, and tirelessly made improvements to these manuscripts.

Special thanks to OIMB faculty: Dr. Cynthia Trowbridge, for teaching me about coastal ecology in Oregon and during research opportunities in Ireland, CMLC Director Trish Mace for volunteer opportunities and support, Dr. Craig Young for genuine interest in my project and SEM access, Dr. Maya Watts for endless kindness and teaching me everything I know about parasites, Dr. Brian Bingham for statistical analysis advice, and librarians Barb Butler and Clara Robbins for helping me get access to any resource I needed for this project.

I would like to thank my high school biology teacher, Pam Doyle, for introducing me to OIMB eight years ago. I would also like to thank the OIMB community for making OIMB feel like my home-away-from-home. Special thanks to the graduate students: Caitlin Plowman, Nicole Nakata, Christina Ellison, Dr. Jenna Valley, Kara Robbins, Alexa Romersa, Mike Thomas, Carly Salant, Reyn Yoshioka, Nicole Moss, Zofia Knorek, Hilarie Sorensen, Aliza Karim, and Marco Corrales for their support, comic

relief, and friendships through this crazy adventure. Additional thanks to OIMB facilities staff for helping with project construction and collection of animals; James Johnson, Mike Johnson, Capt. Mike Daugintis and Knute Nemeth.

Additional thanks to my friends and family, especially my parents, whose love and support kept me going through the more difficult times.

Last, but not least, I am extremely grateful for the unwavering love and support from my husband Michael Summers. He has worked tirelessly to help support us, so that I may go to school and pursue my dreams, and I am forever grateful for that. He supports all of my late nights in the lab, far-away research trips, and does not blink an eye at the occasional echinoderm that occupies our freezer.

For my parents, Pete and Bonnie,

who let me play with strange ocean things early on,

and who gave me my brain and taught me how to wield it.

And for my husband Michael,

whose love and support have kept me afloat

through this academic journey.

TABLE OF CONTENTS

Chapter Page

LIST OF FIGURES

Figure Page

Figure Page

Figure Page

LIST OF TABLES

CHAPTER I

GENERAL INTRODUCTION

Ophiuroidea is a class of echinoderms comprised of the basket stars, snake stars and brittle stars. Currently, there are over 2080 known species within the class (Stöhr et al., 2018a). Adults are pentamerous, usually with five simple or branching arms, however species with six and 10 simple arms do exist. Adult body disc sizes can range from 2 mm to 140 mm and can be covered in disc scales, grannules, and / or spines. Ophiuroids have a water-vascular system through which they pressurize tube feet used in locomotion, respiration, and feeding (Farmanfarmaian, 1966; Fedotov, 1930; Hyman, 1955). Their bodies are supported by a calcareous endoskeleton made from calcium carbonate, which constitutes a high fraction of total body mass. Ophiuroids also possess specialized mutable collagenous tissue (Farmanfarmaian, 1966; Hyman, 1955; Pechenik, 2015). This tissue allows for rapid autotomization of arms and sometimes body discs; this easily induced autotomization behavior gave the group its common name: the brittle stars.

Gorgonocephalus eucnemis

Gorgonocephalus eucnemis, first described by Müller and Troschel in 1842, is a basket star known as the Gorgon's head sea star (Fig. 1A). The color of these animals is highly varied and can include white, tan, pink, orange, salmon, yellow and maroon. Like all ophiuroids, the central body disc is markedly distinct from the arms. The disc of *G. eucnemis* is strikingly accentuated with 5 pairs of pale spoke-like plates called radial shields. The central disc has been measured up to 14 cm in diameter (Lambert, 2007) and maximum diameter lengths (arm-tip to arm-tip of un-broken arms) can reach up to 60 cm (Lambert and Austin, 2007). Here in southern Oregon the largest the largest *G. eucnemis* animal I have collected had a disc diameter of 7.1 cm and a maximum diameter of 80 cm (pers. obsv.).

Gorgonocephalus eucnemis inhabits rocky or muddy seafloors in the Pacific, Atlantic and Artic Oceans in the Northern Hemisphere at depths ranging from 15 to 150

meters but as deep as 2,000 meters in association with various genera of soft corals (Rosenberg et al., 2005). These active suspension feeders anchor themselves to the substratum (rocks, corals, etc.) and feed by unfurling their dichotomously branched arms into the current and occasionally making sweeping motions. The arms are supported by strong intervertebral ossicles, muscles, mutable collagenous tissue (Rosenberg et al., 2005), and possibly, with the aid of the water vascular system (Pechenik, 2015). The arms of *G. eucnemis* create a basket-like shape that may be efficient for capturing planktonic prey (Warner, 1977). Warner (1982) suggests that euryaline (Order: Euryalida) ophiuroids fit into the category of predatory suspension feeders due to the looping and ensnaring action of the arms similar to that of the carnivorous ophiurine (Order: Ophiurida) ophiuroids. Prey items discovered in the gut contents include, but are most likely not limited to: copepods, ostracods (Hendler et al, 1984), euphausiids, fish larvae and embryos (Lambert, 2007), chaetognaths and mysids (Emson et al, 1991).

Ophiothrix suensonii

Ophiothrix suensonii (Lütken, 1856), is a large, tropical brittle star, known as the sponge-dwelling brittle star, due to its close association with various sponge species (Fig. 1B). It can be found on fringing and soft-coral reefs within the Caribbean Sea, the Gulf of Mexico, and the Atlantic Ocean as far south as Brazil, from depths of 1 meter up to approximately 100 meters (Hendler et. al., 1995). These suspension feeding ophiuroids occur on mangroves, sponges, gorgonians and even milliporid hydrocorals (Hainey, pers. obsv.). During the day these brittle stars lie flat on their chosen substrata (sponge, root, coral etc.) then move to the highest points of their substrates at night to extend their arms into the current to catch drifting plankton and detritus (Hendler et. al., 1995). Particles that are collected during suspension feeding are compacted into a bolus and transported to the mouth via tube feet. Yellow and dark purple are the most abundant colors of this species, but they can also be found in a wide variety of colors such as: orange, yellow, grey, dark purple, lavender, pink, and red. Disc colors are usually the same as the arms, however the radial shields can be a lighter shade of the disc color with pigment spots in orange, dark yellow, purple or black. The most distal portion of the radial shields, dorsal to the articulating surface, often has a very light patch of color, sometimes appearing

white. This species also has a distinctive dorsal stripe down the length of each arm which is usually crimson, purple, or black (Hendler et. al, 1995).

Ophiothrix spiculata

Ophiothrix spiculata (Le Conte,1851), the Western spiny-brittle star, is a medium-sized temperate to tropical brittle star (Fig. 1C) commonly found in kelp forests, rocky reefs and the intertidal, ranging from northern Chile to Moss Beach, San Mateo County, California, with a small, disconnected population in the waters surrounding Victoria, British Colombia, Canada. They can be found at depths of 1 to 2059 meters (Lambert and Austin, 2007). This species of brittle star lives within crevices in rocks and kelp hold fasts, and can reach population densities of up to 80 individuals per 0.1 square meter (Lambert and Austin, 2007). This suspension feeder sticks one-to-three arms out of its crevice into the water column and remove plankton and detritus by suspension feeding. Material that is collected during feeding is compacted and moved toward the mouth with tube feet. *Ophiothrix spiculata* comes in a wide variety of colors including: maroon, brown, crimson, orange, yellow olive, plum, pink, and, occasionally blue (Hainey, pers. obsv.; Lambert and Austin, 2007). Several species of fish (rock wrasse, pile perch, and sand bass) actively prey on this species of brittle star (Lambert and Austin, 2007).

Echinoderm Respiration

The success of Echinodermata as a phylum has been contingent upon the evolution of specialized respiratory structures, in the form of invaginations and evaginations of thin tissues, that reside in the spaces between ossicles of the well-developed endoskeleton (Farmanfarmaian, 1966). In extant groups of echinoderms, we find specialized respiratory structures such as, papullae/dermal branchiae (Asteroidea), respiratory trees and papillae (Holothuroidea), tube feet/ podia (Asteroidea, Holothuroidea, Echinoidea, Ophiuroidea, and Crinoidea), and bursae (Ophiuroidea). All echinoderms are highly dependent on the acquisition of dissolved oxygen from the surrounding seawater. Although echinoderms do not have a high requirement for oxygen,

most can only withstand low levels or an absence of oxygen for brief periods of time (Lawrence, 1987) and are not known to inhabit anaerobic waters in nature (Farmanfarmaian, 1966). Echinoderms with greater proportions of calcium carbonate (the main component of ossicles) in their body require less oxygen for basic metabolic maintenance. In general, the slope of a line representing the relationship between rate of oxygen consumption and wet weight is greatest in holothuroids, followed by asteroids and echinoids. The lowest oxygen consumption rate /wet weight (mass) belongs to the ophiuroids, due to their well-developed ossicle system (Lawrence and Lane, 1982). Burrowing echinoderms may have lower respiration rates than their non-burrowing counterparts, however respiration rates for various echinoderms of similar mass are all in the same order of magnitude (Farmanfarmaian, 1966). Respiratory rate is also dependent on the nutritional state, ambient oxygen tension, pH and, sometimes salinity (Farmanfarmaian, 1966). While total oxygen consumption increases with the weight of the animal, the mass specific rate of oxygen consumption decreases with increasing size within a species (Farmanfarmaian, 1966). Respiratory rate has also been observed to increase when echinoderms process food (Farmanfarmaian, 1966).

Farmanfarmaian (1966) demonstrated that oxygen absorbed across the tissue-water interface moves by advection (generated by muscular and ciliary action) in the lumen of the tube foot to the ampulla (Farmanfarmaian, 1966). Once in the ampulla, oxygen diffuses across the ampullar membrane into the coelomic fluid. Advection of perivisceral coelomic fluid is directly responsible for delivery of oxygen to the internal tissues and for removal of carbon dioxide. Since ophiuroids lack ampullae, but possess a unidirectional valve, the oxygen must diffuse through the podial/water vascular system (WVS) membrane once above the valve. Under natural conditions, the greatest distance oxygen can diffuse across echinoderm tissue is approximately 1.5 mm (Farmanfarmaian, 1966). Thus, an echinoderm with body dimensions greater than 3 mm cannot rely on diffusion alone as a sustainable means of oxygenating its tissues and must utilize another specialized structure (e.g. thin tube feet or papullae) or pump water past respiratory exchange surfaces such as respiratory trees, to meet their oxygen needs (Farmanfarmaian, 1966). Two classes of echinoderms that have members that are known to actively pump water past their respiratory exchange surfaces are holothuroids and the asteroids (genus

Pteraster). Holothuroids have specialized respiratory structures such as papillae and respiratory trees. The respiratory trees of holothuroids are attached to the cloacal opening and lie within the body of the animal, within the coelomic fluid. The cloaca pumps sea water into these trees, where oxygen is taken-up, then the tree tubules contract, flushing the water back out the cloaca and the cycle continues (Pechenik, 2015). Reported rates of filling and emptying the respiratory tree are six-to-ten cycles per minute (Nichols, 1969).

Like other asteroids, *Pteraster* takes up oxygen via tube feet and papullae, but it also has a nidamental chamber through which water is pumped over papullae on its aboral surface (Johansen and Petersen, 1971). The nidamental chamber is above the aboral body wall and below the supradorsal membrane (Johansen and Petersen, 1971). Well-developed musculature in the body wall in addition to skeletal ossicles that can slide past one another, allow *Pteraster* to fill and empty the chamber. Upon deflation, body wall muscles contract and the osculum opens, forcing the water in the nidamental chamber, out, then the cycle restarts (Johansen and Petersen, 1971). When comparing the rates of nidamental chamber ventilation at various dissolved oxygen concentrations, *Pteraster* ventilated its nidamental chamber approximately 4 times per minute under hypoxic conditions, compared to a rate of 2 nidamental chamber ventilations per minute under normoxic conditions (seawater held at 11 °C) (Johansen and Petersen, 1971).

Ophiuroid Respiration

Ophiuroids are known to uptake oxygen across their tube-foot membranes, and the bursae in their body discs are presumed to be additional sites of oxygen uptake (Austin, 1966; Hyman, 1955; MacBride, 1906). The bursae are lined with a ciliated epidermis that generates currents which enter through the upper region of each bursal slit and exit from the lower region of the bursal slit (Austin, 1966). In the basket star, *Gorgonocephalus*, all of the bursae are fused together into a large, circumesophageal space and lined by layers of ciliated epidermis and peritoneum (a serous membrane lining the coelomic side of the bursae) (Fedotov, 1926; Hyman, 1955). In *Gorgonocephalus eucnemis*, (Müller & Troschel, 1842) each bursa has its own opening (bursal slit) visible from the oral side of the animal. Some ophiuroids, such as *Gorgonocephalus* and *Ophiothrix*, actively pump their discs which moves an increased volume of water through

their bursae compared to the ciliary current (Hainey, pers. obsv.). This active disc pumping behavior was first observed in species from the genera *Ophiothrix*, *Ophiura*, and *Amphiura* (MacBride, 1906).

Functional Morphology of the Radial Shield-Genital Plate Ossicles

Ophiuroid ossicles are composed of a porous, calcitic microstructure called stereom. The stereom is composed of a fine meshwork of trabeculae, which are a repeated series of calcitic columns or bands. The patterns, or stereom fabrics, found within the trabeculae can be either regular or irregular and are found in echinoid calcitic structures (Blake et al., 1984), as well as ophiuroid ossicles (Hainey, pers. obsv.). The presence of different stereom fabrics at different locations on a calcitic structure may suggest morphological features such as muscle attachments (Blake et al., 1984). In ophiuroids, on the oral side of the body disc, a pair of genital plate ossicles lie at the base of each arm, between the bursal slit and the arm. Although the genital plates are distinguishable and independent, they are firmly attached to the base of each arm by connective tissues. Toward the edge of the disc, each genital plate has an articulating region that abuts the articulating region of the radial shield and is held in place by the abductor muscle, connective tissue and epidermis. Historically, it has been asserted that the radial shield ossicles, in conjunction with the genital plate ossicles and associated muscles are responsible for the mechanical regulation of the roof of the disc, resulting in bursal ventilation, however, this has not been empirically tested.

Thesis Outcomes

This thesis bridges the disciplines of animal behavior in relation to environmental changes and functional morphology with additional attention to microstructure. By applying what we learn from examining the functional morphology and microstructure of certain ophiuroid ossicles to the animal's movements that are generated by the ossicles and corresponding muscles, we can gain new information on ophiuroid biology, ecology, taxonomy, and paleobiology. Chapter II, "*Gorgonocephalus eucnemis* and bursal ventilation," will be published with co-author, Richard B. Emlet.

Figure 1.

A. *Gorgonocephalus eucnemis*. B. *Ophiothrix suensonii*, and C. *Ophiothrix spiculata*

BRIDGE I

Gorgonocephalids are known to regulate the position of the roof of their discs, but its role in respiration has not been empirically tested. In chapter I, I demonstrate the respiratory function of the disc pumping behavior of *Gorgonocephalus eucnemis,* by investigating two environmental conditions that this species would encounter in situ. In one experiment I offered suspended food and in another I reduced the dissolved oxygen in the SW. Under both conditions basket stars increased their rates of bursal ventilation. I estimated the volume of water moved through the disc bursae during non-feeding and feeding intervals. I also measured the dissolved oxygen concentration in aquarium seawater before and after it entered the bursae. These measurements and estimates allowed me to calculate the contribution that bursal ventilation makes to oxygen uptake by the basket star.

CHAPTER II

TITLE:

Gorgonocephalus eucnemis and bursal ventilation

Methods regarding bursal ventilation in response to feeding, and hypoxia, and methods detailing volume approximations were developed by both Richard Emlet and myself. Richard Emlet provided helpful suggestions regarding discussion content and provided re-wording of my original writing in the introduction and discussion sections. I was the primary contributor to this chapter, by running all of the experiments, analyzing all of the data, in addition to doing all of the original writing and figure creation.

AUTHORS:

MacKenna A. H. Hainey and Richard B. Emlet

INTRODUCTION

All echinoderms are aerobic organisms and are highly dependent on the acquisition of dissolved oxygen from the surrounding seawater. Echinoderms have developed specialized respiratory structures, such as dermal branchiae, papillae, papullae, respiratory trees, and utilized other structures secondarily such as the podia, as sites for oxygen uptake (Farmanfarmaian, 1966). The basket star, *Gorgonocephalus eucnemis* (Müller & Troschel, 1842), is a member of the largest Echinodermata class, Ophiuroidea (Stöhr et al., 2018b). Basket stars and other ophiuroids have five pairs of specialized structures called bursae (i.e. genital bursae, respiratory bursae) which are hollow chambers opening to the sea. Bursae occur in the body disc on either side of each arm base and open to the outside environment via bursal slits located where the arms join the disc on the oral side. The bursal epidermis is lined with a ciliated epithelium (Austin, 1966; Hyman, 1955; MacBride, 1906). Spencer and Wright (1966) suggest bursae arose to meet the requirements of living in sediment burrows. Many species who do not live in burrows also have bursae which presumably play a role in reproduction (Spencer and Wright, 1966). The thin highly-folded nature of the *Gorgonocephalus* bursal epidermis has an increased surface area, which suggests that the bursae are ideal locations for oxygen uptake and removal of waste products via diffusion (Fedotov, 1926; Hyman, 1955; Spicer, 2016; see Fig. 1). Some ophiuroid species lack bursae entirely, indicating they are not essential for respiration. However, most species that lack bursae are very small, with disc diameters smaller than 2mm (Austin, 1966), well within the suggested maximum oxygen diffusion distance of 1.5 mm (Farmanfarmaian, 1966). A few larger species lack bursae. *Hemipholis elongata,* and *Hemipholis cordifera* have average disc diameters of ~ 5 mm. These species have developed adaptations to compensate for the lack of bursae, such as the utilization of the respiratory pigment hemoglobin (contained in coelomocytes within the WVS) (Beardsley and Colacino, 1998; Heatwole and Stancyk, 1982), and specialized structures inside the body disc called the Simroth's appendages.

Some species are known to exhibit a disc pumping behavior. This disc pumping motion is achieved by the raising and lowering of the radial shield ossicles with an opposing set of muscles that articulate with the genital plate ossicles (Fig. 2 and Chapter 2). Upon elevation of the body-disc roof, the bursae inflate as water is drawn in (MacBride, 1906). This inflation, followed by a compression of the aboral surface 'roof' of the bursal sacs, is cyclical, and will be referred to as bursal ventilation hereafter.

Historical Record of Disc Pumping in Ophiuroids

In 1880, Lyman reported the radial shields of *Gorgonocephalus sp.* occupy expected positions within the body disc and articulate with the genital plates. He states, "Hinged to the genital plates they regulate the position of the roof of the disk as it is raised or lowered (pg. 255)." Lyman, however, did not report any observations of active disc pumping by the animal at this time. In 1906, MacBride made observations of active disc pumping by *Ophiothrix fragilis*: "Observations on *Ophiothrix* show that in this species at any rate the radial plates can be raised or lowered. When they are raised the centre of the disc is lifted into a cone and water is sucked into the genital bursae whereas when they are lowered the bursae are compressed and water is expelled (pg. 285)." He was also the first to observe this bursal ventilation by disc pumping in the additional genera, *Ophiura* and *Amphiura* (now *Amphipholis*). MacBride also asserted, "its [the bursa's] main function is respiratory," that bursal ventilation was of respiratory nature, and that it may play a role in supplementing oxygen when ambient oxygen concentrations are decreasing. "This forced respiration comes into play when the supply of oxygen is getting scanty" (Mac Bride 1906, pg. 285). The ciliated ectoderm of the bursae is also mentioned for the first time in this passage as well; "…the cilia bringing about a constant inward current of fresh sea-water, the oxygen contained in which diffuses through the thin wall of the sac into the coelomic fluid (pg. 485)." Forty-nine years later, in Hyman (1955) stated, "Bursae are peculiar to ophiuroids and important to their biology. A water current constantly circulates through the bursae for respiratory purposes, and some species pump water in and out of them by movements of the aboral disc wall (pg. 617)." Though not completely exhaustive, this literature review shows over 110 years of assertion and general acceptance of an untested suggestion that bursal ventilation by disc

pumping is a means of respiration, and that it may aid the animal in some manner when oxygen concentrations are low.

Exposure to Hypoxia in Situ

While most epibenthic marine animals do not regularly experience hypoxia, there is an apparent increase in hypoxic and anoxic events worldwide, especially along upwelling zones (Altieri et al., 2017; Bakun et al., 2010). Marine animals that are not used to experiencing hypoxic events will begin to do so as the trend for periodic hypoxia becomes more severe in duration, spatial scale and intensity. Many species of ophiuroids live in habitats that may experience low concentrations of oxygen or periods of hypoxia. Hypoxic ocean conditions have been present for millennia and in some locations may have impacted the evolution of fossil ophiuroid species. Perhaps the exposure to hypoxic periods has shaped the evolution of bursae as sites for oxygen uptake, as well as an ability to increase rate of bursal ventilation during these exposures. When encountering water with low oxygen (hypoxic) or no oxygen (anoxic) some ophiuroids, like *Ophiothrix* (Müller & Troschel, 1840), widen the bursal slits, perhaps allowing movement of a greater volume of water by ciliary current (Austin, 1966). Some species exhibit a behavior called 'arm-tipping' where the ophiuroid stands up on its arm tips raising the disc up higher in the water column, presumably in effort to reach more oxygenated waters (Altenbach et al., 2012; Riedel et al., 2014). Others often attempt to quickly vacate the immediate area by climbing nearby structures or by moving away in a lateral direction (Johnson et al., 2018; Spicer, 2016). Hypoxic events with lengthy persistence times, that cover wide geographic ranges, make it seem unlikely that many slow-moving species such as *Gorgonocephalus* would be able to relocate to oxygen refugia.

Temporary hypoxic conditions along the Pacific Northwest coast are events that have probably occurred regularly over evolutionary time, however, the increasing frequency, lengthening duration, and severity of these events suggest a long-term shift in Eastern Pacific Ocean conditions. Many species of ophiuroid, such as *G. eucnemis,* live within these ecosystems that are now experiencing anomalous periods of hypoxia, and while ophiuroids are mobile they may not be able to escape to more oxygenated waters

when these events occur. MacBride (1906) suggested that the bursal ventilation behavior might "come into play when the supply of oxygen is getting scanty," however this has not been tested. Change in respiration when exposed to environmental hypoxia is one of the first physiological responses observed across multiple taxa (Spicer, 2016). In part, this study investigates whether the bursal ventilation behavior in basket stars can serve as a coping mechanism for short-term exposure to hypoxic ocean conditions. There is an urgent need to inform those looking to manage how detrimental fluctuations in oxygen concentrations affect ecosystems and biodiversity. In addition, there is also an urgent need for information on animal physiological responses, such as hypoxia-induced impacts on respiration, of the affected individual species.

In the present study, I demonstrate that bursal ventilation behavior serves as a means of respiration and explore environmental conditions that may increase ventilation rates. I examine rate of bursal ventilation when exposing the animal to two stimuli encountered in situ: an increase in food availability, triggering a feeding response /digestion, and a decrease in dissolved oxygen to hypoxic levels. In addition, I measured dissolved oxygen levels of water entering and exiting the bursae.

METHODS AND MATERIALS

Collection of Specimens

Three *Gorgonocephalus eucnemis* specimens were collected in February 2015, six specimens in February 2016, and eleven in June 2017 by rectangular dredge (~90 cm X 30 cm frame, 3 cm net mesh diameter catch bag). Sampling took place approximately five kilometers off-shore from Cape Arago, Oregon, USA (in the vicinity of 43^{o} 16' 615" N, 124^{o}27' 475" W) at depths ranging 45-60 meters. Individuals were transported to the laboratory in coolers filled with seawater. Animals were placed into coolers ventral (oral)-side-up to allow air bubbles to escape from their mouths and bursae. At the laboratory, all basket stars were placed into a 500-gallon tub supplied with continuously flowing seawater and aeration.

The basket stars collected in 2015 were used to examine effects of feeding on bursal ventilation rate, body disc volume and, volume of water processed per hour in

feeding and non-feeding individuals, for an undergraduate thesis (Hainey, 2015). The specimens collected in 2016 were used for the same purposes, but the data was not in the thesis. Specimens from the 2017 collections were used to examine responses to hypoxia.

Bursal Ventilation Rates and Feeding

Individual basket stars (n =9), with body disc sizes ranging from 8.8 mm to 64 mm, were placed into an insulated 15-gallon aquarium filled with filtered (5 μm) sea water, held at 11° C (in situ temperature) by a temperature control unit (VWR Scientific model #1141). Constant aeration was supplied to the tank via an airstone and pump. Basket stars were allowed to acclimate to the tank environment for one hour before any data were recorded. Once acclimated, basket stars were video recorded in time-lapse with a GoPro camera (HD Hero 3 Silver Edition®) at a frame-rate interval of 1 frame per 5 seconds. The first hour of time-lapse video recording served as the 'control' as no food supplements were added to the water. However, at the beginning of each control trial, the surface of the water was stirred with a clean turkey-baster. After the first hour of video recording, 50 ml of 'krill smoothie' (equal volumes dried krill and seawater, pureed in a blender) were added to the aquarium with a turkey-baster. Upon addition of the 'krill smoothie' to the aquarium water, time-lapse video recording of the 'feeding manipulation' began, lasting for one hour. An additional, third hour of video recording followed the 'feeding' manipulation to observe any post-feeding behavior. Time-lapse videos were later analyzed by counting the total number of disc pumps in each video (2,160 frames per video = 3 hours of video), for each trial. Videos were played at 10x – 12x real time speed and the number of disc pumps were counted. Bursal ventilation rate was reported as the number of body disc pumps per hour. Aquarium water was changed between each specimen.

Estimated Volumes of Fluid Moved Through Bursae

To calculate the approximate volume of fluid (seawater) moved through the bursae, I measured, using calipers, the disc diameters (radius to opposite interradius) to the nearest 0.1 mm of each basket star in the feeding trials. I took still images from the corresponding time-lapse videos that showed the disc at a fully-inflated and fully-compressed state (one pair of images per basket star). From these images, uploaded to

ImageJ and calibrated from known disc diameter, I measured the height of the disc at the fully-inflated state (2c) and the fully-compressed state (d). I used these measurements to calculate the change in disc volume assuming an oblate spheroid for the fully inflated shape and the lower hemisphere of a deflated oblate spheroid for the compressed shape for each individual (Fig. 3). 'a' is the equatorial radius of the spheroid, and 'c' and 'd' are the distance from center to the pole along the symmetry axis (Eqn. 1).

Eqn. 1

$$\Delta \text{ Volume} = 4/3\pi a^2 c - \tfrac{1}{2}(4/3\pi a^2 d)$$

This equation gave the estimated volume of fluid moved through the bursae in one bursal ventilation cycle. To measure the volume of fluid moved through the bursae for one hour in milliliters per hour (mL/h) during feeding and non-feeding, I multiplied volume of one pump by the number of disc pumps / hour during feeding and non-feeding treatments. Difference in disc pumps per hour between feeding and non-feeding groups were calculated, as well as the percent increase in the volume of fluid moved per hour between non-feeding and feeding states (see table 1). Paired T-tests were run on the data using R v. 3.3.2 (R Core Team 2016).

Bursal Ventilation Rates in Response to Hypoxia

Ventilation rates were measured on 11 individuals. Individual basket stars were placed into an insulated 15-gallon aquarium filled with filtered (5 μm) sea water, held at a constant temperature of 11° C by the same temperature control unit described above. Basket stars were allowed to acclimate to the tank environment for one hour before data were collected. For this experiment "hypoxic conditions or hypoxia" was defined as a concentration of oxygen $\leq$ 3.5 O_2 mg L^{-1} (= 2.45 O_2 ml L^{-1}). This concentration of oxygen was approximately 40-50% of local ambient conditions (range: 7.95-8.32 O_2 mg L^{-1}, 5.57-5.82 O_2 ml L^{-1}; average: 8.16 O_2 mg L^{-1}, 5.71 O_2 ml L^{-1}) and had strong effects on animal behavior. Oxygen concentration demarcations were made with Siebel's (2011) argument in mind, that hypoxic habitats should be defined by the biological response to hypoxic conditions and not by an arbitrary oxygen concentration. Historically, hypoxia has been defined as oxygen concentrations $\leq$ 2.0 O_2 mg L^{-1} (1.4 O_2 ml L^{-1}) (Dashtgard et

al., 2015; Levin et al., 2009 and), however, I chose to use a slightly higher oxygen concentration to avoid basket star mortality. Death occurs after ~ 2 hours at 3.0 mg L^{-1} (n = 1) (M. Hainey, pers. obsv.).

Bursal ventilation rate was measured during three, half-hour intervals at DO levels designated as normoxic (8.0 O_2 mg L^{-1}), hypoxic (3.5 O_2 mg L^{-1}) and post-hypoxic (7.9-8.0 O_2 mg L^{-1}). During each trial one specimen was in the aquarium starting in normoxic conditions; after 30 minutes, medical grade nitrogen gas was bubbled into the water until a dissolved oxygen concentration of 3.5 mg L^{-1} was reached. At this point, the nitrogen gas was turned off and the surface of the water was covered with plastic wrap to limit surface oxygen exchange. Conditions remained at this hypoxic level for another 30-minute interval. After 30 minutes of exposure to hypoxia, the plastic surface cover was removed and ambient air was bubbled into the water until 'normoxic' conditions were reached. Once a 'post-hypoxic' dissolved oxygen concentration of 7.9-8.0 mg L^{-1} was reached the third and final 30-minute interval was recorded. Dissolved oxygen and temperature were continuously recorded over the entire trial using a YSI ODO probe and the accompanying computer software (YSI Pro Series Data Manager 1.1.8 © 2009) (Fig. 4). The animals were video recorded continuously through each oxygen concentration transition with a GoPro camera (HD Hero 3 Silver Edition®) at a time-lapse frame-rate interval of 1 frame per 5 seconds (one disc pump took an average 1.5-2 minutes). Disc pumps were counted during the entire length of each 30-minute interval and doubled to achieve 'bursal ventilation rate.' This process was carried out for each of 11 specimens (n = 11). Body disc sizes (diameter) ranged from 28 millimeters to 75 millimeters. pH measurements were taken at the 15 minute mark of each 30 minute exposure period with a benchtop pH meter (Fisherbrand™ Accumet™ AE150 pH Benchtop Meter), during each trial.

Statistical Analyses Used for Hypoxia Experiment

To test the assumption that the variances between all possible pairs of within-subject conditions are equal, a Mauchly's Sphericity test was run. A repeated measures ANOVA (ANOVAR) and paired t-tests were carried out. All statistics were calculated using R v. 3.3.2 (R Core Team 2016). Since alpha error climbs with each t-test, a

Bonferroni correction (α =0.05/3) was applied to the critical alpha to compensate for this effect.

Oxygen Uptake Within the Bursae

To test if oxygen was being absorbed through tissues inside the bursae, water samples were taken from inside the bursae after the body disc had been at full inflation for at least 30 seconds. Approximately 2-3 mls of water were removed from the bursae using a modified 50 ml Falcon centrifuge tube with a- 30 cm long piece of polyethylene tubing (1.57mm external diameter, PE160 INTRAMEDIC®) secured to a hole at the bottom of the 50 mL falcon tube with 100% silicone adhesive. The free end of this tubing was carefully placed into one of the bursae (through the bursal opening). The basket star would then detect a foreign object in its bursae and close its bursal opening around the tubing. A sample of water from the bursae was then drawn into the falcon tube using a plunger from a 60 mL syringe. After obtaining a sample, the tube was gently removed from the bursae so as to avoid loss of sample. A hole was then poked into the side of the Falcon tube (above the sample but below the plunger) which released the vacuum inside the barrel of the Falcon tube and allowed for removal of the plunger without further aeration of the sample. An oxygen probe (YSI ODO, Model No.626281) was then used to determine oxygen concentration (mg L^{-1}) of the sample while still in the bottom of the Falcon tube. This was repeated for 3 individual basket stars with disc diameters ranging from 40 – 55 mm, that were within the middle of the size range of all animals collected (8 – 75mm). The dissolved oxygen concentrations of the ambient tank conditions were measured by placing the ODO probe directly into the aquarium water, at approximately the middle of the water column. To determine whether collection by syringe and tubing had any influence on oxygen concentration, a 'tube control' sample was taken. For this control, ambient tank water was drawn up into the syringe and measured with the ODO probe in the same manner as the bursae samples. Measured oxygen concentrations taken from the aquarium (ambient), the bursae, and from a tube control were listed in table 2.

Statistical Analyses Used for Oxygen Uptake Experiment

One-tailed t-tests were carried out on the groups: ambient vs. bursae samples, ambient vs tube control samples, and bursae vs. tube control samples. All statistics were calculated using R v. 3.3.2 (R Core Team 2016).

RESULTS

Bursal Ventilation Rates and Feeding

Bursal ventilation rates were significantly higher for the 'feeding' group (mean +/- SE = 31.2 ± 3.87) than for the 'non-feeding' group (mean +/- SE= 20.4 ± 3.36; $t = 5.7$, $df = 8$, $p < 0.001$, $\alpha = 0.05$) (Fig. 5). Each of nine specimens showed an increase in bursal ventilation rate during feeding trials. Once the food was detected by a basket star in the test aquarium, it quickly assumed a feeding position (some arms raised in a parabola, creating a basket shape with tendrils unfurled) and began to move 2-3 arms slowly through the water, looping arm tendrils as the arm hooks accumulated particles of krill. The rate of bursal ventilation increased rapidly once this feeding activity began. Animals maintained their feeding behavior for 45-55 minutes. Bursal ventilation rates remained elevated for an average of 25 minutes after active feeding had ceased.

Estimated Volumes of Fluid Moved Through Bursae

Estimated volumes of fluid moved through the bursae during feeding trials were significantly higher than the volumes of fluid moved through the bursae during non-feeding trials (feeding = 234.4 ± 77.0 mL/h (mean +/- 1 s.e.), non-feeding = 168.5 ± 61.5 mL/h; $t = 2.31$, $df=8$, $p < 0.001$, $\alpha = 0.05$). Note the standard errors are large due to the large range in body sizes and hence bursal volumes (Table 1). There was an average increase of ~ 64% in the volume of fluid moved through the bursae when basket stars were feeding compared to when they were non-feeding (Figure 6, Table 1).

.

Bursal Ventilation Rates in Response to Hypoxia

Bursal ventilation rate, measured in number of disc pumps per hour (bv/h), increased significantly when basket stars were exposed to hypoxic conditions and rates returned to near-original levels when dissolved oxygen levels returned to a normoxic

concentration (normoxic = 17.5 ± 0.4 bv/h (mean +/- 1 s.e.), hypoxic = 28 ± 0.47 bv/h, post-hypoxic = 17.7 ± 0.25 bv/h; $F = 60.27$, $df = 10$; $p<0.05$; Fig. 7). Bursal ventilation rates were significantly different between normoxic and hypoxic conditions ($t = 9.5$ $df = 10$, $p< 0.01$, $\alpha =0.017$; Fig. 7A), and between hypoxic and post-hypoxic conditions ($t= 8.6$, $df = 10$, $p< 0.01$, $\alpha =0.017$; Fig. 7B). There was no statistical difference between normoxic and post-hypoxic conditions ($t = -0.17$, $df = 10$, $p= 0.87$, $\alpha =0.017$; Fig. 7C). Bursal ventilation rate for all 11 animals increased during hypoxic conditions and then decreased after return to normoxic conditions (Fig. 8).

Oxygen Uptake Within the Bursae

Dissolved oxygen concentrations from water samples taken from the bursae and the aquarium water (ambient) differed significantly ($t = 6.73$, $df = 2$, $p = 0.01, 0.05$, $\alpha = 0.05$). Ambient samples contained a higher level of dissolved oxygen (8.84 ± 0.17 mg O_2 L^{-1}) than water samples taken from within the bursae (7.44 ± 0.17 mg O_2 L^{-1}). The tube control contained an insignificantly higher dissolved oxygen concentration (8.92 ± 0.15 mg L^{-1}, $t = -2.81$, $df = 2$, $p = 0.11$, $\alpha = 0.05$) than water samples taken directly from the aquarium (Fig. 9). 'Bursae' and 'tube control' samples were also significantly different from one another ($t = -7.29$, $df = 2$, $p = 0.009$, $\alpha = 0.05$).

Observations Associated with Feeding and Hypoxia

Once pureed krill was added to the experimental aquarium, the basket stars quickly unfurled their arm tendrils. Within 45 seconds of adding the krill, basket stars had unfurled all of the arm tendrils that were being utilized for food capture and began to move around the tank on the arms that were not involved in food capture. The feeding arms swept slowly through the water and the tendrils of the sweeping arms coiled as krill particles collected on the arm hooks. Coiled tendrils were then brought below the disc unfurled slightly, some were inserted into the mouth, and food was removed as the tendrils were pulled across the oral papillae and out of the mouth, leaving the krill particles on the esophageal side of the jaws. Basket stars exhibited feeding behavior beginning a few seconds after food was introduced to the aquarium and lasted an average duration of 50 minutes (Figure 10).

During the hypoxia experiment, I observed a gradual decrease of coordination as the exposure time to hypoxic conditions lengthened. In normoxic conditions basket stars appeared to have fine motor control over arms both involved in locomotion and clinging, or arms that were raised into the water. They were able to uncurl and re-curl arm tendrils into tight coils and could adequately grasp structures in the aquarium. However, as nitrogen gas was bubbled into the aquarium the basket stars seemed to lose the ability, or just stopped forming tight arm tendril coils. This was a gradual process occurring over the first few minutes of addition of nitrogen gas. Basket stars were mostly stationary in normoxic conditions, however, approximately 2 minutes after aquarium conditions reached ~3.5 O_2 mg L^{-1} basket stars abruptly began to move around the tank, appearing to 'stumble' when they failed to bring locomotory arms out from beneath the disc, displaying poor coordination of arms. At this time bursal ventilation rates were elevated. Bursal ventilation rates had noticeably increased around the 8-10-minute mark of adding nitrogen (~6.0 O_2 mg L^{-1}). The stars continued to move for approximately 10-20 minutes (of the 30-minute hypoxia exposure time) and then ceased locomotion. When stars stopped moving their arms appeared limp, though some formed very loose coils. Bursal ventilation rates remained elevated once the basket stars stopped moving around the tank for the remainder of the duration in hypoxic conditions. Arm condition (limpness) and motor control appeared to improve gradually as the nitrogen was replaced with air, and oxygen saturation began to return to near-normoxic conditions. Bursal ventilation rates also declined to near- normoxic rates as the oxygen saturation climbed. It appears that the basket stars need to respire at an elevated rate post-feeding, perhaps to aid in the digestion process (Fig. 10A). However, when recovering from exposure to hypoxia, the decrease in bursal ventilation rate was relatively rapid, and synchronized with the return of oxygen to the water (Fig 10B).

DISCUSSION

Bursal Ventilation Rates and Feeding

The bursal ventilation rates during feeding periods were significantly higher than rates from non-feeding trials. The sharp increase in activity once food was introduced (arm movement) seems to be a reasonable reason why bursal ventilation increased as

feeding started. Each arm, including all of its bifurcations, is powered by intervertebral muscles, which like any muscle, requires more oxygen when doing more work. Bursal ventilation may be a way to increase oxygen delivery to the arms, once oxygen is transported across the bursal linings and delivered to the fluid in the coelom, which may travel down the crescentic coelom extensions into the arms. These coelomic extensions lie on the aboral surface of the arm in the narrow space that lies between the lateral and aboral arm plates, and the vertebral arm ossicles (Hyman, 1955). However, it is unlikely that oxygen taken in through the bursae will make it out to the most distal ends of the arms. It is more likely that oxygen absorption and distribution at the distal portions happens locally through the podia. Bursal ventilation may also increase during feeding activities because digestion requires increased metabolism which requires more oxygen. This may explain why ventilation rates remain elevated after they stopped feeding.

Disc pumping after feeding has been observed in other species, such as *Ophiarachna incrassata*. Wakita (2018 and unpublished) noticed *O. incrassata* specimens would rhythmically pump their discs after feeding in repetitive cycles lasting 20 – 70 seconds. In contrast, disc pumping in *G. eucnemis* is cyclical and continuous. In *Gorgonocephalus* disc pumping behavior is present before, during, and after feeding activity, but differs in rate.

Like all animals, basket stars create waste products such as nitrates, nitrites and ammonia. Because ophiuroids have a blind gut (no anus, cloaca) and no designated nephridial system, Austin (1966) suggested regular bursal ventilation helps with the removal of nitrogenous waste products once they are transported through the layers of tissue into the bursal cavities.

Bursal Ventilation Rates in Response to Hypoxia

Bursal ventilation rates were significantly higher during hypoxia treatments. The hypoxia exposure resulted in an approximate 60% increase in average bursal ventilation rate when compared to both the normoxic and post-hypoxic conditions (compared to the 64% increase between non-feeding and feeding rates). During this experiment, not only was there a significant increase in bursal ventilation rate, but also a noticeable decrease in coordination of the arms involved with locomotion. This lack of coordination of the arms

in periods of low oxygen could be explained by inadequate oxygen absorption by the podia, leaving the arms muscles starved for oxygen resulting in poor motor function. The sudden increase in locomotion in response to the dropping oxygen concentration may be an effort to find water with a higher oxygen saturation. Escape, or avoidance behaviors are a common response of marine animals that may experience periodic hypoxia (Burnett and Stickle, 2001).

Hypoxic events along the North American Pacific Northwest coast have occurred regularly over the past few thousand years, exposing the local fauna to fluctuating oxygen concentrations (Erhardt et al., 2014). Perhaps increased bursal ventilation in response to hypoxic conditions has evolved in *Gorgonocephalus* and other ophiuroids as a mechanism to increase the amount of water processed for respiratory purposes. Due to their ability to increase their rates of respiration via bursal ventilation adult *G. eucnemis* may be able to cope with and survive less severe hypoxic events that are not too long lasting or too extensive spatially. Because *Gorgonocephalus* (local to Oregon waters) tolerates a fairly narrow temperature range (7-12° C), hypoxic events that coincide with an increase in temperature above 12°C could have negative consequences for populations. In the laboratory, a sustained increase in temperature of (approximately) 1-2 degrees above the normal range has proven lethal for *Gorgonocephalus* after a few days (pers. obsv.). In slightly elevated temperatures, basket stars begin to autotomize arms starting with the most proximal tendrils. If the stressed basket stars are not placed into cooler water once autotomatization has begun entire arms will drop off and the animal will die shortly thereafter (M. Hainey, unpublished observations).

When the nitrogen gas was pumped into the test aquarium, it displaced the oxygen and other dissolved gasses such as carbon dioxide. This displacement of dissolved gasses caused the pH of the seawater to rise slightly (+ 0.04) in each trial. Despite pH being on a log scale, this change is negligible and is well within the change in pH a basket star could experience in situ. In 2016 the Pacific Marine Environmental Laboratory (PMEL), a branch of the National Oceanic and Atmospheric Administration carried out a series of hydrographic cruises along the western shore of North America, on the continental shelf. At a location North of Cape Arago (44.200, -124.140), the PMEL cruise recorded a pH

range of 0.70 at depths of 47 and 73 meters, well within *Gorgonocephalus* habitat (Greeley, 2016).

Oxygen Uptake Within the Bursae

The rate of bursal ventilation increased by an average of 64% when basket stars were feeding, compared to non-feeding, with a corresponding 64% average increase in the volume of fluid moved through the bursae by bursal ventilation. When exposed to hypoxic conditions, basket stars increased their rates of bursal ventilation an average of 60%, when compared to bursal ventilation rates in normoxic conditions. Although approximate volumes of fluid moved through the bursae were not measured for the hypoxia exposure experiment, we can expect to see an approximate increase in fluid moved through the bursae to be around 60% (in the hypoxic conditions) based on what I found with the feeding experiment. The response of *Gorgonocephalus* to reduced oxygen availability make it an oxyregulator (Spicer, 2016). Adult basket stars are large with some of the most voluminous body discs known among ophiuroids. The oblate spheroidal shape of the disc restricts its surface area relative to its volume and the ability to absorb oxygen through the epidermis of the body disc. Perhaps utilizing the bursae as respiratory surfaces has allowed ophiuroids like *Gorgonocephalus* to grow to the large sizes we find today.

If *Gorgonocephalus eucnemis* takes up oxygen via its bursae, how much of this oxygen contributes to the total oxygen demand? Based on the 'in bursae and ambient' measurements of DO of the three specimens multiplied by the approximate bursal exchange volume (0.012L) for basket stars in this size range and by the average number of bursal ventilations in one hour (20) I estimate 0.35 mg oxygen taken up within the bursae per hour. I used the mass specific metabolic rate measured by LaBarbara (1982) from two individuals (average: 12.2 µl O2 g wet mass $^{-1}$ hr $^{-1}$) multiplied by one of my specimen's wet mass (194.4 g) to estimate that my specimen would use approximately 3.4 mg O_2 hour^{-1}. These calculations suggest that bursal ventilation only accounts for ~10 % of the estimated demand of the whole animal. I have probably underestimated the bursal contribution for three reasons. First, the modified Falcon-tube apparatus exposed the bursal water samples to a small volume of air (0.2ml) trapped in the system, despite

the plunger being pushed down as far as possible into the barrel. Even though this trapped air only accounts for ~10 -15% of the total sample volume, it may have increased the concentration of oxygen in the bursal water samples, and decreased the estimate of DO removed from ambient water. Second, I sampled the water inside the bursae once the disc roof had been fully elevated for approximately 1 minute and there was no obvious further expansion. Because a cycle of filling and emptying lasts for 1-1.5 minutes and DO is removed during the entire cycle, I also probably underestimated the amount of DO removed from ambient water. Third, the specimens studied by LaBarbera had wet masses that were ~5x and ~20x smaller than my average individual, and therefore, should have higher mass specific metabolic rates than the larger one used in my study, leading to a potential overestimate of metabolic O_2 demand.

The perivisceral coelom of the disc continues into the base of each arm occupying the space between the vertebral ossicles and the lateral and aboral arm shields (Hyman,1955). Because of the coelom presence in the arm bases, we hypothesized oxygen taken up in by structures within the disc may also be utilized by regions in the arm bases. Gorgonocephalus also have arms with many intervertebral muscles that consume more oxygen when doing work, so it would not be unreasonable to suggest any oxygen taken up from within the podia would be quickly consumed locally. Oxygen taken up by podia might not make it to the body disc before consumption by arm muscles, which is why I hypothesize continuous bursal ventilation is necessary to fulfill basic metabolic needs, especially concerning processes that occur within the disc. This has yet to be tested empirically but is of interest for future study.

These experiments have demonstrated a very strong link between bursal ventilation and respiration and suggest that bursal ventilation is indeed a means of respiration. However, respiration by oxygen up-take through the bursae may only supply a fraction of what is needed for basket stars to survive. These experiments also demonstrated the basket stars' ability to increase the rate of bursal ventilation in response to certain stimuli such as increased food availability or a decrease in available oxygen, suggesting this species is an oxyregulator. Their ability to increase bursal ventilation rate in response to hypoxic conditions suggests that basket stars may be able to offset the

effects of hypoxic conditions on a short-term basis, however mortality will incur if the exposure intensity, duration or spatial scale are too great. More studies such as this one are needed to add to our understanding of the major physiological responses of marine animals to hypoxia as more and more organisms will begin to encounter chronic or periodic hypoxic environments in the future.

Table Legends

Table 1. Measurements and estimates from experimental animals used in the feeding experiment: disc diameter, disc volumes (fully expanded and compressed), bursal ventilation rates, and the volumes of fluid moved through the bursae per hour.

Table 2. The oxygen concentrations taken from the ambient aquarium water, the bursae, and from a tube control, for 3 specimens.

Tables

Table 1.

Specimen	1	2	3	4	5	6	7	8	9
Disc Diameter (mm)	8.8	9	11.9	26.4	34	41	48	48	64
Volume Full (mL)	0.22	0.29	0.54	5	12	23.4	31	31.2	83.6
Volume Compressed (mL)	0.13	0.15	0.32	3.1	6.2	10.7	18	11.6	42.9
Volume / Disc pump (mL)	0.09	0.14	0.22	1.93	5.79	12.72	12.97	19.6	40.67
Disc pumps / hour, Feeding	28	53	39	24	36	24	38	26	13
Disc pumps / hour, Non-feeding	11	40	30	13	16	15	26	23	10
Difference	17	13	9	11	20	9	12	3	3
mLs moved / hour, Feeding	2.52	7.42	8.58	46.32	208.44	305.28	492.86	509.60	528.71
mLs moved / hour, Non-feeding	0.99	5.6	6.6	25.09	92.7	190.8	337.3	450.7	406.7
Difference	1.53	1.82	1.98	21.23	115.74	114.48	155.56	58.90	122.01
% increase from NF to F (% mLs/h)	155	33	30	85	125	60	46	13	30

Table 2.

Treatment	Ambient	From bursae	Tube control
Animal #	DO (mg L^{-1})	DO (mg L^{-1})	DO (mg L^{-1})
1	9.04	7.76	9.07
2	8.99	7.18	9.06
3	8.5	7.38	8.62

Figure Legends

Figure 1. Drawings of sections through the body of *Gorgonocephalus eucnemis,* modified from Fedotov (1924 figures 6 and 11). A. A section though the body disc perpendicular to the oral-aboral axis and aboral to the arm frame. B. A section through the body disc parallel to the oral-aboral axis and bisecting a radius.

Figure 2. Illustration of one bursal ventilation cycle viewed from the side of an animal (aboral is up and oral is down in the image.

Figure 3. Overlay of the closest matching shapes used to calculate change in disc volume.

Figure 4. An example of the changes in dissolved oxygen (DO) during one trial of the experiment with water that was normoxic, hypoxic and post-hypoxic. DO plot was shown by a graph in the YSI Pro Series Data Manager [1.1.8] interface.

Figure 5. A. Box plot comparing bursal ventilation rates during nonfeeding (grey) and feeding (black) trials. (n= 9). Box - 50th percentile of the data set, derived using the lower and upper quartile values. Error bars - 95% confidence intervals, x - mean, horizontal lines - median. B. Bar graph comparing rates of bursal ventilation for individual specimens during nonfeeding (grey) and feeding (black). Corresponding disc sizes are listed below the x-axis.

Figure 6. Bar graph comparing the estimated volumes of fluid moved through the bursae during non-feeding (grey) and feeding (black) trials. To reveal differences in volume, the data are shown as two plots with different y-axes for smaller and larger individuals. Corresponding disc sizes are listed below the x-axis.

Figure 7. Box plots comparing the rate of bursal ventilation for A, normoxic (black) vs. hypoxic (dark grey); B. hypoxic (dark grey) vs. post-hypoxic (light grey); and C, normoxic (black) vs. post-hypoxic (light grey) conditions. Box - Box - 50th percentile of the data set, derived using the lower and upper quartile values. Error bars – 95% confidence interval, x – mean, horizontal line – median, circles – outliers. Note the different scale for the y-axis in C.

Figure 8. The trends in bursal ventilation rate for each of 11 specimens and average changes in pH across treatments. Left y-axis-bursal ventilation rate. Right y-axis – average change in pH, bars – 1 s.e.

Figure 9. Bar graph comparing the mean dissolved oxygen concentrations (DO) of water samples taken from inside the bursae and test aquarium. Ambient DO (black), DO inside the bursae (grey), and 'tube control' (diagonal stripes). Lines - 1 s.e.

Figure 10. Ventilations rates through time for two specimens in the feeding study (A) and two specimens in the hypoxia study (B). A. Black bracket denotes time period where specimens were actively feeding. Specimen #1 (black) and specimen #5 (grey), oxygen concentration (dashed black line). B. Grey dashed line)- the start of nitrogen gas flow, (Grey dotted line) – nitrogen gas off, surface covered with plastic, (Black dotted line) – air pumps turned on, (Black dashed line)- O_2 levels match beginning normoxic conditions Specimen #1(black) is different from the individual in A, and specimen #2 (grey).

Figure 1.

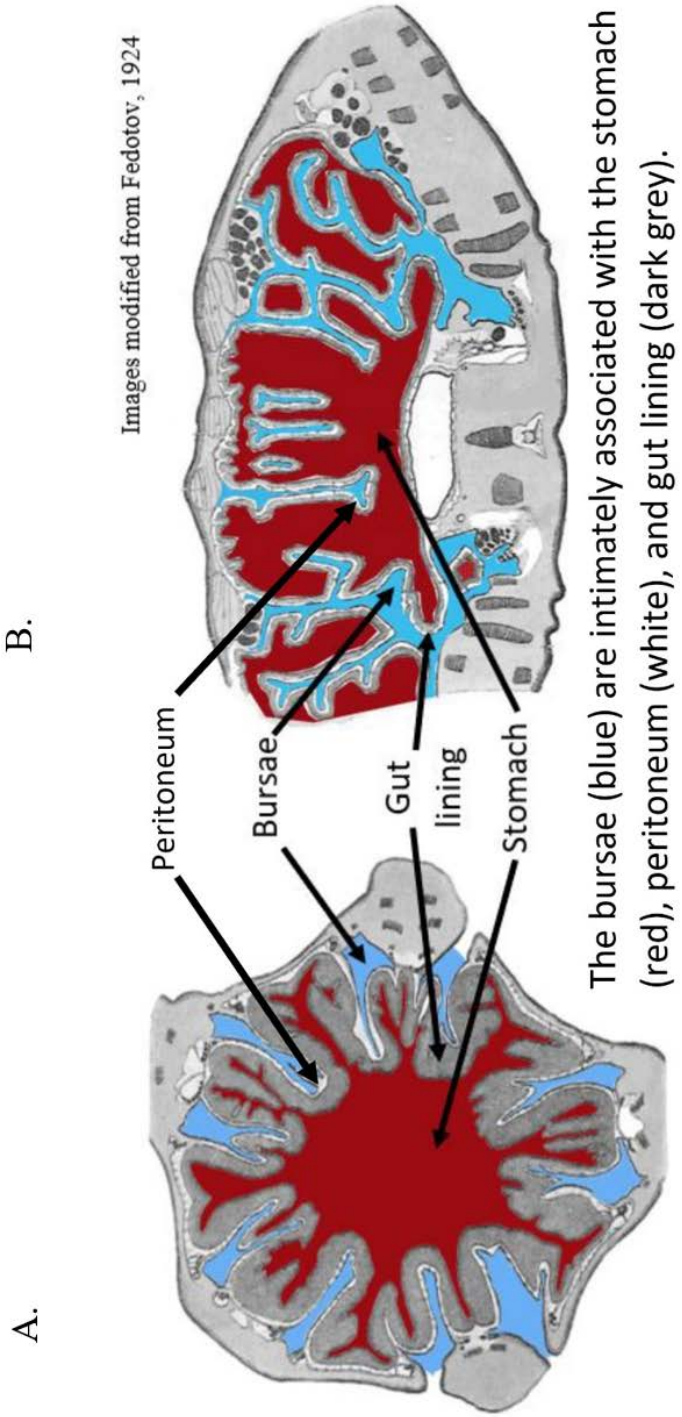
A.
B.
Images modified from Fedotov, 1924
Peritoneum
Bursae
Gut lining
Stomach
The bursae (blue) are intimately associated with the stomach (red), peritoneum (white), and gut lining (dark grey).

Figure 2.

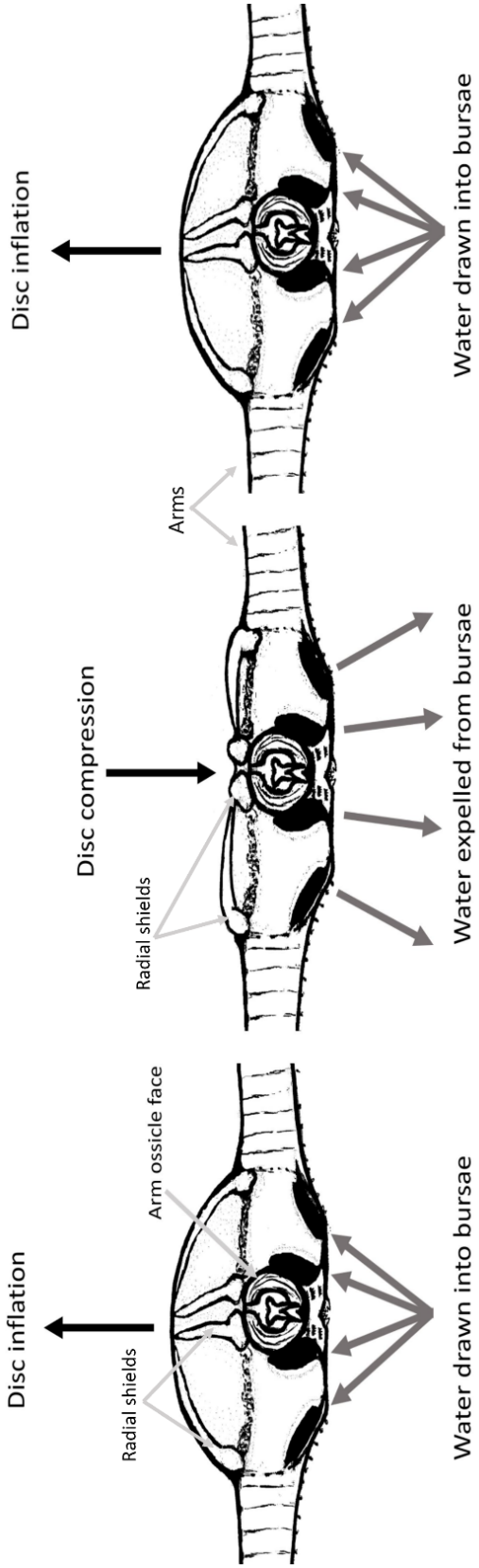
Disc inflation
Water drawn into bursae
Arms
Disc compression
Radial shields
Water expelled from bursae
Arm ossicle face
Disc inflation
Radial shields
Water drawn into bursae

Figure 3.

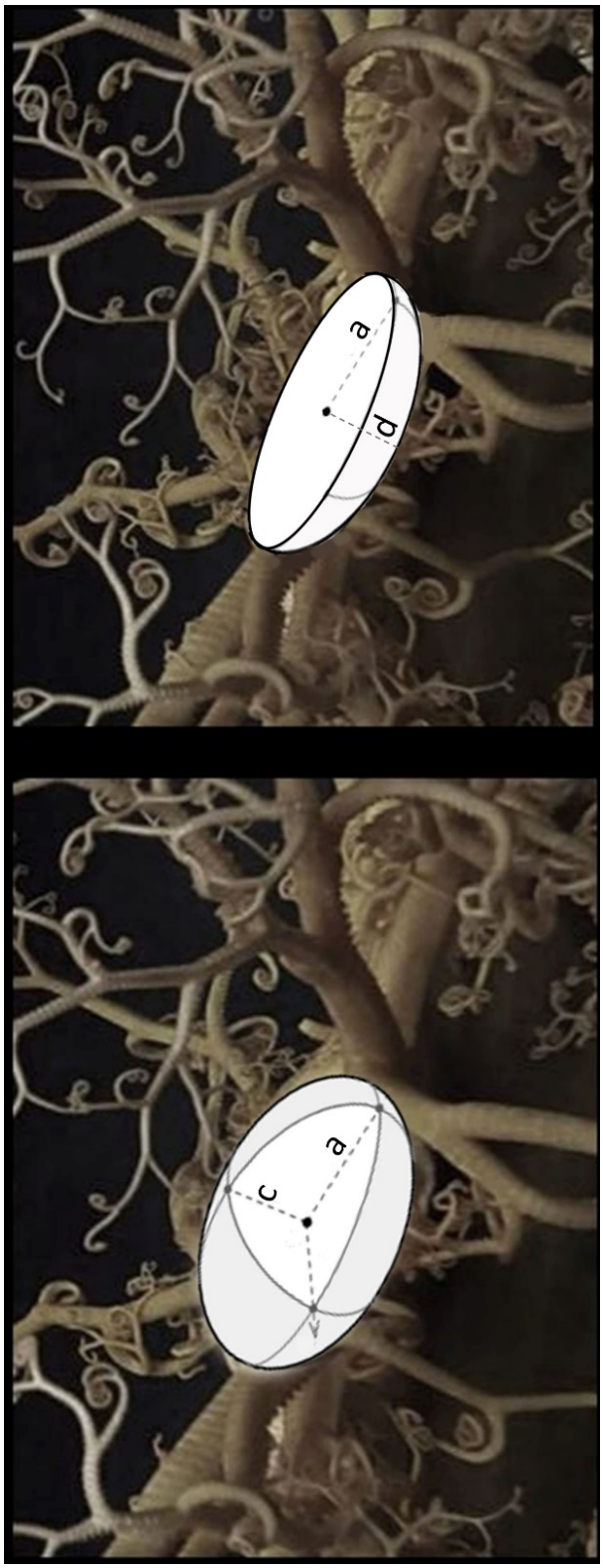

Figure 4

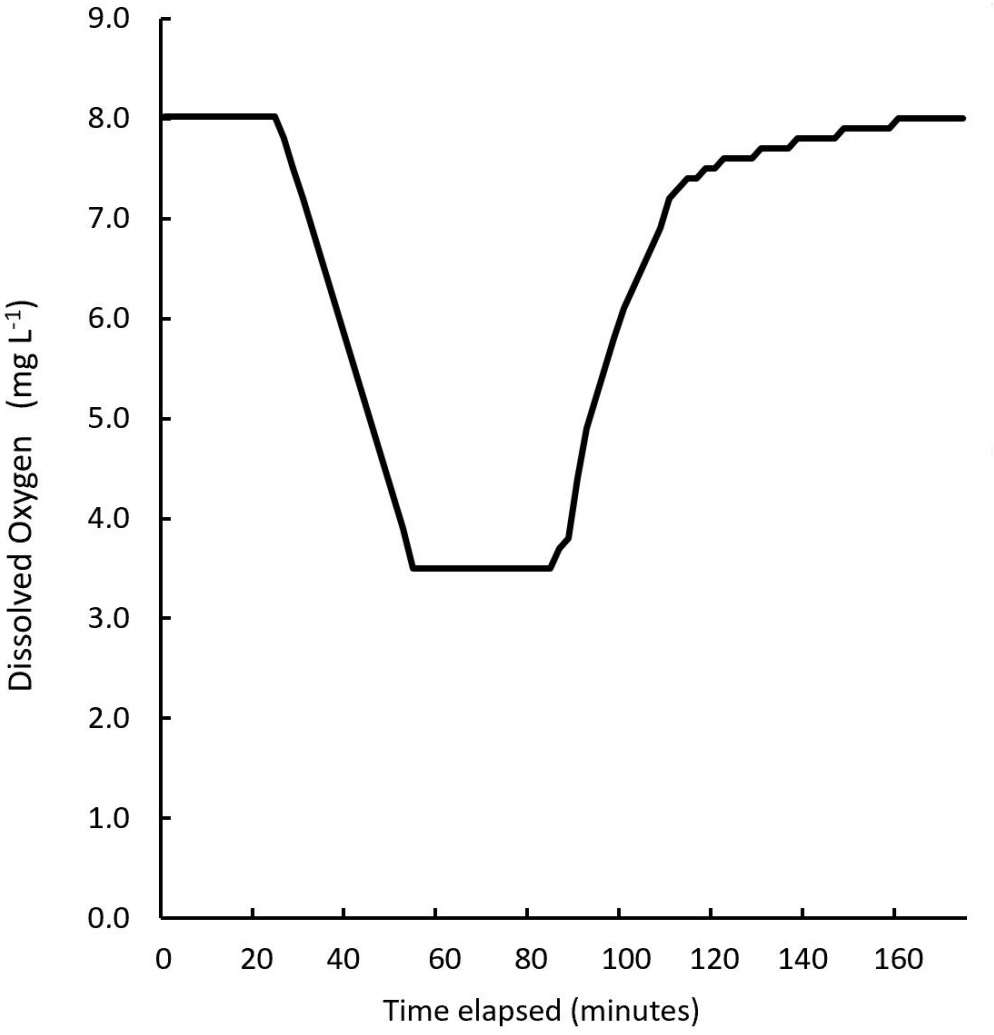
9.0
8.0
7.0
6.0
5.0
4.0
3.0
2.0
1.0
0.0
Dissolved Oxygen (mg L-1)
0
20
40
60
80
100
120
140
160
Time elapsed (minutes)

Figure 5.

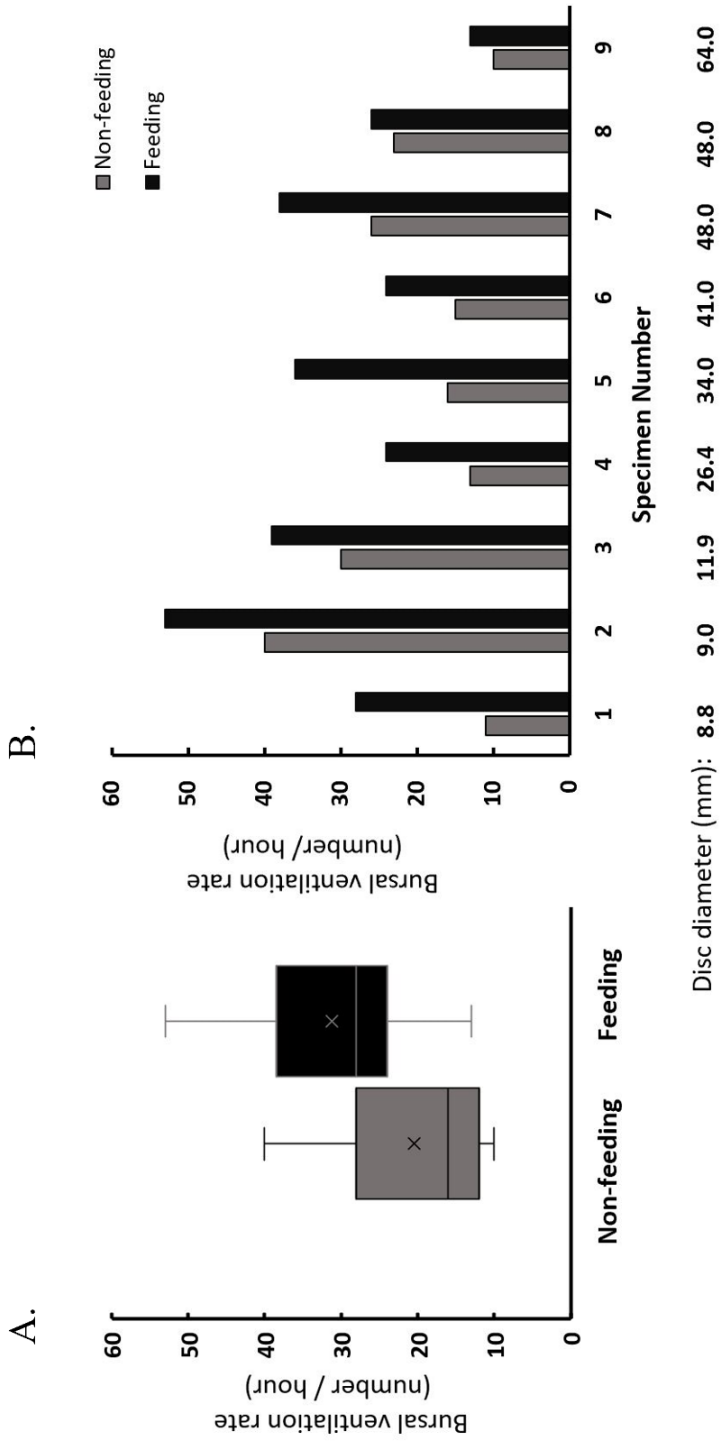
A.
Bursal ventilation rate
(number / hour)
0
10
20
30
40
50
60
Non-feeding
Feeding
B.
Bursal ventilation rate
(number/ hour)
0
10
20
30
40
50
60
Non-feeding
Feeding
1
2
3
4
5
6
7
8
9
Specimen Number
Disc diameter (mm):
8.8
9.0
11.9
26.4
34.0
41.0
48.0
48.0
64.0

Figure 6

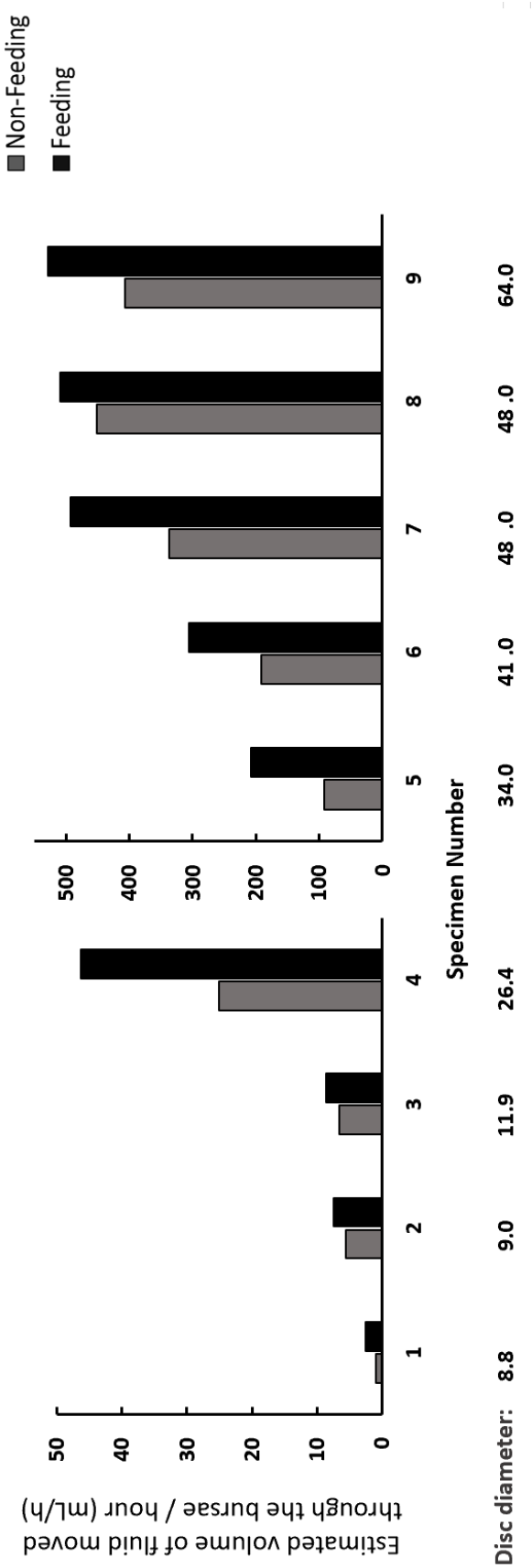
Non-Feeding
Feeding
Estimated volume of fluid moved through the bursae / hour (mL/h)
0
10
20
30
40
50
0
100
200
300
400
500
Specimen Number
1
2
3
4
5
6
7
8
9
Disc diameter:
8.8
9.0
11.9
26.4
34.0
41 .0
48 .0
48 .0
64.0

Figure 7.

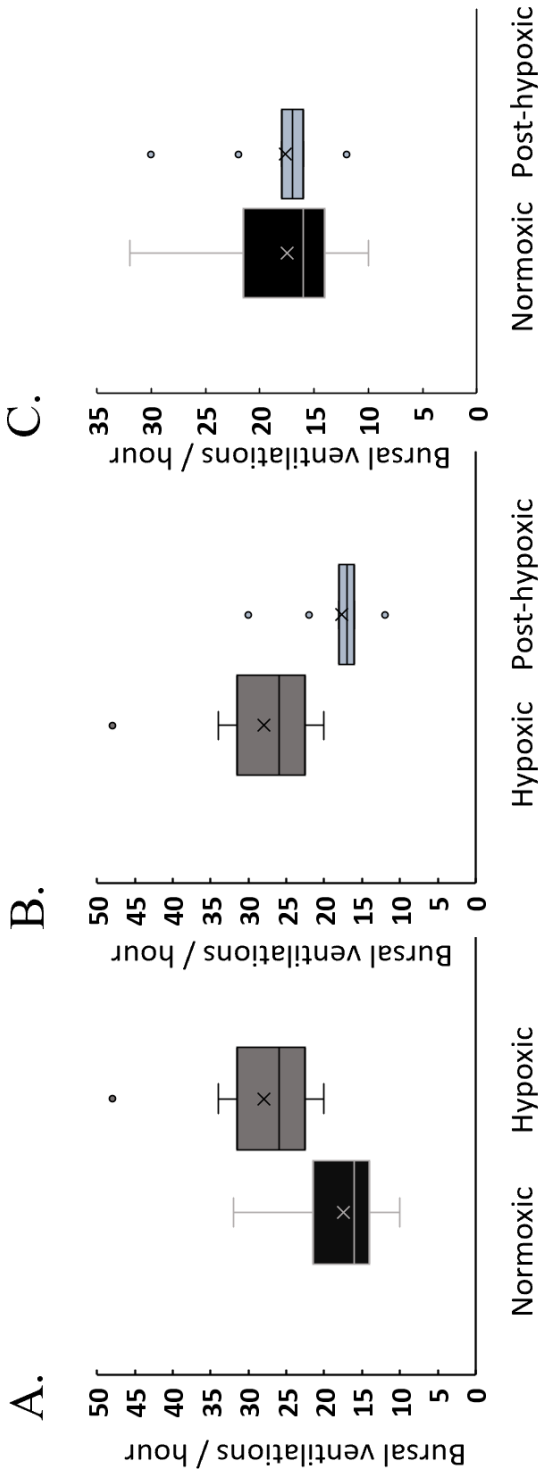
A.
B.
C.
Bursal ventilations / hour
0
5
10
15
20
25
30
35
40
45
50
Normoxic
Hypoxic
Post-hypoxic

Figure 8.

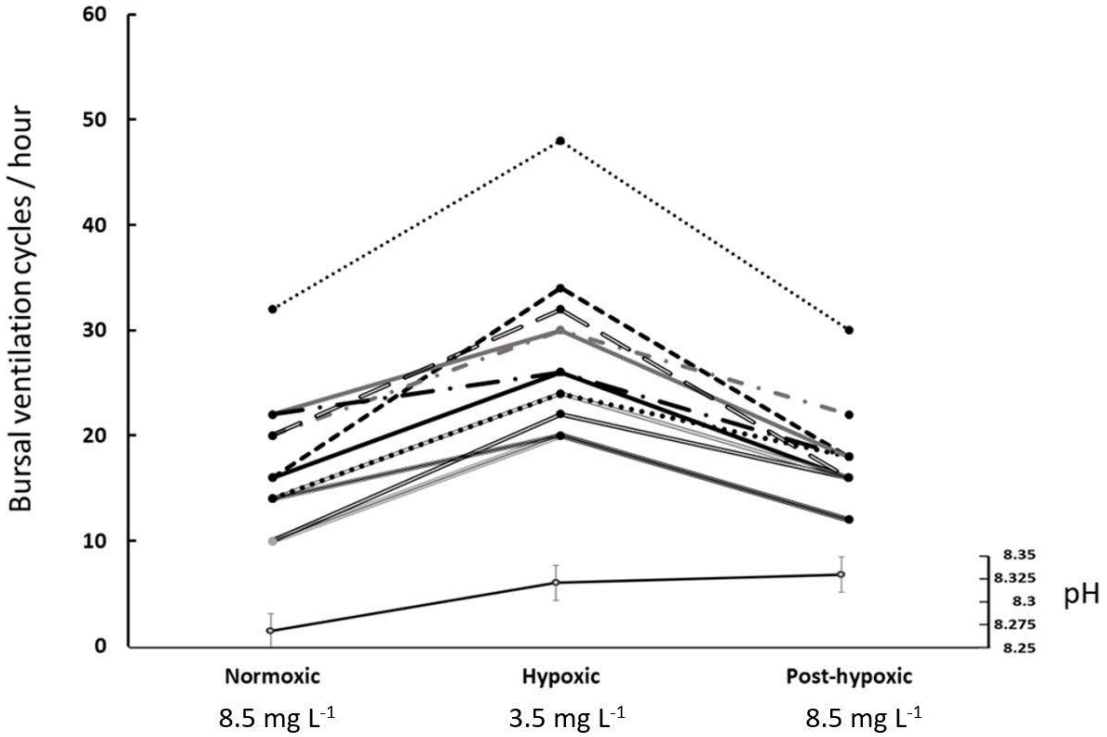
Bursal ventilation cycles / hour
60
50
40
30
20
10
0
8.35
8.325
8.3
8.275
8.25
pH
Normoxic
Hypoxic
Post-hypoxic
8.5 mg L-1
3.5 mg L-1
8.5 mg L-1

Figure 9.

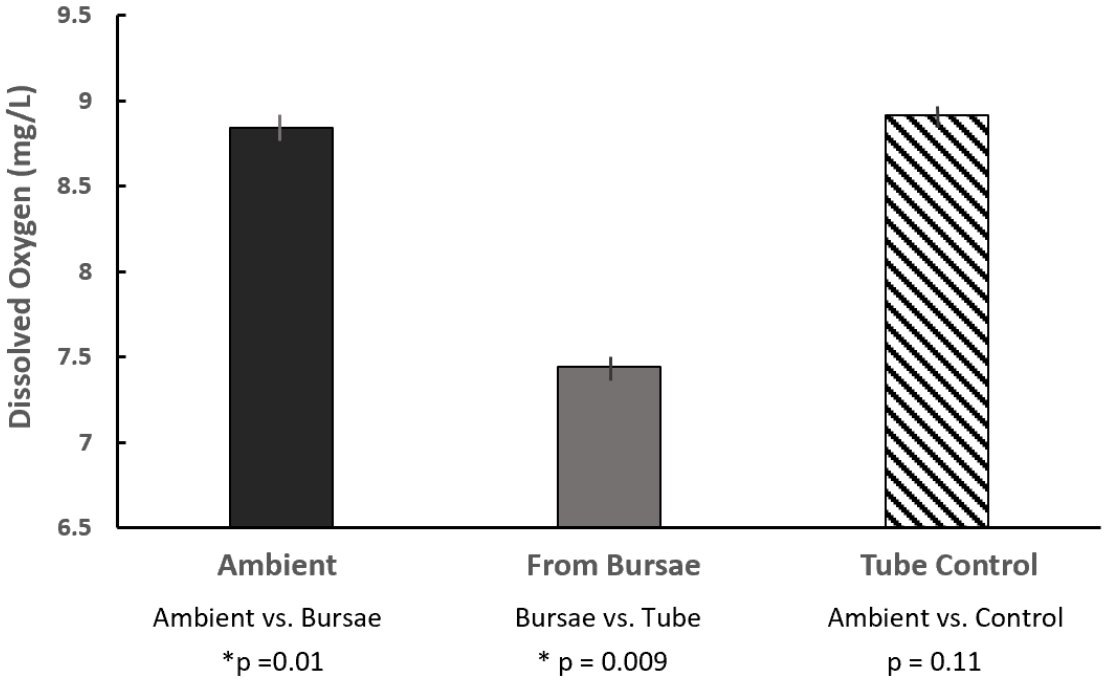
Dissolved Oxygen (mg/L)
9.5
9
8.5
8
7.5
7
6.5
Ambient
From Bursae
Tube Control
Ambient vs. Bursae
*p =0.01
Bursae vs. Tube
* p = 0.009
Ambient vs. Control
p = 0.11

Figure 10.

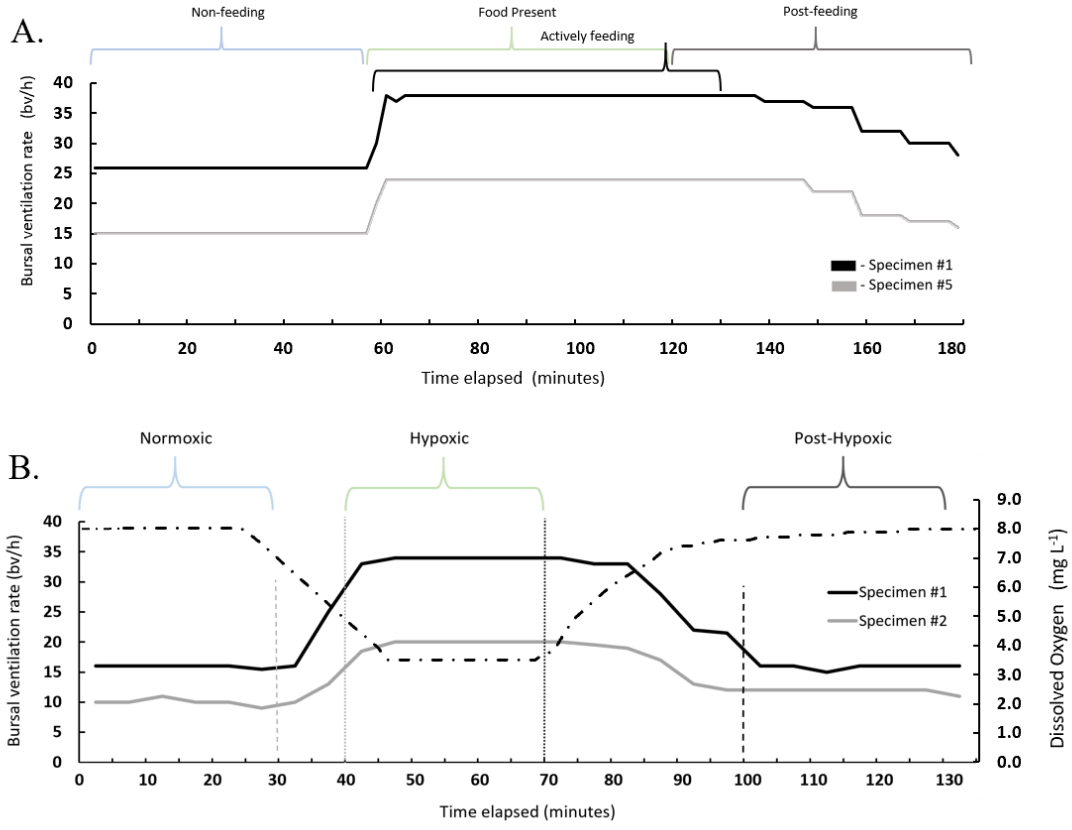
A.
Non-feeding
Food Present
Actively feeding
Post-feeding
Bursal ventilation rate (bv/h)
Time elapsed (minutes)
- Specimen #1
- Specimen #5
B.
Normoxic
Hypoxic
Post-Hypoxic
Bursal ventilation rate (bv/h)
Dissolved Oxygen (mg L-1)
Time elapsed (minutes)
Specimen #1
Specimen #2

BRIGDE II

Chapter III concerns the behavior of bursal ventilation observed in two ophiothricids from two different climate zones: *Ophiothrix suensonii* from the tropics and *Ophiothrix spiculata* from a temperate region. *Ophiothrix suensonii* has a range that includes areas of the Caribbean Sea that are subject to periods of hypoxia in shallow reef ecosystems. *Ophiothrix spiculata* is found along the coast of California and Mexico, and is subject to upwelling-induced hypoxia within the California Current system. Both species are abundant and contribute substantial biomass to their respective ecosystems, yet they remain overlooked when considering energy flow through the ecosystems. Both geographic locations have observed an increase in the frequency and magnitude of hypoxic events, often resulting in ecosystem dead zones. In chapter III, I examine the behavior of these two species of ophiuroids when exposed to hypoxic conditions. I pay particular attention to the rate of bursal ventilation, and analyze the increase in bursal ventilation rate when moving the specimens from normoxic to hypoxic conditions, then back to normoxic conditions. I consider whether these two species are oxyregulators that use bursal ventilation as a means of respiration and whether this behavior may help them survive hypoxia events.

CHAPTER III

TITLE:

Ophiothrix suensonii, Ophiothrix spiculata, and bursal ventilation

AUTHORS:

MacKenna A. H. Hainey

INTRODUCTION

Echinoderms are aerobic organisms and are highly dependent on the dissolved oxygen in ambient seawater. All echinoderms have specialized respiratory structures to help them acquire oxygen from their surroundings. Asteroids have papullae or dermal branchiae, holothuroids have papillae and internal respiratory trees, and most ophiuroids have bursae (genital bursae, respiratory bursae). All classes of echinoderms take up oxygen across their podial (tube-foot) membranes, including the echinoids and crinoids (Binyon, 1972; Farmanfarmaian, 1966; Lawrence, 1987). Ophiuroids constitute the largest class of echinoderms (Stöhr et al., 2018), and are found in every ocean basin of the world. Five pairs of bursae reside in the body disc on either side of each arm base as hollow chambers opening to the outside environment via bursal slits, located where the arms join the disc on the oral side. The bursae are thought to be a feature that evolved to meet the oxygen demands of species that lived in sediment burrows (Spencer and Wright, 1966). Many species also use bursae for brooding their young (Spencer and Wright, 1966). The lining of the bursae has qualities such as a thin, (usually) ciliated and highly folded epithelial lining which increases surface area to volume ratio. Bursae have two mechanical means of seawater flushing, making them ideal structures for respiratory purposes (Spicer, 2016). By the first method the ciliated epithelium of each bursa generates a current that circulates water through the bursa, while open (Austin, 1966; Hyman, 1955; MacBride, 1906). The second means of bursal ventilation is muscular pumping of the disc.

Some species of ophiuroid have been observed exhibiting a disc pumping behavior (MacBride, 1906; Hainey, pers. obsv.). This behavior is the result of the raising and lowering of the radial shields (Hainey, Chapter 2). In species such as *O. suensonii* and *O. spiculata*, bursal ventilation by disc pumping is constant. Upon elevation of the disc roof, seawater is drawn into the bursal slits, bathing the bursae in fresh seawater. When the disc roof is lowered, the water in the bursae is forced out through the bursal slits (MacBride, 1906; Hainey, pers. obsv.). Bursal ventilation by disc pumping draws in

a greater volume of water than the passive ciliary currents, which suggests this bursal ventilation behavior may be important in the acquisition of oxygen under certain biological demands or ecosystem changes. After observing this active disc pumping behavior, MacBride (1906) was the first to suggest this behavior might play a role when oxygen is "getting scanty."

Though the majority of epibenthic marine fauna are not regularly exposed to hypoxic conditions, in the past two decades scientists have observed an increase in the number of hypoxic events world-wide, especially along the west coasts of continents in up-welling zones (Altieri et al., 2017; Bakun et al., 2010; Levin et al., 2009). These events are also increasing in magnitude (reaching up into shallower depths), and intensity (moderate to extreme hypoxia, bordering on anoxia) (Chan et al., 2008; Erhardt et al., 2014). Upwelling zones along the west coasts of continents have naturally occurring seasonal hypoxia if the oxygen concentration of the upwelled water is low, but the extent of the upwelled hypoxic water usually stays within the oxygen minimum zone (below ~300 m depth for N. America). In the past decade researchers have observed hypoxic water reaching depths as shallow as approximately 100 m - 70 m (Chan et al., 2008; Erhardt et al., 2014), exposing many species to anomalous conditions to which they are not adapted physiologically, often resulting in mass mortality (Chan et al., 2008). Hypoxia can occur by other means. In Panama, nutrient enrichment, or eutrophication, associated with human activities is resulting in hypoxia events at increased frequencies (Altieri et al., 2017; Johnson et al., 2018).

In the present study, I demonstrate that bursal ventilation behavior serves as a means of respiration by exploring whether environmental hypoxia induces an increased rate in bursal ventilation. I used two species of brittle star within the genus *Ophiothrix,* that may experience natural, mild hypoxia in situ, but are both in geographic locations where hypoxia has been reported to be increasing in frequency, magnitude and intensity for different reasons (i.e. upwelling or eutrophication).

METHODS AND MATERIALS

Ophiothrix suensonii

Collection of Specimens

Ten *Ophiothrix suensonii* specimens were collected by hand at depths of 2-5 m from shallow reefs near the Bocas Research Station (BRS)of the Smithsonian Tropical Research Institute (STRI), Bocas del Toro, Panama. Specimens were transported in a bucket of seawater to the laboratories at BRS, transferred into a sea table and supplied with continuous flowing seawater and aeration. Water temperature averaged 26°C.

Bursal Ventilation and Hypoxia

Individual brittle stars with disc sizes ranged from 8.1 - 14.9 mm were placed into a modified 2-liter aquarium. The plastic aquarium (23.1cm L x 15.2 cm W x 16.8 cm H) was fitted with false-floor constructed from bamboo dowels and black tulle fabric (1 mm diameter mesh size). A vertical tank partition was also constructed from bamboo dowels and black tulle. As a filling port, a 2 cm diameter opening was made in the floor of the plastic aquarium and fitted with a PVC elbow joint, sealed with 100% silicone (Fig. 1). The portion of the elbow joint inside of the aquarium was attached to a 15mL Falcon tube 'diffuser' which had ~60 1mm perforations. The portion of the elbow joint on the outside of the aquarium was attached to 2 meters of 5/8" tubing. The entire aquarium unit was placed over a portable stir-bar pad, and a magnetic stir bar was placed in the aquarium below the false floor. An air stone was placed on one side of the aquarium behind the tank partition. As an outflow port, a 2 cm diameter opening was made at the top of the aquarium side-wall and another 2-meter-long length of 5/8" diameter tubing was attached with 100% silicone (Fig. 1). Before the start of each trial, 2 buckets were filled with 5 liters of fresh seawater from the sea tables. One bucket remained outside while the other was brought into the lab to cool to ~24°C (room temperature). This cooler seawater was poured into a 2-liter filtering flask, which was attached by rubber tubing to a vacuum pump (Air-Cadet model no. 7530-40). The flask was sealed with a rubber stopper and the vacuum was run for approximately 30 minutes to pull dissolved oxygen from the seawater, until hypoxic levels were reached (~3.2 O_2 mg l^{-1}).

At the start of each trial, the aquarium was filled with two liters seawater at ambient outside temperature (26° C). An individual brittle star was placed into the aquarium and allowed to acclimate for 30 minutes prior to the start of the experiment. The stir bar was spinning below the false floor and aeration via airstone behind the

partition was supplied during this acclimation period. After the acclimation period, the brittle star was recorded for 30 minutes, in normoxic conditions (~6.4 O_2 mg l^{-1}). At the end of this time the stir bar and the aeration were turned off. The normoxic water was displaced by feeding the cooler, hypoxic water (re-checked for dissolved oxygen concentration ~3.2 O_2 mg l^{-1} and temperature ~24°C) into the aquarium through the bottom port connected to a flask elevated above the aquarium. The upper tubing carried the warmer, normoxic water out of the tank..Video recording of this transition from normoxic to hypoxic water was continuous, however the 'hypoxic 30-minutes' began once the entire volume of normoxic water was replaced with hypoxic water, and the surface of the water was covered with a thin sheet of plastic (to limit surface-oxygen exchange). After the 30-minute hypoxic period, the plastic was removed, and the aeration and the stir bar were turned on, bringing the dissolved oxygen concentration back up to normoxic levels (~6.4 O_2 mg l^{-1}), taking an average of 30 – 40 minutes. Once normoxic levels were achieved the last 'post-hypoxic' 30-minute period began. Aquarium water was changed between each specimen. This procedure was repeated for a total of 8 specimens (n=8). All recordings were done with a GoPro camera (Hero 3 Silver Edition®) at a time-lapse frame rate of 1 frame/ 2secconds

Dissolved oxygen and temperature were continuously recorded over the entire trial using a YSI ODO probe and software (YSI Pro Series Data Manager 1.1.8 ©, Fig. 2). Videos were played at 8x – 10x real time speed and the number of disc pumps were counted during the entire length of each 30-minute interval (normoxic, ~6.4 O_2 mg L^{-1}, hypoxic, 3.2 O_2 mg L^{-1}, and post-hypoxic, 6.0-6.4 O_2 mg L^{-1}), then doubled to achieve 'bursal ventilation rate' (number of disc-pumps/hour).

Statistical Analyses Used for *O. suensonii* Hypoxia Experiment

To test the assumption that the variances of the differences between all possible pairs of within-subject conditions are equal, a Mauchly's test for sphericity was run. A repeated measures ANOVA (ANOVAR) and paired t-tests were carried out. Because alpha error climbs with each t-test, a Bonferroni correction ($\alpha = 0.05/3$) was applied to the critical alpha to compensate for this effect. Rates of bursal ventilation for each animal

were plotted to illustrate a common trend observed among the animals used in this experiment All statistics were calculated using R v. 3.3.2 (R Core Team 2016).

Accounting for Temperature

To determine if the slight drop in water temperature (26° to 24°C) affected the rate of bursal ventilation when transitioning from the ambient normoxic water to the cooler hypoxic water, three trials were run by manipulating only temperature. Oxygen levels were normoxic (~6.4 O_2 mg L^{-1}) throughout the temperature transition. Three *O. suensonii* specimens were used in this exercise. For the first 30 minutes, the temperature was 26° C, then cooler (24° C) water was introduced from the bottom of the aquarium in the same manner mentioned above for the hypoxic water. Animals were recorded for 30 more minutes for the 24° C water exposure. Video recording with a GoPro (Hero 3 Silver Edition®) and bursal ventilation rate calculations were conducted as described above. A paired t-test was run on the data using R v. 3.3.2 (R Core Team 2016).

Ophiothrix spiculata

Twenty specimens were purchased from Marinus Scientific, LLC, whose divers collected the specimens off Long Beach, California in January, 2017. After receiving specimens at OIMB in Oregon, they were brought up to room temperature (~ 16° C) with aeration supplied by air stone and pump. Once they appeared to have recovered from shipping (approx. 2 hours), they were placed into an isolated 5-gallon aquarium with a built-in filtration system and water pump. This aquarium was maintained at 15- 17° C.

Bursal Ventilation and Hypoxia

Individual brittle stars (n = 8), with body disc sizes ranging from 4-6 mm, were placed into a custom-built cage with an attachment for a GoPro camera (Fig. 3). This custom cage was constructed from half of a clear, plastic container, white plastic mesh (pore diameter 2mm), 25-lb test fishing line and hot glue. The arm that connected the GoPro to the cage was constructed from section of plastic and bamboo dowels. The cage was connected to the plastic arm by a wing-nut (glued to the bottom of the cage by the wings) and a plastic screw, inserted backward through the wing-nut and glued to the arm surface (this allowed the cage to swivel in place in one focal plane). The GoPro camera

(in a waterproof housing) was attached to a flat piece of slate which anchored the entire unit. Once a brittle star was placed into the cage, the entire unit (with camera and slate weight) was submerged in an insulated 15-gallon aquarium filled with filtered (5 μm) seawater, held at a constant temperature of 15° C (in situ temperature) by a temperature control unit (VWR Scientific model #1141). Constant aeration was supplied to the tank via air pump and airstone. Brittle stars were allowed to acclimate to the cage-tank environment for one hour before any data were recorded. Once acclimated, brittle stars were video recorded in time-lapse with a GoPro camera (HD Hero 3 Silver Edition®) at a frame-rate of 1 frame per 2 seconds.

Oxygen concentration levels were chosen based on Siebel's (2011) argument that hypoxic habitats should be defined by the biological response to hypoxic conditions and not by an arbitrary oxygen concentration (the same rationale was applied to *O. suensonii* experiments). In other research, hypoxia has been defined as oxygen concentrations $\leq$ 2.0 O_2 mg L^{-1} (Levin et al. 2009 and Dashtgard et al. 2015), however, I chose to use a higher oxygen tension; for this experiment "hypoxic conditions or hypoxia" was defined as a concentration of oxygen $\leq$ 3.4 O_2 mg L^{-1}. This concentration of oxygen was approximately 50% that of local ambient conditions (range: 7.8-8.0 O_2 mg L^{-1}; average 8.0 O_2 mg L^{-1}) and had obvious effects on animal behavior. Aquarium water was changed between each specimen.

Rate of bursal ventilation was measured during three, half-hour intervals at DO levels considered to be normoxic (8.0 O_2 mg L^{-1}), hypoxic (3.4 O_2 mg L^{-1}) and post-hypoxic (7.8 - 8.0 O_2 mg L^{-1}). One specimen was in the chamber during each trial, starting in normoxic conditions; after 30 minutes, medical grade nitrogen gas was bubbled into the water until a dissolved oxygen concentration of 3.5 mg L^{-1} was reached. At this point, the nitrogen gas was turned off and the surface of the water was covered with plastic to limit surface oxygen exchange. Conditions remained at this hypoxic level for another 30-minute interval. After 30 minutes of exposure to hypoxia, the plastic surface cover was removed and ambient air was bubbled into the water until 'normoxic' conditions were reached. Once a 'post-hypoxic' dissolved oxygen concentration of 7.9-8.0 mg L^{-1} was reached the third and final 30-minute interval was recorded. Dissolved

oxygen and temperature were continuously recorded over the entire trial using a YSI ODO probe and software (YSI Pro Series Data Manager 1.1.8, Fig. 4). Video recording was continuous through each oxygen concentration. Time-lapse videos were later analyzed; each video (2,700 frames per video = 1 trial run), was played at 8x – 10x real time speed and the number of disc pumps was counted for each 30-minute interval (normoxic, hypoxic, post-hypoxic), then doubled to achieve 'bursal ventilation rate' (number of disc-pumps/hour). pH measurements were taken at the 15 minute mark of each 30 minute exposure period with a benchtop pH meter (Fisherbrand™ Accumet™ AE150 pH Benchtop Meter), during each trial.

Statistical Analyses Used for Hypoxia Experiment

To test the assumption that the variances of the differences between all possible pairs of within-subject conditions are equal, a Mauchly's Sphericity test was run. A repeated measures ANOVA (ANOVAR) and paired t-tests were carried out. Because alpha error climbs with each t-test, a Bonferroni correction ($\alpha = 0.05/3$) was applied to the critical alpha to compensate for this effect. Rates of bursal ventilation for each animal were plotted to illustrate a common trend observed among the animals used in this experiment All statistics were calculated using R v. 3.3.2 (R Core Team 2016).

RESULTS

Ophiothrix suensonii - Observations Associated with Exposure to Hypoxia

During the hypoxia experiment *Ophiothrix suensonii* specimens were relatively stationary in normoxic conditions then, rapidly moved around the aquarium once hypoxic water displaced the normoxic water. Movement was continuous throughout the 30-minute hypoxic exposure time, however, toward the end of the 30 minutes (~last 10 minutes) brittle stars started showing signs of uncoordinated movement such as repeatedly moving up one of the aquarium walls, then falling off and landing oral-side-up on the false floor. The amount of time a brittle star took to right itself also appeared to increase as the 30-minute hypoxia duration went on. Brittle star coordination appeared normal during normoxic and recovered during the post-hypoxic periods, although very little movement was observed during these periods.

Ophiothrix suensonii - Bursal Ventilation Response to Hypoxia and Temperature

Bursal ventilation rate in *O. suensonii*, measured in number of bursal ventilations (i.e. disc pumps) per hour, (bv/h) increased significantly when brittle stars were exposed to hypoxic conditions (Fig. 5). Rates of bursal ventilation returned to near-original levels when dissolved oxygen levels returned to a normoxic concentration (normoxic = 308.5 ± 10.9bv/h (mean +/- 1 s.e.), hypoxic = 415.75 ± 20.5 bv/h, post-hypoxic = 329.25 ± 11.7 bv/h; $p<0.05$, $F = 44.09$, $df = 7$).

Bursal ventilation rates were significantly different between normoxic and hypoxic conditions ($t = 6.8$ $df = 7$, $p< 0.001$, $\alpha =0.017$ (Fig. 5A), and between hypoxic and post-hypoxic conditions ($t= 7.9$, $df = 7$, $p< 0.001$, $\alpha =0.017$) (Fig. 5B), however, there was no statistical difference between normoxic and post-hypoxic conditions ($t = -2.5$, $df = 7$, $p= 0.05$, $\alpha =0.017$) (Fig. 5C). Rates of bursal ventilation for each animal were plotted to illustrate a common trend observed among the animals used in this experiment (Fig.6).

The rate of bursal ventilation was not significantly different between the ambient 26° C seawater and the 24° C seawater ($t = -3.79$, $df = 2$, $p = 0.063$, $\alpha = 0.05$). 26° C seawater (282.7 ± 20.5 bv/h (mean +/- 1 s.e.), 24° C seawater (293 ± 22.5 bv/h). However, there were no noted differences in behavior between the two temperatures. All brittle stars slowly moved around the chamber, making occasional stops.

Ophiothrix spiculata -Observations Associated with Exposure to Hypoxia

Ophiothrix spiculata specimens were observed moving around the cage during normoxic and hypoxic periods. During normoxic conditions, the movement of *O. spiculata* appeared to be exploratory in nature, covering the floor and walls of the cage. Once oxygen concentration levels reached ~ 4.0 O_2 mg L^{-1}, this movement increased dramatically and became less coordinated. At this point, ophiuroids were attempting to climb up towards the top of the cage. Once aeration was turned back on and the dissolved oxygen concentrations returned to normoxic levels the climbing movements slowed, and in some specimens stopped.

Ophiothrix spiculata- Bursal Ventilation Response to Hypoxia

Bursal ventilation rate of *O. spiculata*, measured in number of bursal ventilations (disc pumps) per hour, (bv/h) increased significantly when brittle stars were exposed to hypoxic conditions. Rates of bursal ventilation returned to near-normoxic levels when dissolved oxygen levels returned to a normoxic concentration (normoxic = 261 ± 22.1 bv/h (mean +/- 1 s.e.), hypoxic = 334 ± 31.6 bv/h, post-hypoxic = 275.8 ± 26.5 bv/h; $p<0.05$, $F = 44.09$, $df = 7$). Bursal ventilation rates were significantly different between normoxic and hypoxic conditions ($t = 6.17$, $df = 7$, $p< 0.001$, $\alpha =0.017$ (Fig. 7A), and between hypoxic and post-hypoxic conditions ($t = 6.99$, $df = 7$, $p< 0.001$, $\alpha =0.017$) (Fig. 7B) however, there was no statistical difference between normoxic and post-hypoxic conditions ($t = -2.51$, $df = 7$, $p= 0.04$, $\alpha =0.017$) (Fig. 7C), (Fig.8).

DISCUSSION

Rates of bursal ventilation were significantly higher for both *O. suensonii* and *O. spiculata* during exposure to hypoxic conditions when compared to bursal ventilation rates during exposure to normoxic and post-hypoxic conditions. When the nitrogen gas was pumped into the test aquarium while examining *O. spiculata*, it displaced the oxygen and other dissolved gasses such as carbon dioxide. This displacement of dissolved gasses caused the pH of the seawater to rise slightly (Avg. + 0.04) in each trial. Despite pH being on a log scale, this change is regarded as negligible (Waldbusser, G., personal communication). It is unknown if the change in pH had an effect on animal behavior, however it seems unlikely.

The hypoxia exposure resulted in a 35% increase in average bursal ventilation rate for *O. suensonii* and a 28% increase in average rate of bursal ventilation for *O. spiculata*. Both species also exhibited increased movement and decreased coordination of arms during exposure to hypoxic conditions; several *O. suensonii* specimens fell off aquarium walls as hypoxia duration lengthened. Increased movement may have increased rates of bursal ventilation as well. The increase in movement in both species, in response to the dropping oxygen concentration, particularly, movement in the upward direction, may be an escape or avoidance behavior. These avoidance behaviors are a common response found in marine animals that experience periodic hypoxic conditions (Burnett and

Stickle, 2001; Johnson et al., 2018). In ophiuroids, documented avoidance behaviors include migration out of crevices and movement upward in elevation, aggregating at the nearest, highest point in elevation in an effort to find oxygen refugia (Altieri et al., 2017; Johnson et al., 2018). Because increased locomotion would increase the aerobic demand of the animal, perhaps the greater increase in average bursal ventilation rate documented in *O. suensonii* was due to the increase in locomotion during hypoxic periods. Whereas the O. spiculata specimens were moving before the hypoxia exposures and showed a lower bursal ventilation rate increase. Some ophiuroids also display a behavior called 'arm-tipping,' where the animal supports its weight on its arm tips, raising the disc as high as possible in the water column (Altenbach et al., 2012; Stachowitsch et al., 2012).

Few echinoderms are known to actively ventilate their respiratory structures, with the exception of the holothuroids. The holothuroids utilize cyclical pumping of the cloaca to fill their internal respiratory trees with seawater, from which oxygen is extracted (Nichols, 1969). Asteroids in the genus *Pteraster* are also known to actively pump seawater past their respiratory surfaces (dermal branchiae), however, unlike other genera of asteroids, *Pteraster* have a specialized nidamental chamber which lies above the aboral body wall and below the supradorsal membrane (Johansen and Petersen, 1971). *Pteraster* also has well developed musculature within the body wall in addition to skeletal ossicles that can slide past one another. Water enters the nidamental chamber through small holes in the supra dorsal membrane called spiraculae. This allows *Pteraster* to fill and empty the chamber. Upon deflation, body wall muscles contract and the osculum opens, forcing the water out of the nidamental chamber; then the cycle repeats (Johansen and Petersen, 1971). While rate of respiratory tree ventilation under hypoxic conditions has not been investigated in holothuroids, *Pteraster* doubles its rate of nidamental chamber ventilation (from 2 to 4 ventilations/ minute) when transitioned from normoxic to hypoxic conditions (Johansen and Petersen, 1971).

Hypoxic events are increasing in frequency, duration, and intensity in both tropical and temperate climates (Bakun et al., 2010; Grantham et al., 2004; Johnson et al., 2018). In September, 2010 Altieri et al. (2017) documented mass reef-wide mortality within the vicinity of Bahiá Almirante, in the Bocas del Toro region of Panama, due to an

extreme hypoxia event. They noted widespread coral bleaching and death, and mortality of crustaceans, gastropods and echinoderms. Seven years later, in September 2017, another hypoxic event of the same magnitude occurred in the same region (Johnson et al., 2018). Johnson et al. (2018) observed many mobile invertebrate species, including ophiuroids aggregating at the highest possible points on the reef (often mounding corals) in an effort to escape the low-oxygen conditions, however survivorship was not recorded within these aggregations. Both the 2010 and the 2017 hypoxic events were within 16 km from where I collected my *O. suensonii* specimens.

During the past 2 decades, in the Temperate climate zone, the California Current has been experiencing up-welling driven hypoxia at greater magnitudes (i.e. reaching shallower depths), and intensities (Bakun et al., 2010; Grantham et al., 2004). Kelp forests and rocky reef ecosystems in this zone are of particular concern when trying to predict the larger, ecosystem-wide impacts of these hypoxic events (Low and Micheli, 2018). However, we cannot accurately predict ecosystem-wide impacts, until we understand how these environmental changes affect the physiology of the individual.

Ophiuroids are one group of marine animals, whose physiology, in relation to environmental change, remains relatively understudied, however, their populations make significant contributions to species abundance, diversity, and biomass within benthic communities worldwide (Hyman, 1955). In addition, these populations are often overlooked when considering energy flow through an ecosystem. In the tropics, Hendler et. al. (1995) reports ophiuroid densities can range from 20 to 40 individuals per square meter. However, while collecting the specimens used in this study I observed 50 + individuals occupying one large sponge colony (*Callyspongia vaginalis*), occupying less than 1 square meter, with multiple individuals occupying the same osculum (Fig. 9A). *Ophiothrix spiculata* has also been observed living in very high densities (Fig. 9B); particularly in Southern California where population densities as high as 80 individuals per 0.1 square meter have been observed (Lambert and Austin, 2007). With such high population densities, effects on the immediate environment, such as cumulative respiration and carbon cycling must be present.

Like bivalves and gastropods, ophiuroids sequester calcium carbonate and incorporate it into the structural components of their body. This is at the cellular level by capturing carbon molecules from the seawater, then converting this carbon into calcium carbonate by mineralization. This newly formed calcium carbonate is then secreted by specialized cells that build the ossicles. Gram for gram, ophiuroids should be able to sequester as much carbon from seawater as bivalves or gastropods, however this has not been directly compared. Historically, organisms such as foraminiferans, coccolithophores, corals, or bivalves such as oysters have been the main focus of carbon biomineralization studies, however recently, echinoderms have been considered as well (Ambrose et al., 2001; Lebrato et al., 2010; Minge et al., 1998). When evaluating the approximate global contribution of echinoderms to the marine carbon cycle Lebrato et al., (2010) concluded, on a global scale, echinoderms produce approximately 0.861 Pg (petagram = 1trillion kg) of calcium carbonate per year (almost 1 billion metric tons). In many different habitat types, such as rocky reefs, or silty-benthos, ophiuroid aggregations often dominate the area (Ambrose et al., 2001; Minge et al., 1998) and as the largest class of echinoderms, they certainly constitute a large fraction of calcium carbonate produced by echinoderms per year. Minge et al., (1998) measured the calcium carbonate production of a dense aggregation of *Ophiothrix fragilis* and found these ophiuroids produce approximately 0.7 kg $CaCO_3$ m^{-2} $year^{-1}$. Large aggregations such as these also contribute to the total respiration of an area. Ambrose et al. (2001) investigated the role echinoderms play in benthic remineralization (production of calcium carbonate) in the Chuckchi Sea as well as the approximate contribution to total faunal respiration. By examining the echinoderms that dominated the benthos in that area (4 ophiuroids, 1 echinoid) they concluded that these epibenthic dwellers are responsible for 25% of the total respiration that occurs in that area and that, these echinoderms (mostly ophiuroids) are very important contributors (based on biomass) in the remineralization process in the Arctic.

Considering overall ophiuroid importance and contribution to the process of carbon sequestering and remineralization in their respective habitats, anomalous ocean conditions such as wide-spread, intense hypoxic events could prove deadly for these large populations. This could ultimately impact the flow of energy and the flow of carbon

through certain ecosystems. However, in order to better predict what might happen to respective ecosystems if these large populations of ophiuroids were absent, we must understand how fluctuations in environmental conditions affect the physiology of the individual.

Hypoxic events along the North American West Coast in the California Current, have occurred regularly over the past few thousand years, exposing the local fauna to fluctuating oxygen concentrations (Erhardt et al., 2014). Reef systems within the Caribbean Sea have also probably experienced fluctuations in oxygen over geologic time. Currently researchers from the Smithsonian Tropical Research Institute (Panama) and Texas A&M are carrying out a project examining reef cores to determine the frequency of historical hypoxia in the Bocas del Toro region (O'Dea, 2018).

Perhaps increased bursal ventilation in response to hypoxic conditions has evolved in *O. suensonii* and *O. spiculata* as a mechanism to increase the amount of water processed for respiratory purposes. Due to their ability to increase their rates of respiration via bursal ventilation adult ophiothricids may be able to cope with and survive some hypoxic events as long as they have access to structures on which they can escape oxygen depleted stratified water layers, or the hypoxia is mild enough that compensatory bursal ventilation will make up for the lower oxygen concentration.

Figure Legends

Figure 1. Schematic of the experimental aquarium used in the hypoxia experiment for *Ophiothrix suensonii*

Figure 2. An example of the changes in dissolved oxygen (DO) during one trial of the experiment with *Ophiothrix suensonii* with water that was normoxic (n), hypoxic (h) and post-hypoxic (p). DO plot was shown by a graph in the YSI Pro Series Data Manager [1.1.8] interface.

Figure 3. Photograph of the custom-built brittle star cage attached to the GoPro camera, next to the YSI probe. All of these are submerged in the experiment aquarium.

Figure 4. An example of the changes in dissolved oxygen (DO) during one trial of the experiment with *Ophiothrix spiculata* with water that was normoxic (n), hypoxic (h) and post-hypoxic (p). DO plot was shown by a graph in the YSI Pro Series Data Manager [1.1.8] interface.

Figure 5. Rates of bursal ventilation for *Ophiothrix suensonii* in different levels of dissolved oxygen. Box plots comparing the rate of bursal ventilation for A, normoxic (diagonal stripes) vs. hypoxic (black); B. hypoxic (black) vs. post-hypoxic (grey); and C, normoxic (diagonal stripes) vs. post-hypoxic (grey) conditions. Box - Box - 50th percentile of the data set, derived using the lower and upper quartile values. Error bars – 95% confidence interval, x – mean, horizontal line – median, circles – outliers. Note the different scale for the y-axis in C.

Figure 6. The trends in bursal ventilation rate for each of 8 specimens of *Ophiothrix suensonii* across treatments.

Figure 7. Rates of bursal ventilation for *Ophiothrix spiculata* in different levels of dissolved oxygen. Box plots comparing the rate of bursal ventilation for A, normoxic (diagonal stripes) vs. hypoxic (black); B. hypoxic (black) vs. post-hypoxic (grey); and C, normoxic (diagonal stripes) vs. post-hypoxic (grey) conditions. Box - Box - 50th percentile of the data set, derived using the lower and upper quartile values. Error bars –

95% confidence interval, x – mean, horizontal line – median, circles – outliers. Note the different scale for the y-axis in C.

Figure 8. The trends in bursal ventilation rate for each of 8 specimens of *Ophiothrix spiculata* across treatments.

Figure 9. A. Photograph taken in waters surrounding Bocas del Toro, Panama showing over 50 *O. suensonii* species residing on one *Callyspongia vaginalis* colony. B. Photograph of approximately 15-20 *Ophiothrix spiculata* individuals occupying the apex of a porous rock, arms extended into the current. Taken in Monterey Bay, California.

Figures

Figure 1

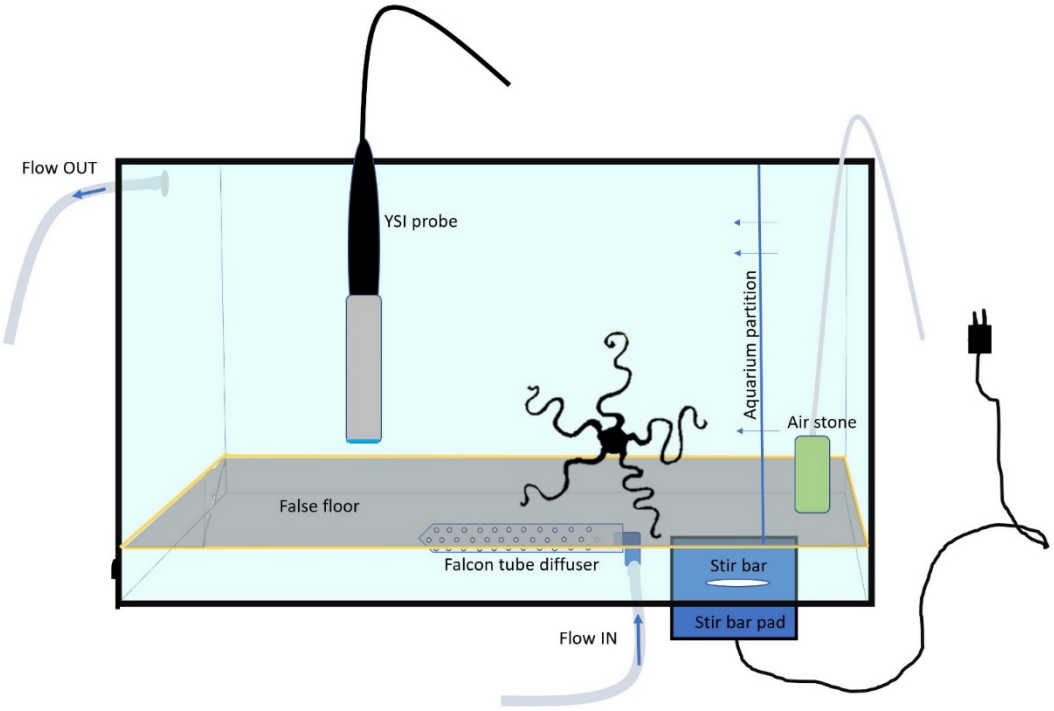

Figure 2

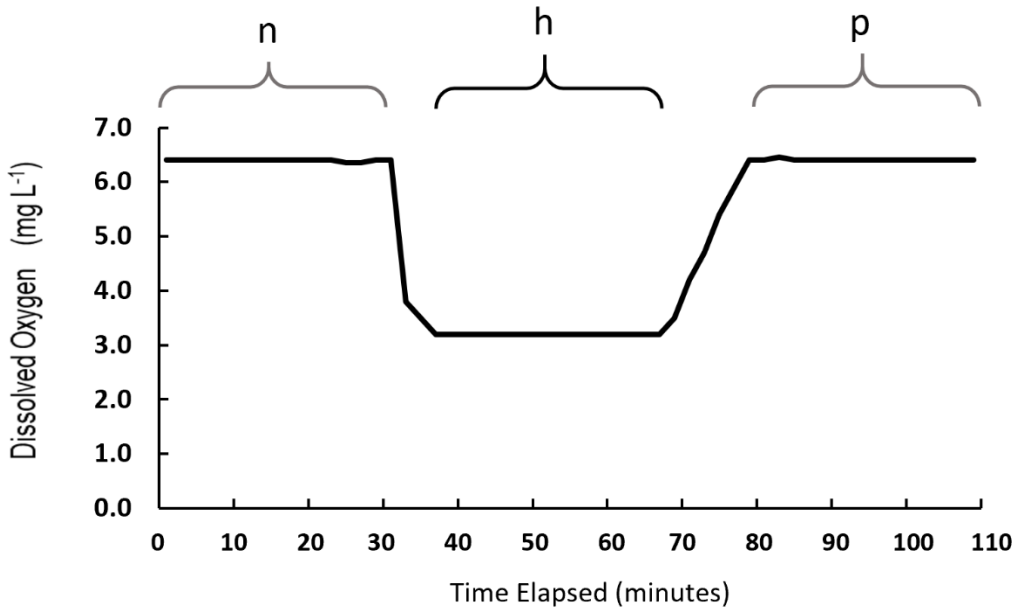
n
h
p
7.0
6.0
5.0
4.0
3.0
2.0
1.0
0.0
Dissolved Oxygen (mg L-1)
0
10
20
30
40
50
60
70
80
90
100
110
Time Elapsed (minutes)

Figure 3

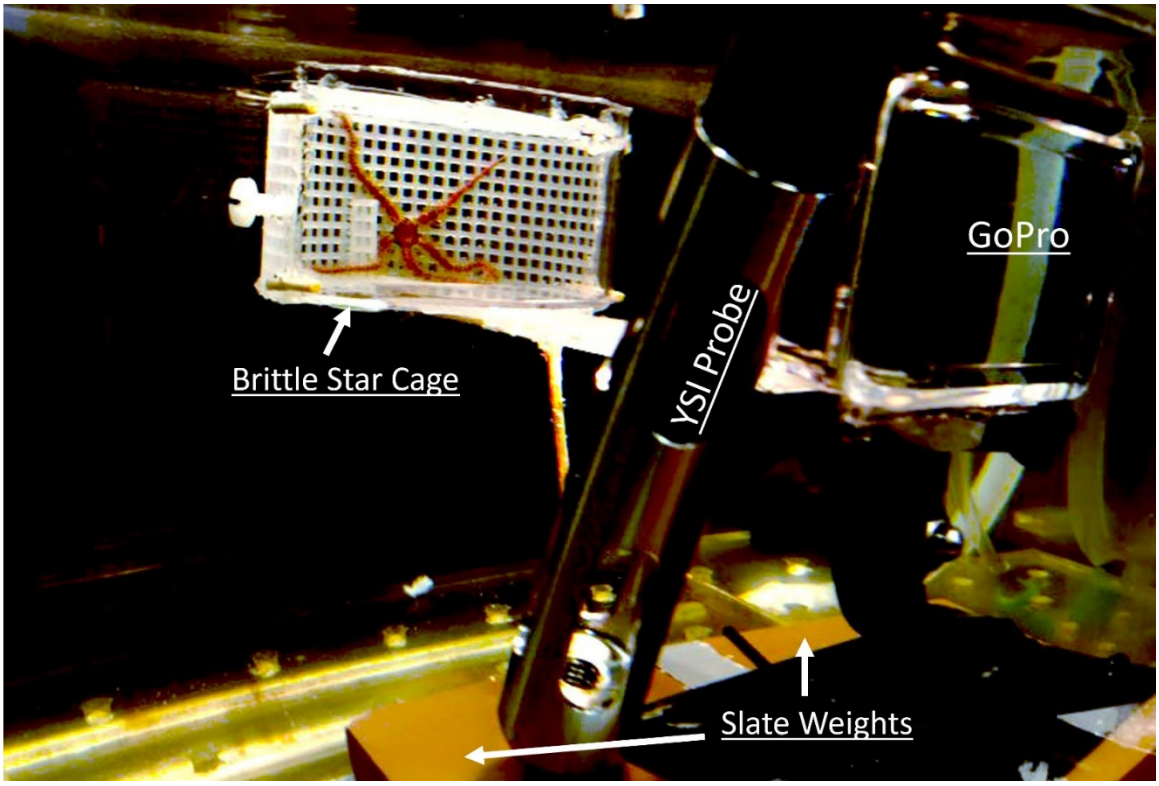

Figure 4

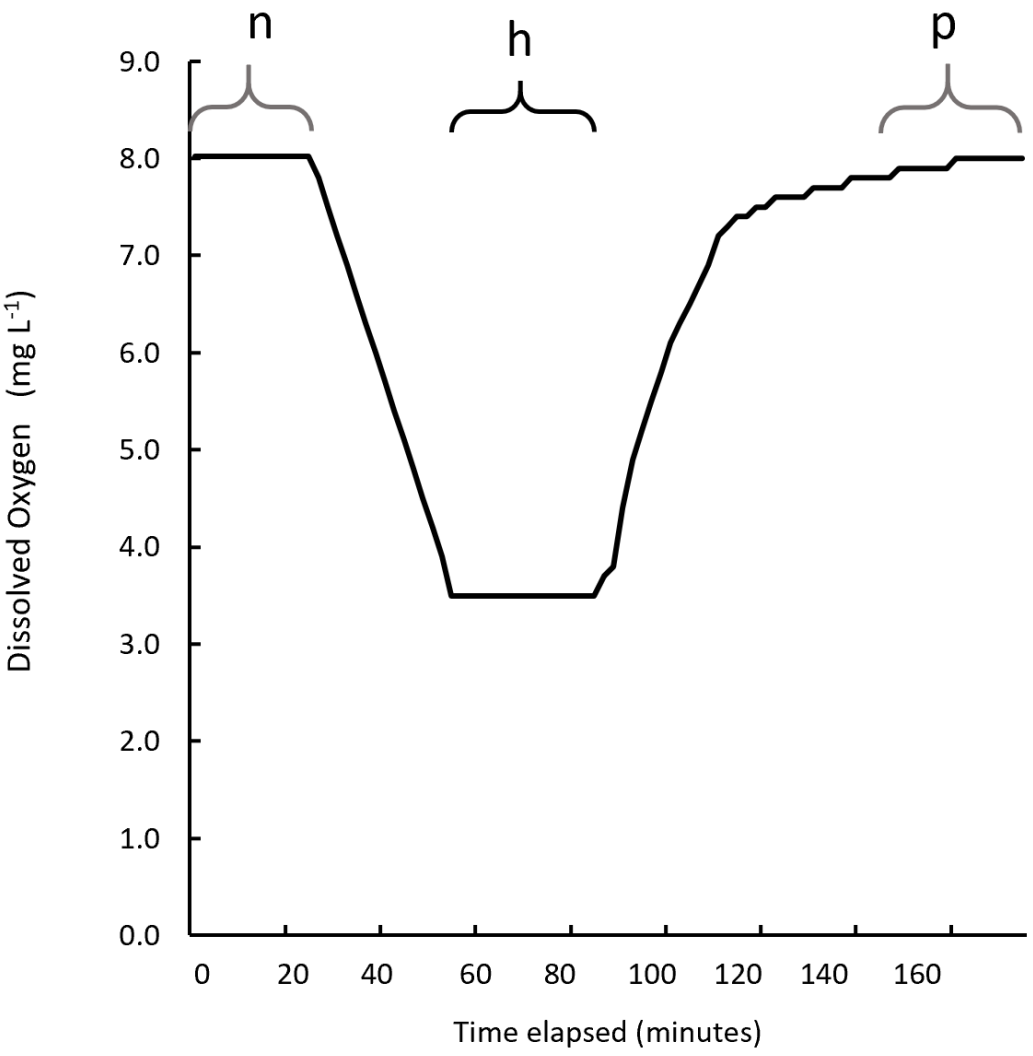
n
h
p
9.0
8.0
7.0
6.0
5.0
4.0
3.0
2.0
1.0
0.0
Dissolved Oxygen (mg L-1)
0
20
40
60
80
100
120
140
160
Time elapsed (minutes)

Figure 5

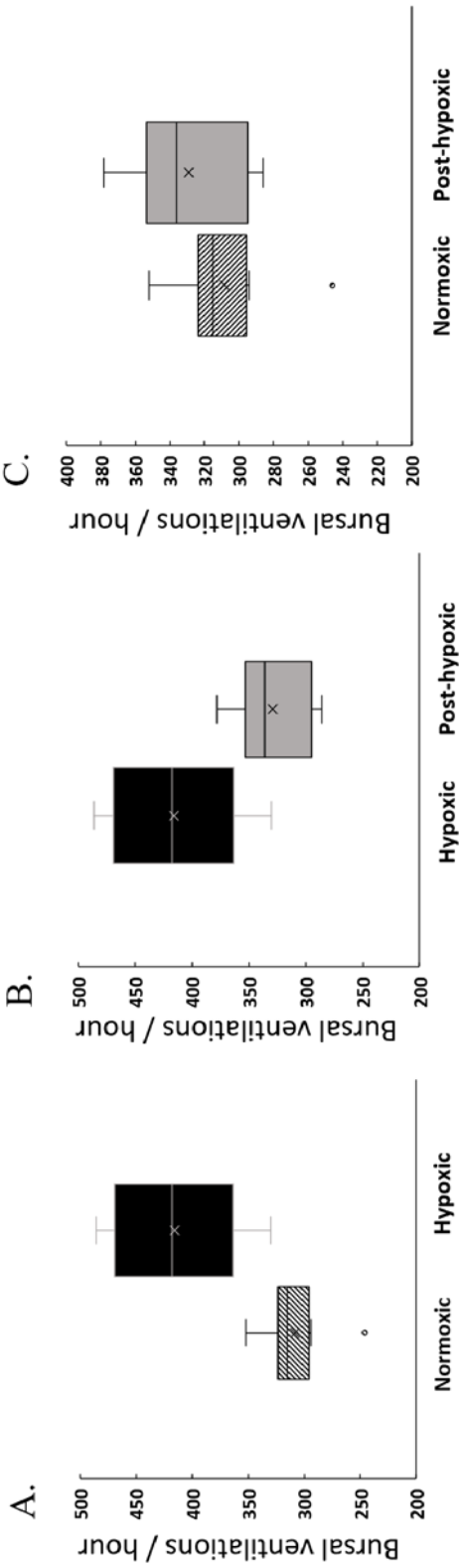
A.
B.
C.
Bursal ventilations / hour
500
450
400
350
300
250
200
400
380
360
340
320
300
280
260
240
220
Normoxic
Hypoxic
Post-hypoxic

Figure 6

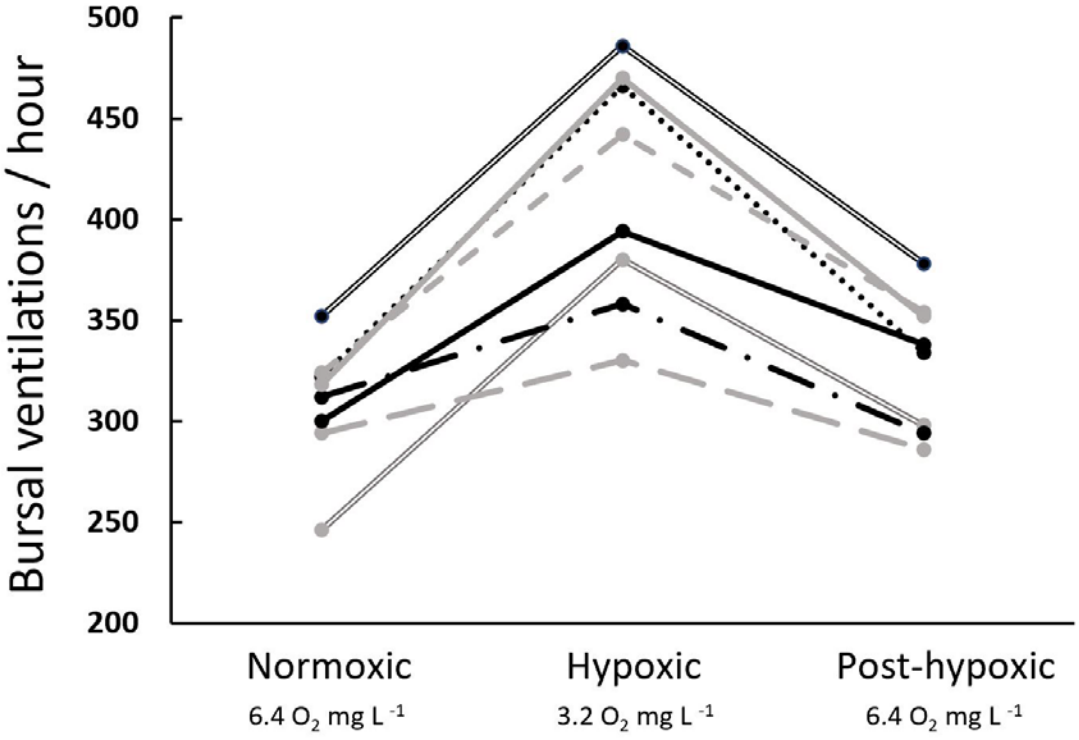
Bursal ventilations / hour
500
450
400
350
300
250
200
Normoxic
6.4 O_2 mg L^{-1}
Hypoxic
3.2 O_2 mg L^{-1}
Post-hypoxic
6.4 O_2 mg L^{-1}

Figure 7

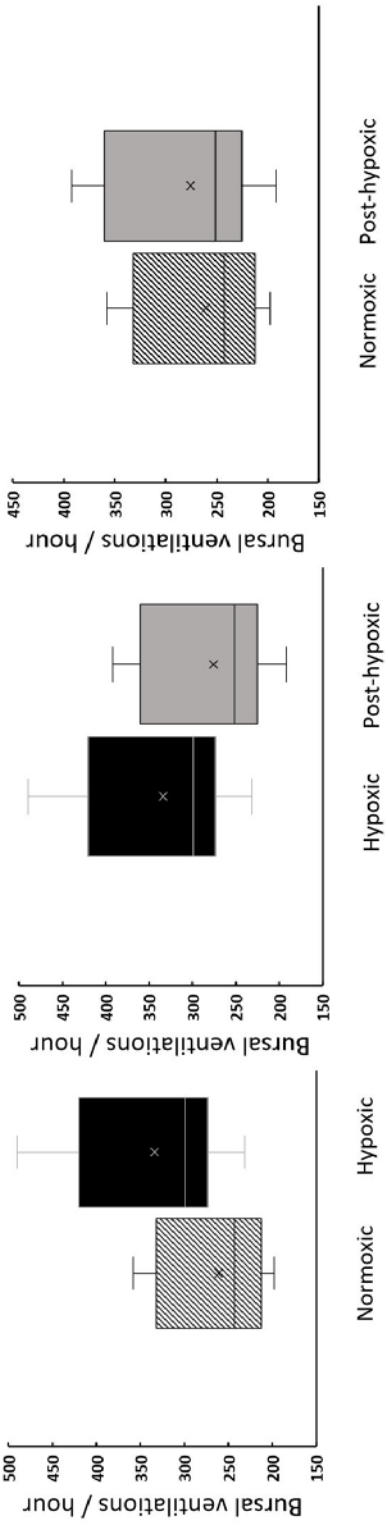
Bursal ventilations / hour
500
450
400
350
300
250
200
150
Normoxic
Hypoxic
Hypoxic
Post-hypoxic
Normoxic
Post-hypoxic

Figure 8

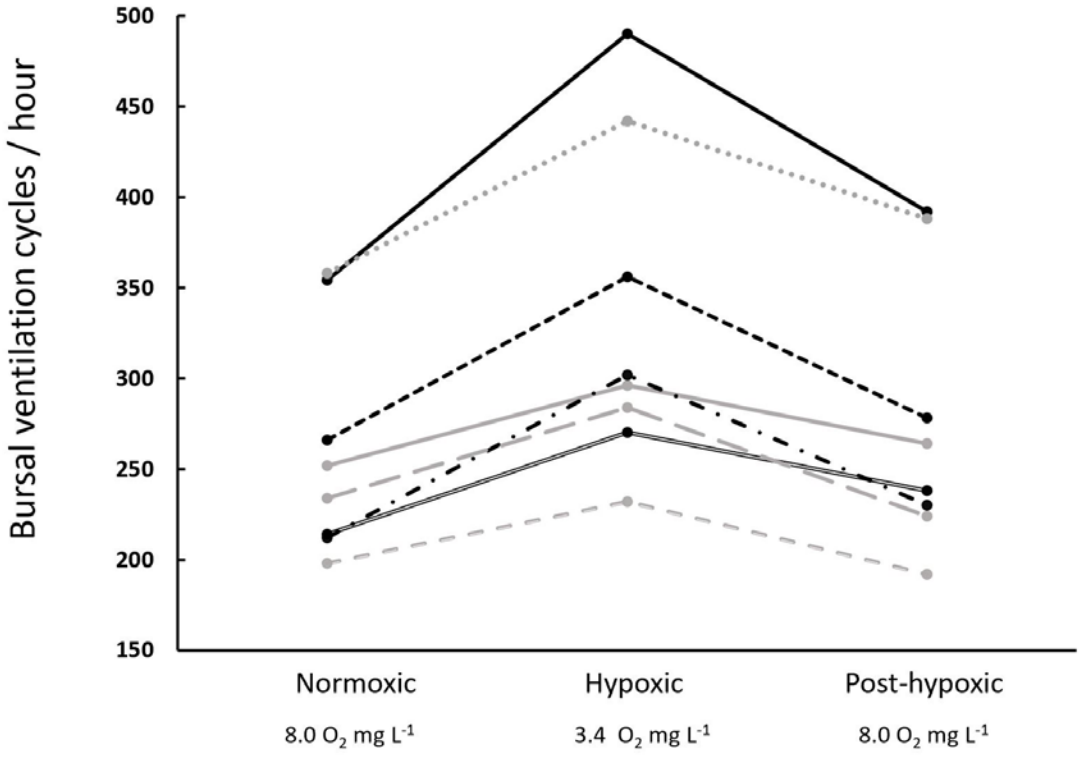
Bursal ventilation cycles / hour
500
450
400
350
300
250
200
150
Normoxic
8.0 O_2 mg L^{-1}
Hypoxic
3.4 O_2 mg L^{-1}
Post-hypoxic
8.0 O_2 mg L^{-1}

Figure 9

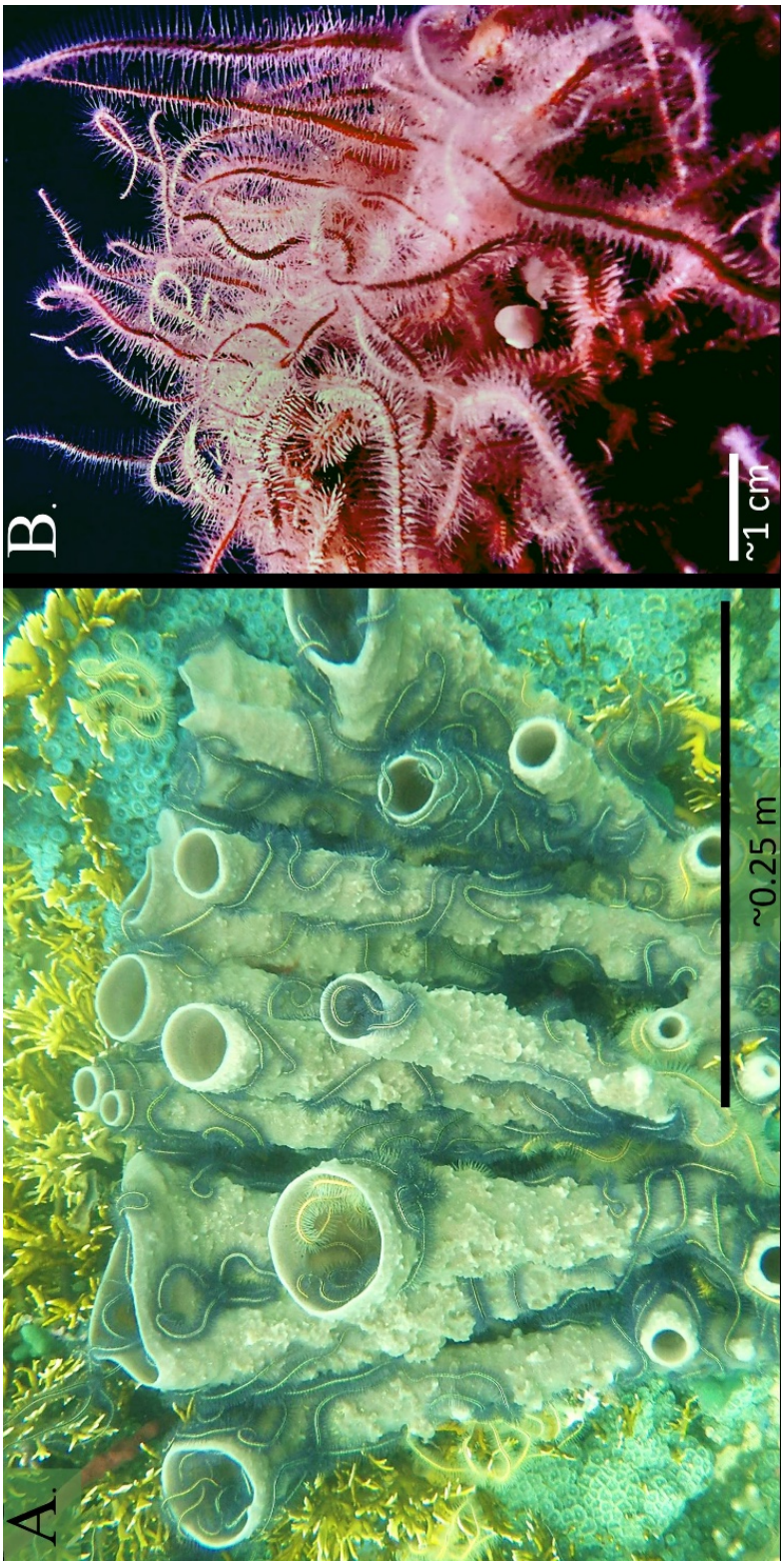

BRIDGE III

Chapter II concerns the functional morphology and microstructure of ossicles that are responsible for the disc pumping movement of bursal ventilation in 3 ophiuroids: *Gorgonocephalus eucnemis, Ophiothrix suensonii, and Ophiothrix spiculata*. The radial shields are highly modified ossicles found throughout the majority of Ophiuroidea. The radial shield gives structure and support to the disc. In some species it works in conjunction with the genital plate and connecting muscles to regulate the position of the roof of the disc. By anesthetizing muscles that connect radial and genital plates, I show that the radial shield – genital plate ossicle complex is responsible for the regulation of the roof of the body disc. I discuss the similarities and differences found in the radial shield microstructure of the 3 aforementioned species, and I compare the shapes and relative sizes of radial shields among related ophiuroids that differ in ways that might be expected to influence morphology of their radial shields. I examine species pairs that a) possess and lack bursae, b) are viviparous and oviparous, c) are large-bodied and small-bodied. I also examine and compare a radial shield from the genus *Ophiura*, the proposed sister-clade to *Gorgonocephalus*.

CHAPTER IV

TITLE:

Morphology and function of radial shields and genital plates in two ophiuroid genera – *Gorgonocephalus and Ophiothrix*

AUTHORS:

MacKenna A. H. Hainey

INTRODUCTION

The Echinodermata class, Ophiuroidea includes basket stars, snake stars and brittle stars of a wide range of sizes that fill multiple ecological niches. Early members of this class emerged in the early Ordovician, approximately 500 million years ago (Stöhr et al., 2012). To date, members of Ophiuroidea are found in all of the worlds' ocean basins, in habitats including; polar sea floor, temperate rocky reefs, tropical reefs, estuary mud flats, and the deep sea (Hyman, 1955; O'Hara et al., 2014). Ophiuroidea is also the largest class of echinoderms, currently boasting 2,087 species (Stöhr et al., 2018b). Ophiuroids have a wide variety of arm-types that can range from simple to bifurcating or dendritic, heavily spined, or lacking spines. Arm lengths can vary from just a few millimeters, up to half a meter and body disc sizes can range from ~1 – 80mm in diameter. An interesting feature in the evolution of ophiuroids is the emergence of a specialized ossicle, the radial shield, with earliest records belonging to the genus *Aganaster* (Hotchkiss and Haude, 2004; Thuy et al., 2014). One of the main functions of radial shields of extant ophiuroids is to work in conjunction with the genital plate to raise and lower the roof of the disc (MacBride, 1906). Ophiuroids have also evolved specialized respiratory structures called bursae which are inpocketings in the body disc at the base of the arms. These bursae are flushed with seawater when the radial shields raise and lower the roof of the body disc (MacBride, 1906; Hainey, Chapters 2 and 3), a behavior I call bursal ventilation. In order to provide groundwork for an improved understanding of ophiuroid radial shield morphology and how that relates to respiratory behaviors, this study focuses on two genera of ophiuroids from the families *Gorgonocephalidae* and *Ophiothricidae.*

The Radial Shield-Genital Plate Complex of *G. eucnemis*

The first accounts of the radial shields and genital plates in a gorgonocephalid came from Lyman, who noted that the radial shield and the genital plates articulate together and raise and lower the roof of the disc (Lyman, 1880, p.255). Only the radial shields were mentioned in the original description of *Gorgonocephalus eucnemis* and were referred to as "ribs of the disc" (Müller and Troschel, 1842). In *G. eucnemis* the radial shields are visible on the aboral side of the disc and usually covered in epidermis

that is lighter in color than the epidermis on rest of the disc (Fig. 1A). MacBride (1906) later observed disc pumping behavior by movement of the radial shields in members of the genera *Ophiothrix, Ophiura, and Amphiura*. However, no detailed description of the radial shields and genital plates has been made.

The Radial Shield-Genital Plate Complexes of *O. suensonii* and *O. spiculata*

In their description of the genus *Ophiothrix* Müller and Troschel (1840) mention the presence of 10 radial 'signs' (shields) which could be naked, sparingly covered, or have a complete armament (with granules or spinules). Ophiothricid radial shields and their associated epidermal coverings are characters used to distinguish species, particularly in keys (Granja Fernández et al., 2014; Lambert and Austin, 2007; and Light et al., 2007). The majority of radial shields are examined from the aboral side as they sit embedded in the disc epidermis. However, the use of scanning electron microscopy imaging is a commonly used tool in zoology and biology, and an increasing number of ossicles have been examined separate from the entire animal (Martynov, 2010; O'Hara et al., 2018; Stewart, 2000; Stöhr et al., 2012; Thuy and Stöhr, 2016)..

This study compares the morphology of the radial shield-genital plate complexes of one gorgonocephalid (*Gorgonocephalus eucnemis*) and two ophiothricids (*Ophiothrix suensonii, Ophiothrix spiculata*). Major differences between the ophiothricids and the gorgonocephalid in articulation of their radial shields and genital plates are highlighted in descriptions and illustrations of their microstructural. Radial shield-genital plate function in *Gorgonocephalus eucnemis* is empirically tested and descriptions are recorded. These data are complemented by an examination of radial shields from other ophiuroids across a broad range of respiratory specialization and taxonomy.

MATERIALS AND METHODS

Collection of Specimens

Nine *G. eucnemis* specimens were collected in February 2016, and 17 in June 2017 by rectangular dredge (~90 cm X 30 cm frame, catch bag with 3-cm mesh diameter), approximately 5 kilometers off-shore (in the vicinity of 43^{o} 16' 615" N, 124^{o} 27' 475" W) Cape Arago, Oregon, USA at depths ranging 45-65 meters. Individuals,

turned ventral (oral)-side-up to allow air bubbles (associated with exposure to air while on deck) to escape from mouth and bursae, were transported back to the laboratory in coolers. At the laboratory, all living basket stars were placed in a 500-gallon tank supplied with aeration and continuously flowing seawater. Specimens that died during or shortly after the collection were preserved in 95% ethanol (EtOH) and were later used to study ossicle morphology. Four specimens from the collection in June 2017 were used in the experiment on functional morphology.

Ten *Ophiothrix suensonii* specimens were collected by hand while snorkeling from the fringing, shallow reefs around the Smithsonian Tropical Research Institute, Bocas del Toro, Panama (9.35148° N, -82.258981° W). Eight of these specimens were used in a respiration study, however the remaining two were anesthetized in a 50/50 solution of seawater and 7.5% concentration $MgCl_2$, then fixed in 95%, EtOH. The two specimens that were fixed in EtOH were used to study morphologies of the radial shield and genital plate.

Ophiothrix spiculata specimens were collected by dredge (~90 m depth) in the waters off Catalina Island, California in June 2015 (33° 26'.668 N, 118° 27'.609 W). Two specimens were used in studies of ossicle morphology.

Ossicle Morphology

For all species used in this study, one radius was removed from each of the preserved specimens (four *G. eucnemis,* two *O. suensonii,* and two *O. spiculata).* Each removed radius included one fifth of the body disc, one arm, one pair of radial shields and one pair of genital plates (e.g. Fig. 1, E). While the tissues were still saturated with EtOH, the dermis was peeled away from the underlying ossicles and muscles. Gut, gonad, and bursae tissue were removed. Each attached arm was shortened to seven vertebral arm ossicles (or after the first bifurcation for *G. eucnemis*). Once soft tissues were sufficiently removed, I allowed the EtOH to evaporate and each radius to dry (Fig. 1, B, C, D). The individuals from which I removed the radii had disc diameters of: *G. eucnemis* 65mm, 45 mm, 32 mm, and 22 mm; *O. suensonii* 15 mm, 14 mm; *O. spiculata* 9mm, 10mm.

For *Gorgonocephalus*, I photographed the entire, dried ossicle complex and illustrated one articulating set of radial shield and genital plate ossicles (Fig. 2). A pair of radial shields and genital plates were removed from a fifth individual with a disc diameter of 20mm. Soft tissues were removed from these ossicles by soaking in a solution of household bleach (NaClO) and deionized water (1:1 by volume). Cleaned ossicles were rinsed in deionized water for 1 minute then placed in small wells of 95% EtOH for 5 minutes. The ossicles were then dried under a warm lamp for 20 minutes and placed on an aluminum stub and vacuum coated with a fine layer of gold. Ossicles were examined and images recorded using a scanning electron microscope (SEM made by Vega Tescan). For each SEM image, Image- J software was used to measure the pore diameters at the surface of the stereom at each region of interest on the ossicles (i.e. articulating surfaces, muscle attachment sites, genital plate spoke, radial shield midrib, and radial shield $CaCO_3$ plates). I took ten measurements at each region of interest and calculated the average pore diameters for each location.

For *O. suensonii*, in addition to the single radius removed from each of two individuals (see Fig. 1 C, D), a whole individual (previously preserved in EtOH) was placed into a solution of household bleach (NaClO) and deionized water (1:1 by volume) until all soft tissues were dissolved, leaving only the ossicles. Ossicles were rinsed for 5 minutes with deionized water to eliminate any residual NaClO, soaked in 95% EtOH for 5 minutes, and dried under a warm lamp for 20 minutes. A pair of radial shields and genital plates were picked out of the dry ossicles, secured with double sided tape to an aluminum stub, vacuum coated with gold, then examined using SEM imaging. Images were made with a camera attached to the SEM and ossicles were illustrated to show overall structure.

For *O. spiculata*, the second (of two) preserved specimen was placed into a solution of household bleach (NaClO) and deionized water (1:1 by volume) until only ossicles remained. These ossicles were rinsed with deionized water for 5 minutes, soaked in 95% EtOH for 5 minutes, then dried under a warm lamp for 20 minutes. A pair of radial shields and genital plates were prepared for SEM imaging in the same manner as for ossicles of O. *suensonii*. Illustrations of the ossicles were made to show overall structure.

The Function of the Radial Shield-Genital Plate Complex

To empirically test the function of the radial shield genital plate complex (RSGPC), I placed basket stars, one at a time, into a temperature controlled, aquarium (75.5 L), held at a constant temperature of 11° C. Each basket star (n= 4) was allowed to acclimate to the aquarium for one hour before the experiment began and was video-recorded for 5 minutes prior to the treatments to ensure all RSGPCs were fully functional. I used Rose Bengal (Acid Red 94) to label the pair of radial shields I was going to alter. This was done by 'stamping' the epidermis covering the targeted radial shields with cotton swap soaked in stain. After staining the epidermis of the radial shields, a 0.5 ml syringe fitted with a 28-gauge needle was loaded with a solution of 14% (by volume) magnesium chloride ($MgCl_2$) in distilled water. Approximately 0.2 ml of the $MgCl_2$ solution was injected into the abductor muscle, near the radial shield and genital plate articulating surfaces. For a control treatment, sterilized seawater (0.45 µm filtered, boiled, and checked for salinity) was injected into the abductor muscle in place of the $MgCl_2$. There was no acclimation period after staining and injections. Two basket stars were used in each treatment group. Basket stars in both the control and $MgCl_2$ treatment group were kept submerged during the staining and injection process. Following injection, the basket stars were video-recorded (GoPro HD Hero 3 Silver Edition®) in time-lapse (1 frame per 5 seconds) while they moved around the aquarium for 30 minutes post treatment. Direct observations were made of all four animals during the experiment. I evaluated movement in time-lapse videos with the program GoPro Studio (© 2018) at a frame rate of 2 frames /second. Basket star behaviors were noted as were positions of the treated radial shields. Still images that best represented the effect of $MgCl_2$ treatment were singled out from the video for Figures 7 and 8. This experiment was not performed on *O. suensonii* nor *O. spiculata* as their abductor muscles were too small to inject with $MgCl_2$ without causing significant damage to the muscles and other structures.

RESULTS

Ossicle Morphology

Gorgonocephalus eucnemis: The radial shields of *G. eucnemis* are long, spoke-like ossicles (Fig. 1A). Each ossicle has a condyle-like process on the distal end (Fig. 2, rsdp) that elongates into a point at the proximal end (Fig. 1B, and Fig. 2). Occasionally, a radial shield may branch resulting in 2 (rarely 3) proximal points. The elongated part of the radial shield is composed of a ventral midrib and distinct dorsal plates of $CaCO_3$ in various stages of fusion with one another. The midrib is durable and provides support from the ventral (oral) side for the $CaCO_3$ stacked plates (Fig 1B, Fig 2, Fig. 3A). As the animal grows, the stacked $CaCO_3$ plates begin to fuse with one another and the underlying midrib, beginning near the distal process of the radial shield. $CaCO_3$ plates near the pointed, proximal end are younger and the most recently accreted plates. These plates are not fused to one another and are held together with connective tissue (collagen) and by epidermis. When a bleach solution is used on the radial shield ossicles, the connective tissue which binds the shield plates at the points of the radial shield dissolves and proximal plates often flake off in the cleaning dish (Fig. 3B). The midrib comes to an end at the distal portion of the radial shield on the ventral side of the ossicle, where it transitions into a small process to which the adductor muscle attaches (Fig. 3A addm). This process is possibly the hardest portion of the radial shield and is most reliably removed from a specimen intact. On the dorsal surface of the radial shield distal process (Fig 2, rsdp) is a small shelf-like indentation to which the abductor muscle attaches. Between these two muscle attachment sites on the radial shield is a small, concave region that is the surface where the radial shield meets and articulates with the genital plate.

The genital plate, more robust than the radial shield, is firmly and immovably attached by connective tissues to the portion of the arm that lies within the body disc. A large portion of the elongate portion of the genital plate is attached to the vertebral arm ossicles (Fig. 1B). The condyle of the genital plate is composed of three processes (Fig. 3A). The first process is the convex articulating surface, with a small shelf-like projection on the distal face for abductor muscle attachment (Fig. 2 #1, Fig. 3C #1, Fig. 4B). I refer to this process as “Darwin’s Calvaria,” due to its resemblance in shape to the receding hair line and cranium of the late naturalist (Fig. 4A, B). Its distinct shape is a useful

marker to look for when distinguishing disarticulated or broken ossicles. The second process of the genital plate condyle is the site of attachment of a proximate ambital ossicle (Fig. 2 #2 and Fig 3C #2). This second process has small rounded projections itself (2-3 depending on individual ossicle) where the ambital ossicles attach with connective tissue. The ambital ossicles form a flexible frame which runs around the ambitus of the body disc. The third process is a shelf-like projection on the proximal side of the condyle, where the adductor muscle attachment site is located (Fig. 2 #3, and Fig 3C#3).

Differences in Stereom Porosity in the Radial Shield-Genital Plate Complex

The radial shield and genital plates are made up of labyrinthic, and microperforate stereom with varying degrees of porosity depending on the part of the ossicle. For *Gorgonocephalus eucnemis*, the articulating areas on the radial shield and genital plate distal processes are composed of microperforate stereom and have the smallest pore diameters (average pore diameter, 5.5 µm) followed by the muscle attachment sites (average pore diameter, 9.6 µm). The next largest pore diameters belonged to the radial shield midrib (average, 14.3 µm) and the genital plate 'spoke' with average stereom pore diameter of (17.1 µm). The radial shield plates along the dorsal surface of the elongated portion of the radial shield, have the most open stereom (large pore diameters throughout) with the largest pore diameters observed in these ossicles (average pore size, 30.0 µm) (See Fig. 3, A-C).

Ophiothrix suensonii: On the living animal, a pair of radial shields can be found on the disc, at the base of each arm. The radial shield of *O. suensonii* is a flat, scapulate ossicle with a small distal process and site of articulation on the ventral side of the ossicle and a point at the proximal end (Fig. 5A, B and Fig. 6A, B). The sides facing the radii are usually straight and aligned with the radius. The interradial sides tend to have more curvature, and come out at an angle from the proximal tip, making the scapulate shape of the ossicle (Fig. 5A, B and Fig. 6B). The distal edge is concave in this species (Fig. 5A, B and Fig. 6B). The entire radial shield appears to be one, solid structure without fusing of $CaCO_3$ plates at the proximal end. However, the proximal end is very thin and easily

broken with forceps, as is the interradial edge of the radial shields. The dorsal surface of the radial shield is made up of labyrinthic stereom (Fig. 5B).

On the ventral side of the radial shield, the small distal process is a region of increased thickness where the adductor muscle attaches (Fig. 5A, and Fig. 6A). This region is composed of an arc of microperforate stereom. The articulating surface can also be found on the ventral side of the radial shield distal process, is a spoon-shaped depression with an outer flange, and functions in a similar fashion to a vertebrate joint-socket (Fig. 5A and Fig. 6A). When viewed from the ventral side, the site of attachment of the abductor muscle can be found distally and slightly below the edge of the articulating surfaces' flange structure (Fig. 5A and Fig. 6A). The ventral surface of the radial shield is also constructed from labyrinthic stereom (Fig. 5A).

As in *G. eucnemis* the genital plate of O. *suensonii* is more robust than the radial shield and lies firmly attached to the side of an arm, fixed in place by connective tissues (Fig 1C). The genital plate condyle is composed of four rounded projections. The first is the largest and most dorsal projection where the articulating surface is found (Fig 5C #1 and Fig 6C #1). On the distal side of this projection is the abductor muscle attachment site, evident as a small ridge. The second and third small projections of the genital plate condyle are the sites for attachment of the proximate ambital ossicle; these are off-set along the interradial side, giving the appearance of 'rounded-steps' along the condyle (Fig 5C #2,3 and Fig. 6C #2,3). The fourth process, directed proximally, is where the adductor muscle attaches (Fig 5C #4 and Fig. 6C #4). The stereom fabric of this process is microperforate (Fig. 5, C). The elongate portion of the genital plate, including the proximal tip, is composed of a mix of labyrinthic and fascicular stereom.

Ophiothrix spiculata: On live specimens, the radial shields can be found in pairs at the base of each arm. The radial shields of *O. spiculata* are also flat and scapulate, like those of *O. suensonii*, with a small distal process and a pointed, proximal tip (Fig 5D, E and Fig. 6D, E). The plate side facing the radius is straight, aligned with the radius, and is thicker than the interradial side. The interradial side comes out at an angle from the proximal tip, is straight until its distal boundary where it curves gently toward the radius and transitions into the distal side of the plate. The distal side of the radial shield comes

to a blunt point, near the radius, where the distal process is situated (Fig. 5D, E and Fig. 6D, E). The dorsal surface of the radial shield is made up of labyrinthic and irregularly perforate stereom (Fig. 5E). On the ventral side of the radial shield is a small distal process (Fig. 5D and Fig. 6D). Like *O. suensonii*, the distal process for this species is an increased thickness of the distal end of the radial shield indicated by a bean-shaped region of microperforate stereom and is the site for attachment of the adductor muscle (Fig. 5D, 6D). On the distal side of this distal process an articulating surface is found. Like in *O. suensonii* this surface is a slight 'spoon-shaped depression' with an outer flange, however unlike *O. suensonii*, the 'flange-rim' (rounded portion) faces proximally (compare Fig. 5A and D; Fig. 6A and D). Despite the opposite direction, this articulating surface functions like that in *O. suensonii*, by providing a socket-like structure for the articulating surface of the condyle of the genital plate. Most of the ventral side of the radial shield is composed of irregularly perforate, labyrinthic, and some fascicular stereom. The site of attachment of the abductor muscle is comprised of microperforate stereom.

The genital plate of *O. spiculata* is also more robust than its radial shield. Each radius has a pair of elongate genital plates (Fig. 5C, 6C) fixed in place by connective tissues between the genital plate mid region and the underlying vertebral arm ossicles (Fig. 1C, D). For *O. spiculata*, the genital plate condyle has 3 processes, compared to the four found on *O. suensonii's* genital plate condyle. The first, largest, and most dorsal projection is where the articulating surface is found (Fig. 5F #1 and Fig 6F #1). On the distal side of this projection is a large ridge comprised of microperforate stereom, where the abductor muscle attaches to the ossicle. Below the largest process and offset to the interradial side of the condyle is the second process. This process is slightly elongated dorsal-ventrally with a small 'bowl-shaped' depression in the middle (Fig. F #2 and Fig. 6F #2). This depression is the site of attachment for the proximal ambital ossicle and the abradial genital plate. Located proximally, the third process of the genital plate condyle is the second largest process, is composed of microperforate stereom, and is where the adductor muscle attaches to the ossicle (Fig. 5F #3 and Fig. 6F #3). The elongate portion of the genital plate, including the proximal tip, is composed of fascicular and labyrinthic stereom (Fig. 5F). The genital plate of *O. spiculata* is more angular than the genital plates

of both *G. eucnemis* and *O. suensonii*. The genital plates of the latter two species have a curved crescent shape, compared to the 'dogleg' shape of *O. spiculata's* genital plate (compare Figs. 2 and 6C, F).

Despite the differences in shape and size, the radial shield genital plate complexes of *G. eucnemis*, *O. suensonii*, and *O. spiculata* all function is the same way: When the adductor muscle relaxes and the abductor muscle contracts, the radial shield raises the aboral surface of the disk. When the abductor muscle relaxes and the adductor muscle contracts, the radial shield falls, lowering the aboral surface of the disc. Together, the radial shield, genital plate, abductor and, adductor muscles make up the radial shield-genital plate complex (RSGPC).

The Function of the Radial Shield-Genital Plate Complex

All RSGPCs on all of the basket stars were fully functional before the treatments were applied. The two basket stars belonging to the control group (sterile seawater injection) were agitated (rapid increased locomotion) but disc movement was not affected by the injection. The abductor muscle functioned normally, allowing full expansion and compression of the body disc (Figure 7, A-C). The two basket stars in the manipulation group ($MgCl_2$ injection) were also agitated and the abductor muscles of the selected radii were no longer functional, resulting in the loss of the ability to raise the radial shields. The treated RSGPC remained in the compressed state, while the remaining four, untreated RSGPCs were still fully functional and could still raise to expand their portions of the body disc (Figure 8, A-D). Upon injection, the magnesium (Mg^{2+}) in the $MgCl_2$ solution worked as an inhibitor of the Ca^{2+} facilitating effect at the neuron junctions, inhibiting the synaptic transmission across the myoneural junctions, resulting in failure of muscle contractility (West et al., 2014) within the treated RSGPC.

DISCUSSION

Bursal ventilation by ophiuroids aids respiration (Ch. 1), the expulsion of gametes and waste molecules (Hyman, 1955), and ventilatory movements occur in species that brood embryos (Austin, 1966; Hyman, 1955). Movement of water in and out of the bursae can occur via ciliary action (Austin, 1966; MacBride, 1906) and by muscular

action. The radial shield and genital plates along with attached muscles permit rhythmic pumping of the body disc that results in bursal ventilation. Well-developed currents produced by cilia lining the bursal epithelium circulate a small volume of water throughout the bursae continuously, however, a larger volume of water is rapidly drawn into the bursae by the muscle-mediated elevation of the radial shields. The continuous flow of water brought in by the beating cilia certainly contributes to the uptake of oxygen, brood ventilation and removal of waste molecules but for the larger-bodied ophiuroids, ciliary currents alone may not meet biological demands. The muscular ventilation of bursae is performed by radial shields and genital plates and their extreme modification in ophiuroids like basket stars and snake stars may allow them to grow to the large sizes we see today. When magnesium chloride solution was injected into a pair of abductor muscles, the muscle function was inhibited and resulted in failure to raise the two adjoining radial shields. This study empirically confirms the functions of the radial shield-genital plate complexes, in *G. eucnemis,* are to provide structural support for the body disc, and also act as 'levers' which raise and lower the aboral side of the disc. The raising and lowering of the aboral surface of the disc draws water into and expels water from the bursae, resulting in bursal ventilation.

Comparison of Euryalida and Non-Euryalid Radial Shield-Genital Plate Complexes

The radial shield ossicles of species in the order Amphilepidida (genus *Ophiothrix*) are flat (and mostly scapula-like/ sub-triangular in form), while those of species in the order Euryalida have larger, spoke-like radial shields that extend into the central region of the body disc. Despite large differences in morphology of the radial shields, the genital plates of these two groups seem similar in shape. Together, these ossicles form the RSGPC (Fig. 9). The movement of the RSGPC is powered by a pair of opposing muscles - the abductor muscle and the adductor muscle. In each ophiuroid, 10 of these RSGP complexes (one pair per arm) work in unison to raise and lower the roof of the body disc, which results in bursal ventilation.

The genus *Ophiothrix* was chosen for comparison with *Gorgonocephalus* because it was one of the only genera reported to carry out regular disc pumping (Austin, 1966). The radial shields of *O. suensonii* and *O. spiculata* are, not surprisingly, most similar to

one another in shape. *Ophiothrix suensonii* adults are generally larger in total diameter than the adults of *O. spiculata* (Hendler, 1995; Lambert and Austin, 2007) and have proportionally larger radial shields with a more pronounced curvature to the interradial and distal sides than those of *O. spiculata*. Even when *Gorgonocephalus* is small and similar in size to ophiothricids, *Gorgonocephalus* radial shields are spoke-like, or elongate and coming to a tapering point near the center of the disc. The proximal tip is also not solidly fused but is composed of a few $CaCO_3$ plates connected to one another with soft tissue, whereas the radial shield points of the two ophiothricids are solid extensions of the single radial shield plate. Although they vary in size, the genital plates of all three specimens are very similar to one another in shape. The genital plate condyles of *Gorgonocephalus* and *O. spiculata* both have 3 processes: the dorsal process with the articulating surface, the interradial process, where the ambital ossicles/ abradial shield connects, and the proximal facing process where the adductor muscle attachment site is located.

Radial Shields in Brooding vs. Non-Brooding Ophiuroids

To further elucidate any trends present between radial shield shape and function, I examined the presence and absence of a biological demand (within a genus) associated with the radial shields starting with viviparous and oviparous congeners. MacBride, (1906) observed disc pumping behavior in *Amphipholis squamata*, a species known to brood its young. This small ophiuroid rarely reaches disc diameters over 5 mm (Lambert and Austin, 2007). Each radial shield has a mirrored pair, which touch along the majority of their radial sides, only separating from one another at the most proximal ends. The distal edges of the radial shields are at the edge of the disc itself, and the total length of a radial shield makes up approximately one-fifth of the total disc diameter (Fig. 10, A).

Amphipholis pugetana, Lyman, 1860, is also a very small ophiuroid rarely reaching disc sizes larger than 5 mm (Lambert and Austin, 2007; Emlet and Hainey, pers obsv.). Although closely related to *A. squamata*, this species sheds eggs and sperm. The radial shields are very similar in size and shape to those of *A. squamata*. They touch along majority of the radial side, separate at the proximal tips. However, the distal sides (down, Fig. 10, B) of *A. pugetana* are straight and slightly wider than the proximal ends

(up) (Fig. 10, B). There are also some very small disc scales that separate the radial shield distal edges from the disc edge. The radial shield length usually takes up one-fifth the entire disc diameter. Other than the widening of the distal edge of *A. pugetana's* radial shields, superficially there is very little difference between the two species despite their very different reproductive strategies, however *A. squamata* and other members of this genus (e.g., *A. chiajei* and *A. filiformis*) are known to exhibit disc pumping (MacBride, 1906; Woodley, 1975). I examined these two species to determine if the act of brooding and ventilating the young inside the bursae would influence the shape of the radial shield. Based on the comparisons of the external radial shield morphology, I cannot conclude whether the act of brooding and ventilating young in the bursae influence radial shield shape, as the two species' radial shields are very similar in size and shape. Finer resolution examination of both the aboral and oral surfaces of the radial shields, using SEM imaging, needs to be done on cleaned radial shields from both species to further elucidate any apparent differences between the two *Amphipholis* species.

Radial Shields in Ophiuroids With and Without Bursae

To better understand the role radial shields and their shapes play in bursal respiration I examined the superficial shape of radial shield of two species of *Ophiactis*, one with and one without bursae. *Ophiactis virens,* (Sars 1859) has no bursae and is similar in size to *O. quinqueradia*, (Ljungman, 1872) that have bursae. The radial shields of the former are pear seed-shaped (Fig. 10, C). They are rounded and blunt on the distal side facing the disc edge. At their proximal end the shields taper to point and so separate from one another, leaving space between them for other disc scales (Fig. 10, C). These radial shields are approximately one-fourth the diameter of the entire disc. *Ophiactis quinqueradia* also has 5 pairs of radial shields visible on the dorsal disc surface. Each radial shield touches its paired counterpart near the distal end but are separated from one another at the middle and proximal ends (Fig. 10, D). The distal edges of the radial shields are flat, with a slight space between each pair at the most-distal portion (Fig. 10, D). The radial shields are also approximately one-third the total disc diameter. Thus, the radial shields of *O. quinqueradia* take up proportionately more disc area than the radial shields of *O. virens.* Perhaps the lack of bursae and the associated biological functions

that come with them, has rendered large radial shields extraneous, and led to their reduction or lack of development. It is currently unknown if disc pumping behavior is exhibited by *O. quinqueradia* (with bursae), however, Selvakumaraswamy and Byrne (2000) noted there was no pumping of the disc during spawning by the congener *O. resiliens* with bursae.

Radial Shields in Large vs. Small Bodied Ophiuroids

Lyman (1880) first noted that the radial shield ossicles regulate the position of the roof of the body disc in a gorgonocephalid specimens collected during the H. M. S. Challenger expeditions. He reported the radial shields were hinged to the genital plates by muscles, and noted the radial shields were not a solid ossicle and he suggested they are composed of a series of soldered disc scales. I compared large-bodied and small-bodied ophiuroids within the same Order, to see if radial shield shape changes with body size. Euryalids such as *Gorgonocephalus eucnemis, Gorgonocephalus arcticus* (Leach, 1819), and *Astrophyton muricatum (*Lamarck, 1816) are all large-bodied ophiuroids, bearing discs that can grow larger than 50 mm in diameter and disc depths of up to 40 mm (Hainey, pers. obsv. on *G. eucnemis*). Their radial shields are all similar to what Lyman (1880) and I describe, as elongate, spoke-like, comprised of several plates of $CaCO_3$ at the proximal point, and bear a well-developed process with articulating surfaces at the distal end. Small-bodied euryalids, such as *Schizostella bifurcata* (Clark, 1952) appear to have similar radial shields to their large-bodied counterparts (Hainey, pers. obsv. of images from Manrique-Rodríguez and Borrero-Pérez (2017)). *S. bifurcata* is a small basket star that is usually around 4 mm in disc diameter as an adult. A thick dermis covers the radial shields, however, the dorsal surface shape can be seen through the dermis in preserved specimens (Hainey, pers. obsv. of images from Manrique-Rodríguez and Borrero-Pérez (2017)). From a superficial image examination, one can see that the radial shields of this small-bodied euryalid are also well developed, reaching to the near-center of the disc. However, it appears the radial shields of *S. bifurcata* have a greater overall curvature to them (creating a steeper arc) compared to those found in *G. eucnemis*. Perhaps for euryalida, it is radial shield curvature that changes between large-bodied and small-bodied species, preserving the general, spoke-like shape. To date, there

has been no published work done on the radial shields or the general anatomy of *S. bifurcata,* with limited photographs to make radial shield-shape estimates on. More research into this species' anatomy needs to be done in order to make any further meaningful comparisons.

Recent morphological evidence now suggests the order euryalida is actually a sister group to the ophiurid brittle stars (Thuy and Stöhr, 2018). Many ophiuroids, including *Ophiura lutkenii* (Lyman, 1860), are medium-to-large bodied, with most of their radial shields showing through the disc dermis. However, the proximal tip and the radial and interradial sides of the radial shield are embedded below the dermis. Once the soft tissue is removed the entire radial shield shape, which is foliose or leaf-like, is visible. The radial shield is much wider at the distal end and in the middle than at the proximal point (Fig. 10, E). The pairs of radial shields do not touch along their radial sides and (from distal to proximal tip) comprise approximately one-fourth the entire disc diameter. Because of its broad distal region and its elongate proximal region, the radial shield shape looks as if it is a hybrid between the radial shields of non-euryalid ophiuroids and those in Euryalida (Fig. 10 E, F). Radial shield features shared with the non-euryalid members of Ophiuroidea include a dorsal-ventrally flattened appearance and a lower length to with ratio. *Ophiura lutkenii's* elongated radial shield proximal tip is more similar to the proximal tips found in euryalid radial shields (Fig. 10, F); and, when *O. lutkenii* radial shields were macerated in household bleach, these proximal tips often flaked off the main ossicle in the same way did for radial shields of *G. eucnemis* (M. Hainey, pers. obsv.). Radial shields of *O. lutkenii* may be extended by accreting $CaCO_3$ plates to the proximal ends, as observed in euryalids (MacBride, 1906). By comparing the radial shield shape of an ophiurid, with a euryalid we can examine morphological similarities and differences that may help solidify the newly established phylogenetic position of sister-clades, based on molecular and other morphological characteristics (Thuy and Stöhr, 2018).

Using Articulating Ossicles in Paleozoology

Historically, the phylogeny of Ophiuroidea has been split into the orders non-euryalids (simple-armed brittle stars) and Euryalida (basket and snake stars). However,

developing phylogenetic and morphological evidence suggests Euryalida may belong within its sister group Ophiurida (Smith et al., 1995; Stöhr et al., 2012; Thuy and Stöhr, 2018). Ophiuroids are good candidates for fossilization in most marine sediment types because of their high magnesium calcite content, however, their tendency to rapidly decompose after death makes finding intact specimens a rarity. Only on the occurrence of rapid deposition of fine marine sediments, do we find fully-articulated fossil specimens (Twitchett, 2004). Taxonomists agree there needs to be a systematic sampling for ophiuroid fossils as there has been no direct expedition for them and the majority of the taxonomic work today is done using museum specimens. Including more fossil species to the taxonomic literature would add to the working body of knowledge on extinct ophiuroids and potentially give more clues to the lineage and evolution of extant ophiuroid clades (Stöhr et al., 2012). Radial shields and genital plates are distinctive ossicles found only in in ophiuroids, and despite their problematic rapid, post-mortem disintegration, radial shields and genital plates should be readily recognizable in the fossil record, even as isolated microfossils. Searching for fossilized radial shields, may help shed light on the evolution and emergence of these modified ossicles and their role in bursal ventilation behavior. By looking at the ossicle stereom fabrics in SEM images, we can infer where muscle attachment sites, and articulating surfaces are and begin to understand how disarticulated ossicles could function together in the living organism. These radial shield characteristics could apply to fossil ossicles as well. By examining microfossils, especially those with well-preserved stereom fabric textures, we could begin to look at structures such as muscle attachment sites and articulating surfaces and make educated inferences about how extinct organisms once functioned.

By comparing the anatomy and micromorphology of these two very different radial shield-genital plate ossicles, we can begin to make generalities about how their structure, such as stereom fabric type denoting muscle attachment sites and the presence of processes, relates to function (i.e. the elevation and lowering of the roof of the body disc). Despite the differences in size and genera, the RSGPC's of the two examined ophiuroid groups (Euryalida/non-euryalid), function nearly identically to one another.

Figure Legends

Figure 1. **A.** An aboral view of adult *Gorgonocephalus eucnemis* with 5 pairs of spoke-like radial shields. (rs)- two pairs of radial shields **B.** An interradial view of a radial shield-genital plate complex, including arm ossicles, dissected from *G. eucnemis*. The body disc would extend from the middle of the image out to the right. (abdm)- abductor muscle attachment sites, (addm)- adductor muscle attachment sites (aoa)- ambital ossicle attachment site, (de)- dermis/epidermis, (gp)- genital plate, (ivm)- intervertebral arm muscles, (p) – stacked plates of $CaCO_3$, (rs)- radial shield, (vao)- vertebral arm ossicles. **C.** An interradial view of the genital plate (gp) of *O. suensonii.* Body disc would extend from the center of the image out to the left. (adm)- adductor muscle, (aoa) - ambital ossicle attachment site, (ivm) – intervertebral muscle. **D.** Dorsal view of one radius of *O. suensonii* with the dermis and one radial shield removed. (gp)- genital plate, (ivm) - intervertebral muscle, (rs)- radial shield, (vao) – vertebral arm ossicle. **E.** *O. spiculata* with one radius removed before maceration.

Figure 2. Illustration of the interradial side of the radial shield-genital plate complex of *Gorgonocephalus eucnemis*; abductor and adductor muscles omitted for simplicity. (abdm)- abductor muscle attachment site, (addm)- adductor muscle attachment site, (aoa)- ambital ossicle attachment site, (gp)- genital plate, (gpc)- genital plate condyle (Darwin's Calvaria), (mr)- radial shield midrib, (p)- thin $CaCO_3$ plates making up the proximal end of the radial shield, (rsdp)- radial shield distal process, (1,2,3) – genital plate condyle processes (see text).

Figure 3. Images taken with a scanning electron microscope detailing the differences in porosity of various structures found in the radial shield-genital plate complex of *Gorgonocephalus eucnemis*. **A.** Ventral view of the radial shield distal process; (aa)- articulating area, addm- adductor muscle attachment site, (mr) – radial shield midrib. **B.** Dorsal view of the radial shield, proximal (left) distal (right); (mr)- radial shield midrib, (p)- radial shield CaCO3 plates. **C.** Image of the interradial-side of the genital plate condyle; **(**abdm)- abductor muscle attachment site, (aa)- articulating surface, addm- adductor muscle attachment site, #1-3 – genital plate condyle processes (see text).

Figure 4**.** Figure comparing the shape similarity between **A.** Charles Darwin's head and receding hair line and **B.** "Darwin's calvaria" - the dorsal side of the genital plate condyle including the articulating surface and the abductor muscle attachment site for *Gorgonocephalus eucnemis.*

Figure 5. Images taken with a scanning electron microscope detailing the similarities and differences between the radial shields and genital plates of *Ophiothrix suensonii* **(A – C),** and *O. spiculata* **(D – E). A.** Ventral view of radial shield, proximal tip broken. (abdm)- abductor muscle attachment sites, (addm)- adductor muscle attachment sites (aoa)- ambital ossicle/ abradial genital plate attachment site, (gp)- genital plate, (rs)- radial shield, dotted lines – edge of disc, (1-4) – genital plate condyle processes (see text). **B.** Dorsal view of radial shield. **C.** Genital plate, interradial side. **D.** Ventral view of radial shield. **E.** Dorsal view of radial shield. **F.** Genital plate, interradial side.

Figure 6. Illustrations detailing the similarities and differences between the radial shields and genital plates, excluding the stereom fabrics, of *Ophiothrix suensonii* **(A – C)**, and *O. spiculata* **(D – E). A.** Ventral view of radial shield (distal portion only). **B.** Dorsal view of radial shield. **C.** Genital plate, interradial side. **D.** Ventral view of radial shield (distal portion only). **E.** Dorsal view of radial shield. **F.** Genital plate, interradial side. (abdm)- abductor muscle attachment sites, (addm)- adductor muscle attachment sites (aoa)- ambital ossicle/ abradial genital plate attachment site, (gp)- genital plate, (rs)- radial shield, (1-4) – genital plate condyle processes (see text).

Figure 7. An image series showing that injection of sterile seawater injection into the abductor muscles of *Gorgonocephalus eucnemis* does not restrict full functionality. **A.** First frame taken during recording and before injection, shows all RSGPC's at full expansion. **B.** 24 seconds, after the injection, all RSGPCs are fully functional and have lowered the radial shields. **C.** 1-minute 2-seconds, all RSGPCs are fully functional and have raised the radial shields. All radial shields continued to rise and fall in unison. (arrows)- center of the disc as it expands and contracts

Figure 8. Image sequence showing the inhibition of the abductor muscles of *Gorgonocephalus eucnemis* of the radial shield-genital plate complex after injection with $MgCl_2$; treated pair of RSGPCs have a magenta stain on the corresponding radial shields. **A.** Immediately after $MgCl_2$ injection the treated radial shields (arrow) hang very low**. B.** 1-minute 2-seconds, after injection the treated radial shield-genital plate complexes are not functional and cannot raise the radial shields, but other radial shields have begun to rise. **C.** The treated radial shield-genital plate complexes remain in place, unable to elevate (2-minutes, 17-seconds after injection. (arrow)- denotes the treated pair of radial shields (also tagged with a magenta stain). **D.** A still image taken from the recording of the experiment (not a part of the A-C sequence) that best displays the muscle contraction inhibiting effect of the $MgCl_2$

Figure 9. Illustrations detailing the general structure of the ophiothricid RSGPC (For comparison with Fig. 2). **A.** A labeled illustration of the RSGPC of *Ophiothrix suensonii*, (abdm)- abductor muscle attachment sites, (abm) -abductor muscle, (adm) -adductor muscle, (addm)- adductor muscle attachment sites, (gp)- genital plate, (rs) radial shield. **B.** Dorsal view illustration of a pair of scapula-like radial shields from *Ophiothrix suensonii.* (rs)- radial shields **(See Figure 2).** Illustration of the interradial side of the radial shield-genital plate complex, abductor and adductor muscles omitted for simplicity. (abdm)- abductor muscle attachment site, (addm)- adductor muscle attachment site, (aoa)- ambital ossicle/ abradial genital plate attachment site, (gp)- genital plate, (gpc)- genital plate condyle, (mr)- radial shield midrib, (p)- thin CaCO3 plates making up the proximal end of the radial shield, (rsdp)- radial shield distal process

Figure 10. Illustrations detailing the different shapes of radial shields in brooding and non-brooding ophiuroids **(A -B)**, ophiuroids without and with bursae **(C -D)**, a medium-large bodied ophiurid **(E)**, and a gorgonocephalid **(F).** A. *Amphipholis squamata*. B. *Amphipholis pugetana*. C. *Ophiactis virens* (no bursae). D. *Ophiactis quinqueradia* (has bursae). E. *Ophiura lutkenii*, dashed line represents the border of the portion of the radial shield that is visible from the dorsal surface, dotted line shows observed point of fracture when macerated. F. *Gorgonocephalus eucnemis*

Figures

Figure 1.

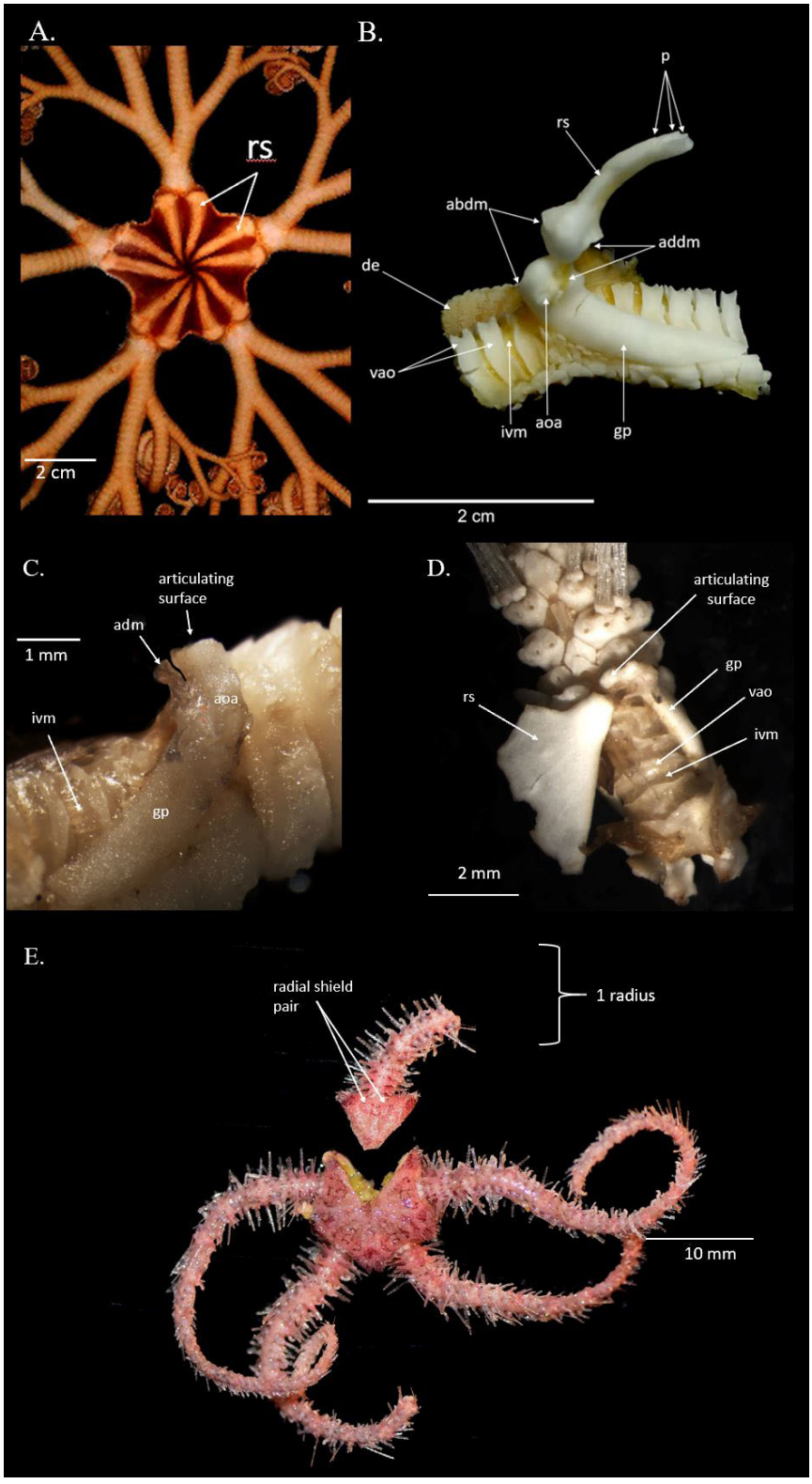

Figure 2.

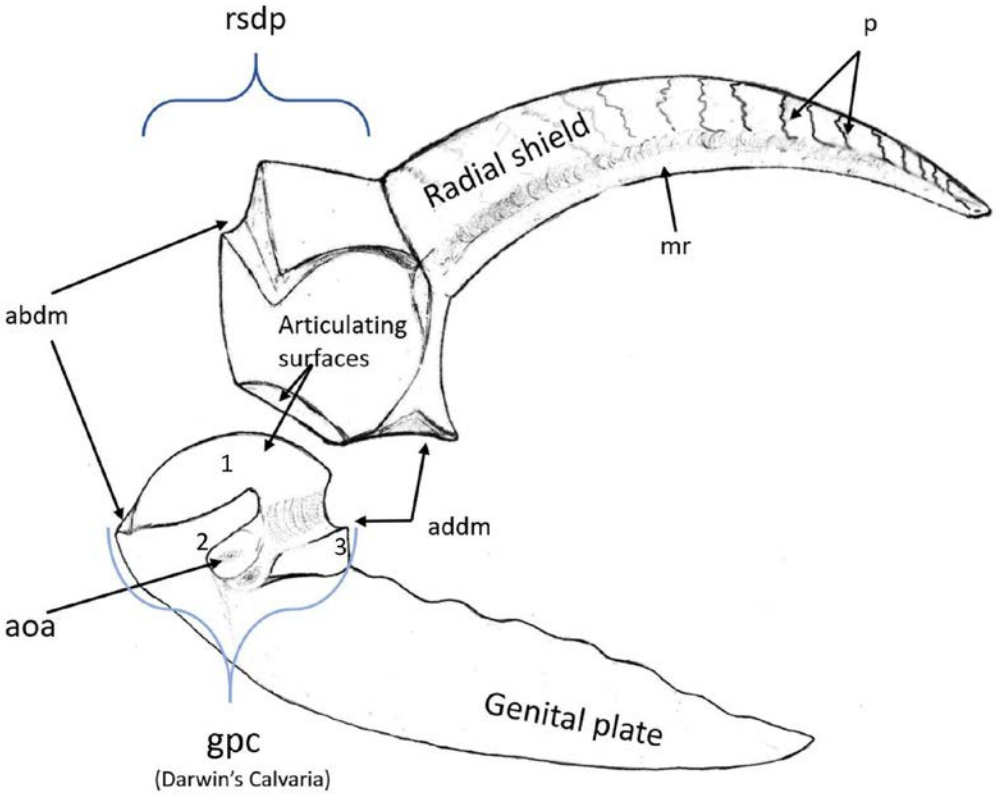
rsdp
p
Radial shield
mr
abdm
Articulating
surfaces
1
addm
2
3
aoa
Genital plate
gpc
(Darwin's Calvaria)

Figure 3.

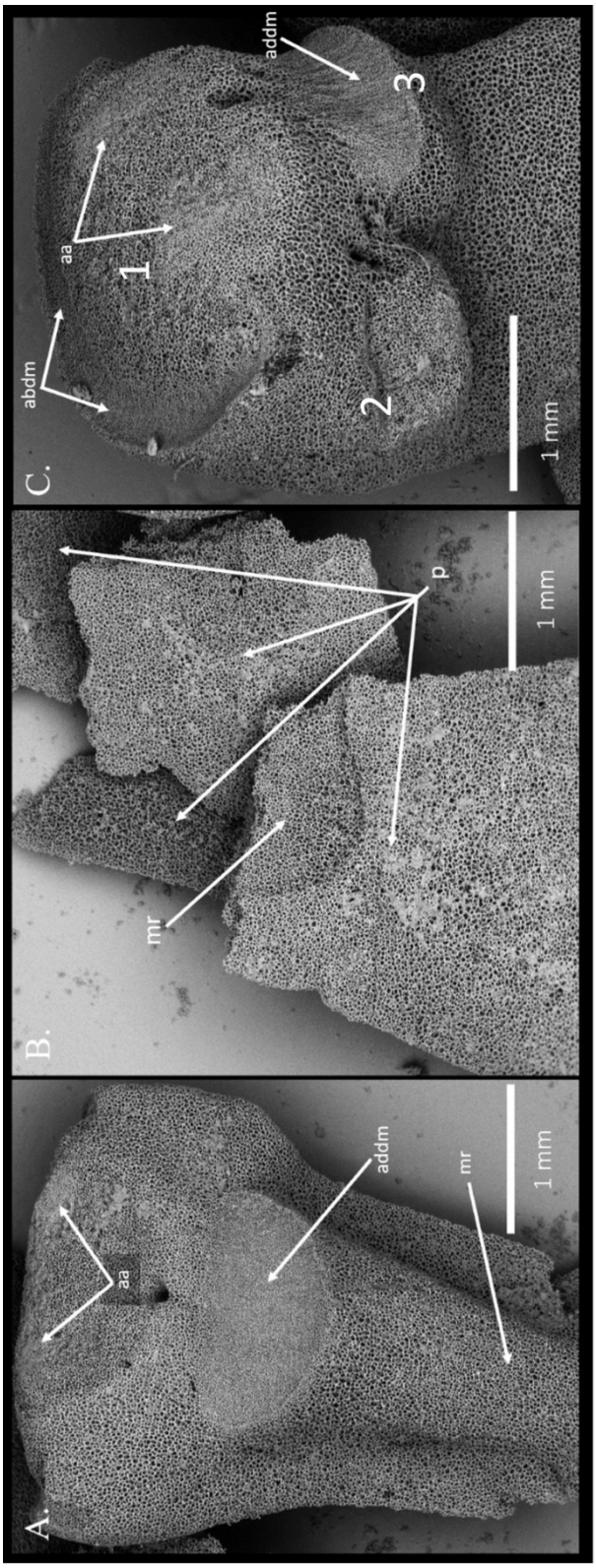

Figure 4.

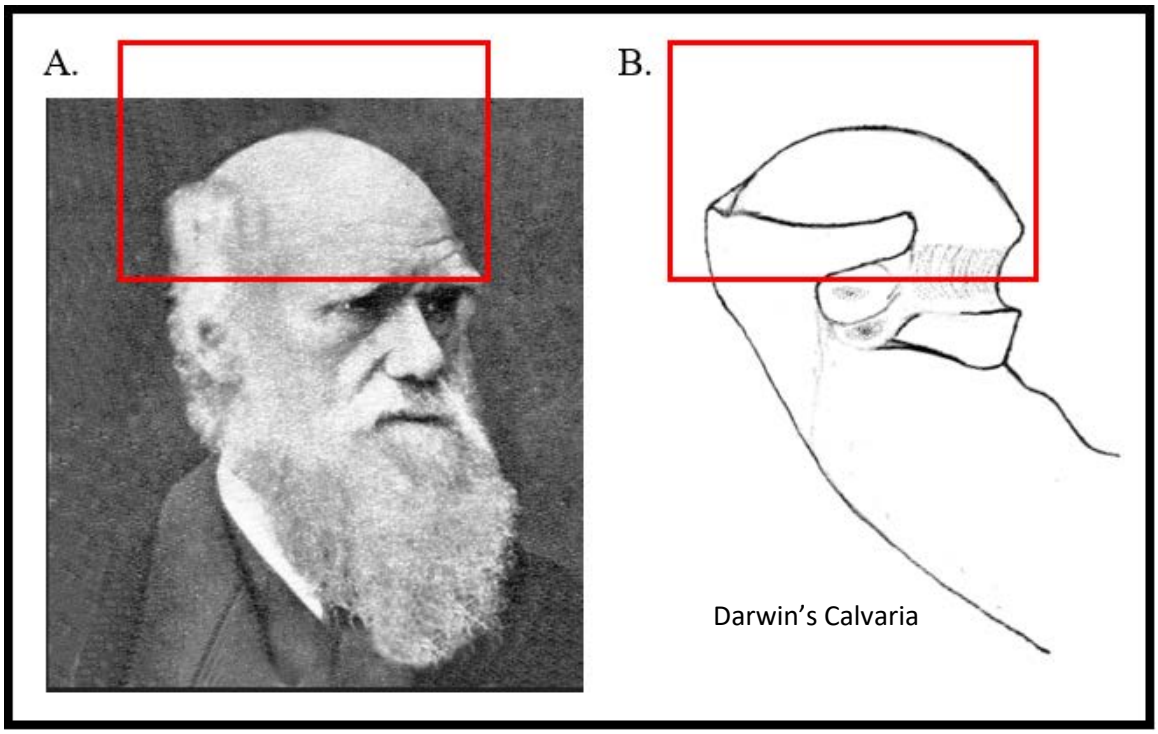

Figure 5.

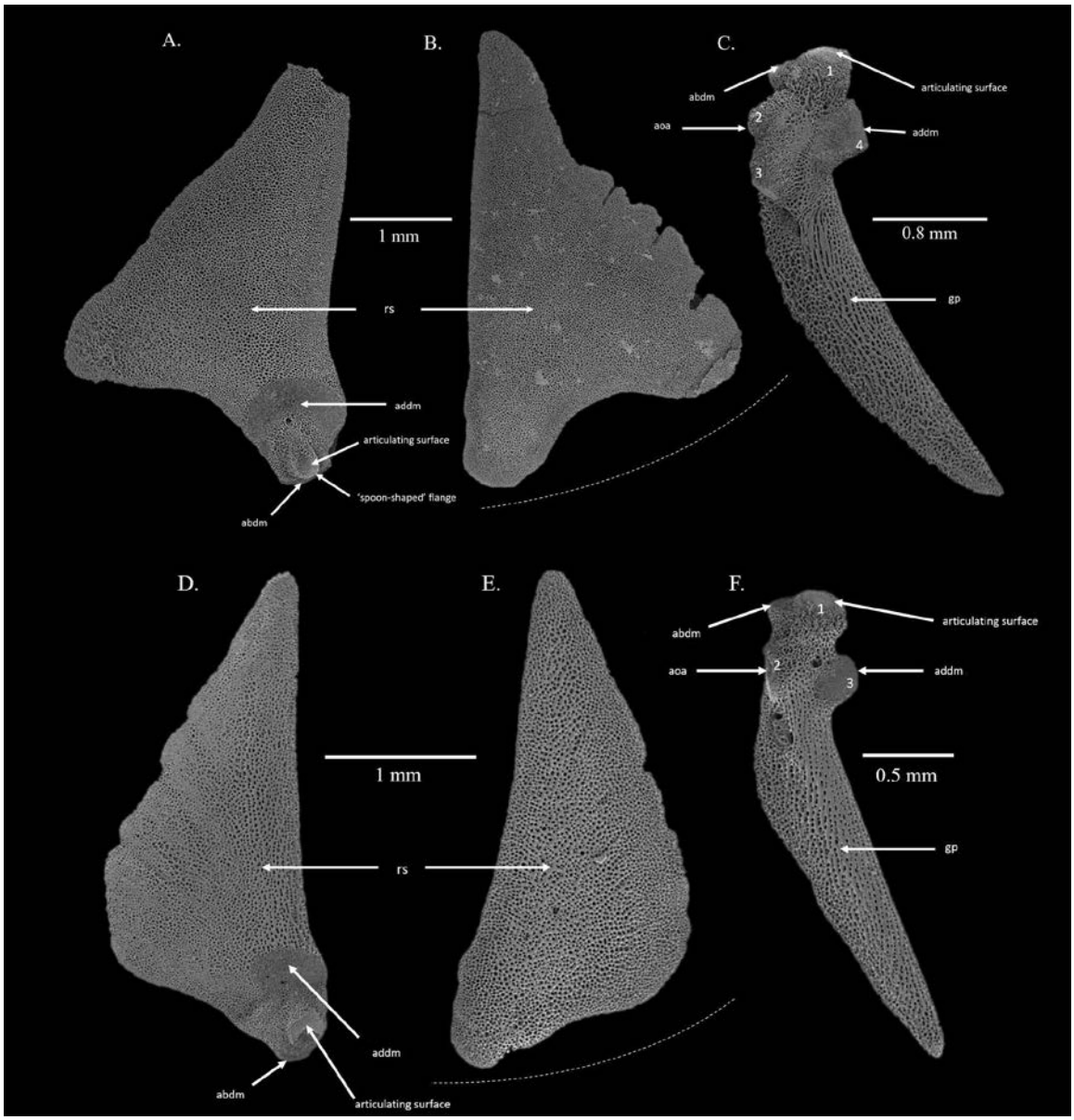
A.
B.
C.
1 mm
rs
addm
articulating surface
'spoon-shaped' flange
abdm
abdm
aoa
1
2
3
4
articulating surface
addm
0.8 mm
gp
D.
E.
F.
1 mm
rs
addm
abdm
articulating surface
abdm
aoa
1
2
3
articulating surface
addm
0.5 mm
gp

Figure 6.

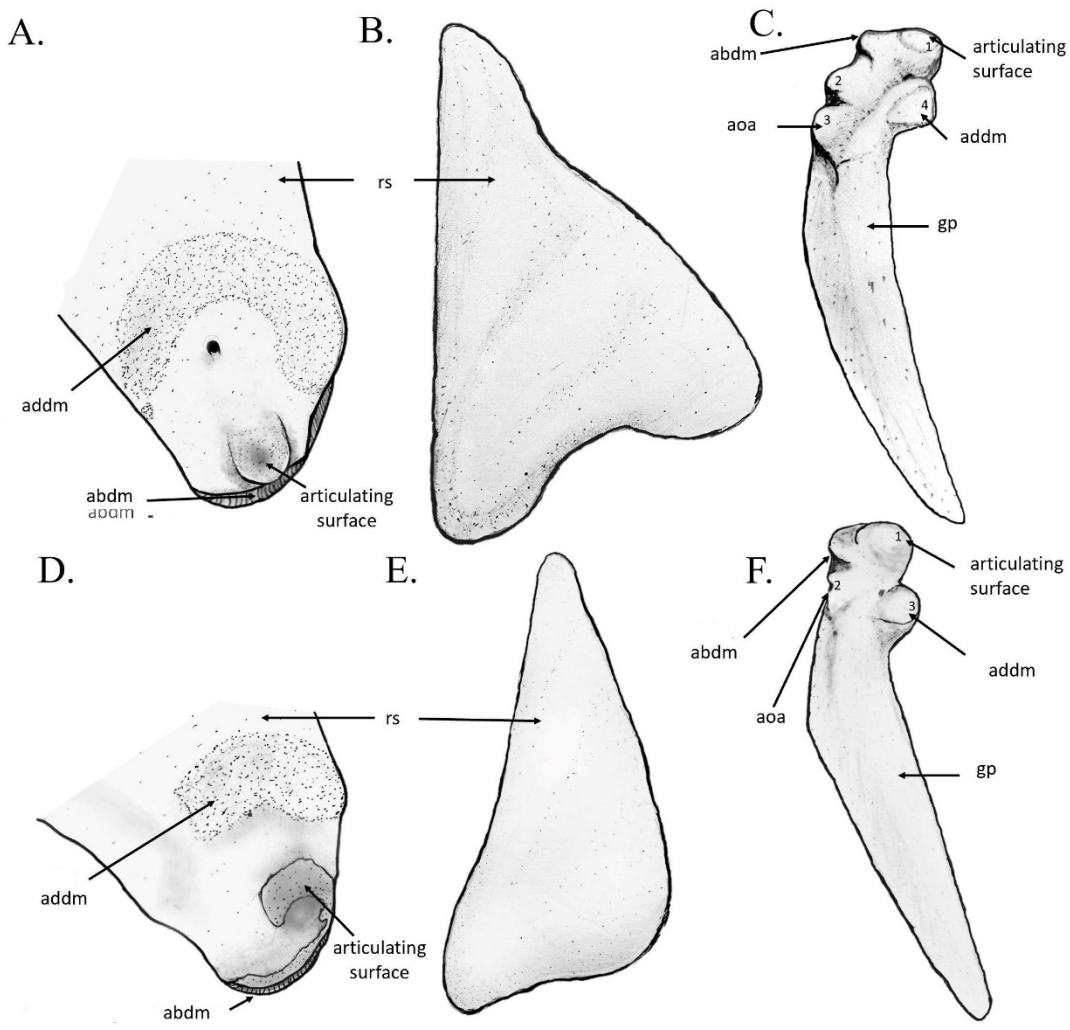
A.
B.
C.
abdm
articulating surface
aoa
addm
gp
rs
addm
abdm
articulating surface
D.
E.
F.
rs
addm
articulating surface
abdm
abdm
articulating surface
addm
aoa
gp

Figure 7.

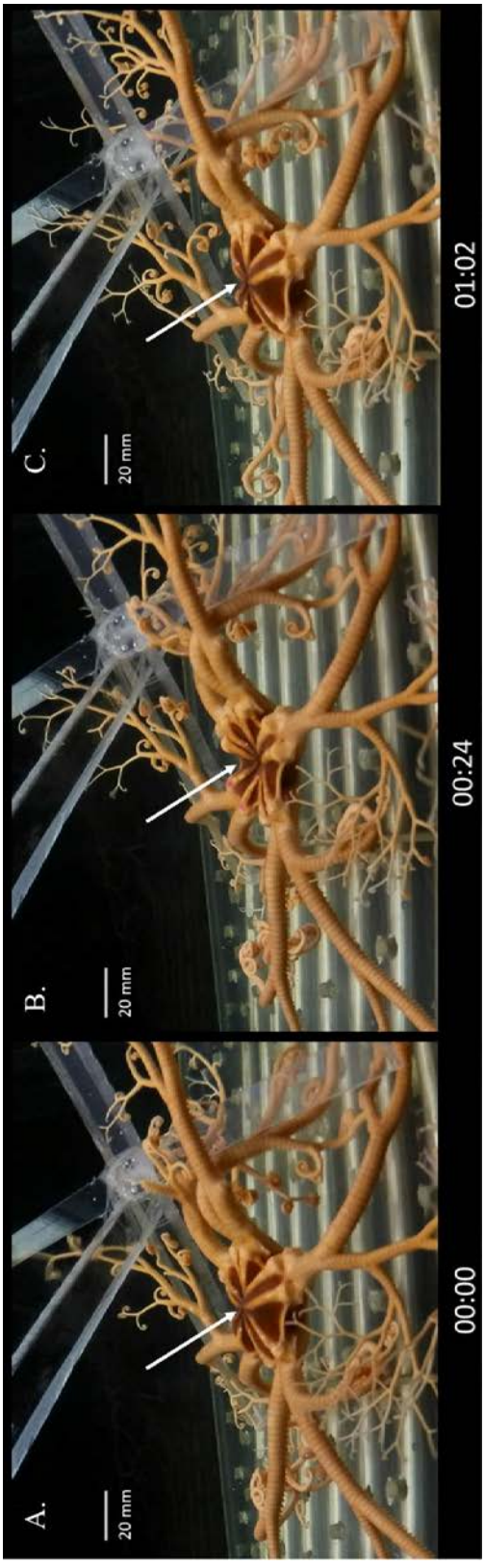

Figure 8.

Figure 9.

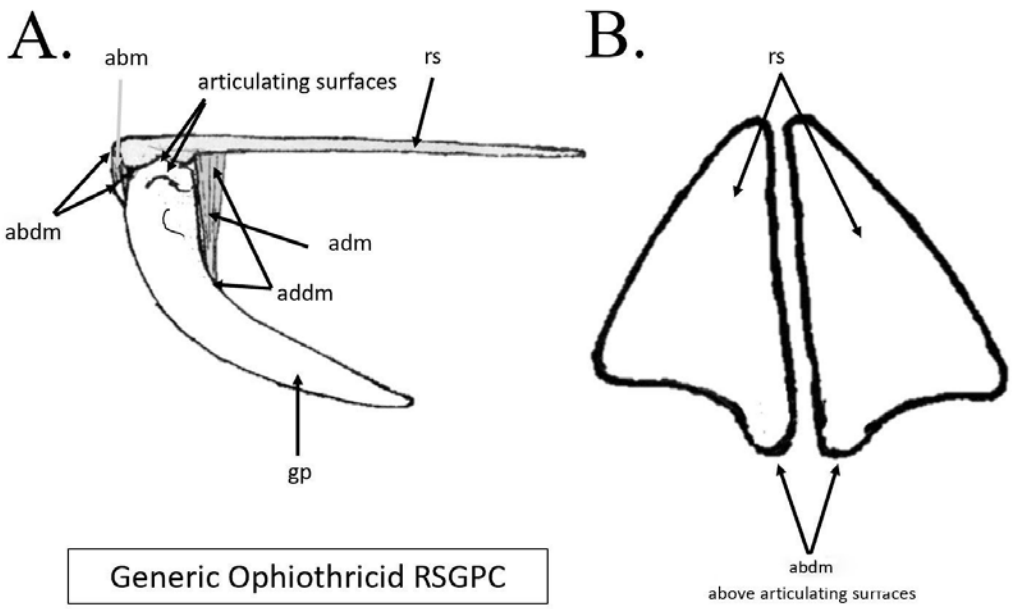
A.
abm
articulating surfaces
rs
abdm
adm
addm
gp
B.
rs
abdm
above articulating surfaces
Generic Ophiothricid RSGPC

Figure 10.

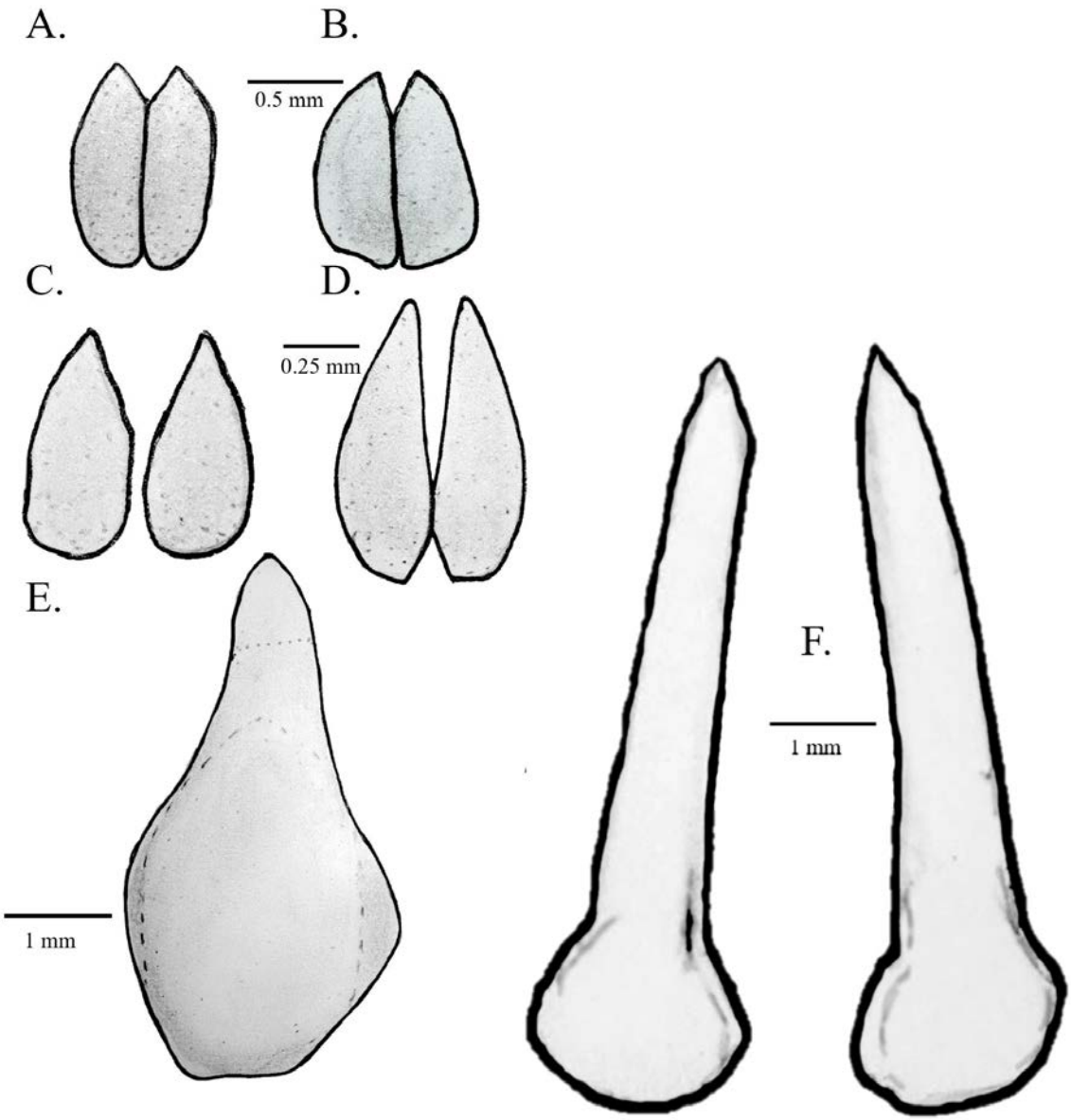

REFERENCES CITED

Altenbach, A. V., Bernhard, J. M. and Seckbach, J. eds. (2012). *Anoxia: evidence for eukaryote survival and paleontological strategies*. Dordrecht: Springer.

Altieri, A. H., Harrison, S. B., Seemann, J., Collin, R., Diaz, R. J. and Knowlton, N. (2017). Tropical dead zones and mass mortalities on coral reefs. *PNAS* 114, 3660–3665.

Ambrose, W., Clough, Tilney and Beer (2001). Role of echinoderms in benthic remineralization in the Chukchi Sea. *Marine Biology* 139, 937–949.

Austin, W. (1966). Feeding mechanisms, digestive tracts and circulatory systems in the ophiuroids *Ophiothrix spiculata* (Le Conte, 1851) and *Ophiura lutkeni* (Lyman, 1860).

Bakun, A., Field, D. B., Redondo-Rodriguez, A. and Weeks, S. J. (2010). Greenhouse gas, upwelling-favorable winds, and the future of coastal ocean upwelling ecosystems. *Global Change Biology* 16, 1213–1228.

Barraclough Fell, H. (1966). The Ecology of Ophiuroids - Locomotion. *Physiology of Echinodermata* 245–65.

Beardsley, A.M., and J.M. Colacino (1998). System-wide oxygen transport by the water vascular system of the burrowing ophiuroid, Hemipholis elongata (Say). pp. 323-328. Echinoderms: San Francisco. Proceedings of the 9th International Echinoderm Conference, R. Mooi and M. Telford (eds). A. Balkema, Rotterdam.

Ben Thuy (2018). Radial Shield Evolution. Personal Communication.

Binyon, J. (1972). *Physiology of echinoderms*. 1st ed. Oxford, New York: Pergamon Press.

Blake, D. F., Peacor, D. R. and Allard, L. F. (1984). Ultrastructural and microanalytical results from echinoderm calcite: Implications for biomineralization and diagenesis of skeletal material. *Micron and Microscopica Acta* 15, 85–90.

Buddenbrock, W. von (1967). *Vergleichende Physiologie. Bd. 5. Physiologie der Erfolgsorgane*. Basel: Birkhäuser Verlag

Burnett, L. E. and Stickle, W. B. (2001). *Physiological Responses to Hypoxia - Coastal hypoxia: consequences for living resources and ecosystems*. (ed. Rabalais, N. N.) and Turner, R. E.) Washington, D.C: American Geophysical Union.

Chan, F., Barth, J. A., Lubchenco, J., Kirincich, A., Weeks, H., Peterson, W. T. and Menge, B. A. (2008). Emergence of Anoxia in the California Current Large Marine Ecosystem. *Science* 319, 920–920.

Clark, A. (1952). A New Genus of Brittle Star (Gorgonocephalidae) -- *Proceedings of the United States National Museum*. 102, 6.

Chu, J. W. F. and Tunnicliffe, V. (2015). Oxygen limitations on marine animal distributions and the collapse of epibenthic community structure during shoaling hypoxia. *Glob Change Biol* 21, 2989–3004.

Dashtgard, S. E., Snedden, J. W. and MacEachern, J. A. (2015). Unbioturbated sediments on a muddy shelf: Hypoxia or simply reduced oxygen saturation? *Paleogeogr. Paleoclimatol. Paleoecol.* 425, 128–138.

Duncan, P. M. (1886). On some Parts of the Anatomy of Ophiothrix variabilis, Dunc., and Ophiocampsis pellicula, Dunc., based on materials furnished by the Trustees of the Indian Museum, Calcutta. *Zoological Journal of the Linnean Society* 21, 107–120.

Emlet, R. B. (1982). Echinoderm calcite: a mechanical analysis from larval spicules. *The Biological Bulletin* 163, 264–275.

Emson, R. H., Mladenov, P. V. and Barrow, K. (1991). The feeding mechanism of the basket star *Gorgonocephalus arcticus*. *Canadian Journal of Zoology* 69, 449–455.

Erhardt, A. M., Reimers, C. E., Kadko, D. and Paytan, A. (2014). Records of trace metals in sediments from the Oregon shelf and slope: Investigating the occurrence of hypoxia over the past several thousand years. *Chemical Geology* 382, 32–43.

Farmanfarmaian, A. (1966). Echinoderm Physiology. *Physiology of Echinodermata* 245–65.

Fedotov, D. M. (1926). Die Morphologie der Euryalae. *Zeitschrift fuer Wissenschaftliche Zoologie Leipzig* 127, pp.403-528.

* Fedotov, D. M. (1930). Zur vergleichenden Morphologie der Ophiuren. *Travaux du Laboratoire de Zoologie Experimentale et de Morphologie des Animaux Leningrad* 1, pp.151-191.

Granja Fernández, R., Herrero Pérezrul, M. D., López Pérez, R. A., Hernández, L., Rodríguez Zaragoza, F., Jones, R. W. and Pineda López, R. (2014). Ophiuroidea (Echinodermata) from coral reefs in the Mexican Pacific. *ZooKeys* 406, 101–145.

Grantham, B. A., Chan, F., Nielsen, K. J., Fox, D. S., Barth, J. A., Huyer, A., Lubchenco, J. and Menge, B. A. (2004). Upwelling-driven nearshore hypoxia signals ecosystem and oceanographic changes in the northeast Pacific. *Nature* 429, 749–754.

Greeley, D. (2016). *National Oceanic and Atmospheric Administration - Pacific Marine Environmental Laboratory - WCOA 16 data*. West Coast of America: NOAA-PMEL.

*Hainey, M. (2015). How Gorgonocephalus eucnemis captures and ingests food - and - does it use bursal ventilation to respire? Undergraduate Honors Thesis, University of Oregon

Hamman, O. (1887). *Beitragezur Histologieder Echinodermen.* Germany.

Hendler, G., Miller, J., Kier, P. and Pawson, D. (1995). *Sea stars, sea urchins, and allies: echinoderms of Florida and the Caribbean*. Washington: Smithsonian Institution Press.

Hendler, G. (1978). Development of Amphioplus abditus (Verrill) (Echinodermata: Ophiuroidea). II. Description and Discussion of Ophiuroid Skeletal Ontogeny and Homologies. *The Biological Bulletin* 154, 79–95.

Hotchkiss, F. (2018). Radial Shield Evolution. Personal Communication

Hotchkiss, F. H. C. and Haude, R. (2004). Observations on Aganaster gregarious and Stephanoura belgica {Ophiuroidea: Ophiolepididae) (Early Carboniferous and Late Devonian age). *Echinoderms: München - Heinze/fer & Nebe/sick (eds)*.

Hyman, L. (1955). *The Invertebrates: Echinodermata*. 1st ed. New York, Toronto, London: McGraw-Hill Book Company Inc.

*ICES Oceanography (2018). ICES Oceanography. *Unit Conversions, Oxygen*.

Johansen, K. and Petersen, J. (1971). Gas Exchange and Active Ventilation in a Starfish, Pteraster tesselatus. *Z. vergl. Physiologie - Springer-Verlag* 71, 365–381.

Johnson, M. D., Rodriguez, L. M. and Altieri, A. H. (2018). Shallow-water hypoxia and mass mortality on a Caribbean coral reef. *Bulletin of Marine Science* 94, 143–144.

LaBarbera, M. (1982). Metabolic rates of suspension feeding crinoids and ophiuroids (Echinodermata) in a unidirectional laminar flow. *Comparative Biochemistry and Physiology Part A: Physiology* 71, 303–307.

Lambert, P. and Austin, W. C. (2007). *Brittle stars, sea urchins and feather stars of British Columbia, Southeast Alaska and Puget Sound*. Victoria: Royal BC Museum.

Lawrence, J. M. (1987). *A functional biology of echinoderms*. Baltimore: Johns Hopkins University Press.

Lawrence, J. M. and Lane, J. M. (1982). The utilization of nutrients by post-metamorphic echinoderms, in M. Jangoux and J.M. lawrence (eds). *Echinoderm nutrition* 331–71.

Lebrato, M., Iglesias-Rodríguez, D., Feely, R. A., Greeley, D., Jones, D. O. B., Suarez-Bosche, N., Lampitt, R. S., Cartes, J. E., Green, D. R. H. and Alker, B. (2010). Global contribution of echinoderms to the marine carbon cycle: $CaCO_3$ budget and benthic compartments. *Ecological Monographs* 80, 441–467.

Levin, L. A., Ekau, W., Gooday, A. J., Jorissen, F., Middelburg, J. J., Naqvi, S. W. A., Neira, C., Rabalais, N. N. and Zhang, J. (2009). Effects of natural and human-induced hypoxia on coastal benthos. *Biogeosciences* 6, 2063–2098.

Light, S. F., Carlton, J. T. and Light, S. F. (2007). *The Light and Smith manual: intertidal invertebrates from central California to Oregon*. 4th ed., completely rev. and expanded. Berkeley, Calif: University of California Press.

Low, N. and Micheli, F. (2018). Lethal and functional thresholds of hypoxia in two key benthic grazers. *Marine Ecology Progress Series* 594, 165–173.

Lyman, T. (1880). *Report on the Ophiuroidea Dredged by H. M. S. Challenger during the Years 1873-76.* 1st ed. Edinburgh.

MacBride, E. W. (1906). Echinodermata – Ophiuroidea. *Library Arkansas Experiment Station*.

Macurda, D. B. (1976). Skeletal modifications related to food capture and feeding behavior of the basket star Astrophyton. *Paleobiology* 2, 1–7.

Martynov, A. (2010). *Reassessment of the classification of the Ophiuroidea (Echinodermata), based on morphological characters. I, I,* Auckland, N.Z.: Magnolia Press.

Minge, A., Davoult, D. and Gattuso, J.-P. (1998). Calcium carbonate production of a dense population of the brittle star Ophiothrix fragilis (Echinodermata: Ophiuroidea): Role in the carbon cycle of a temperate coastal ecosystem. *ResearchGate* 173, 305–308.

*Mortensen, T. (1936). *Echinoidea and Ophiuroidea*. Discovery Reports Cambridge.

Müller, J. and Troschel, F. (1842). *System der Asteriden;* Braunschweig, F. Vieweg und Sohn.

Nichols, D. (1969). *Echinoderms*. 4th (revised) ed. London: Hutchinson.

O'Dea, A. (2018). Historical hypoxia. *Baseline Caribbean*. https://baselinecaribbean.com/2018/03/17/historical-hypoxia/

O'Hara, T. (2018). Radial Shield Evolution. Personal communication.

O'Hara, T. D., Stöhr, S., Hugall, A. F., Thuy, B. and Martynov, A. (2018). Morphological diagnoses of higher taxa in Ophiuroidea (Echinodermata) in support of a new classification. *European Journal of Taxonomy*.

Patent, D. H. (1969). The Reproductive Cycle of *Gorgonocephalus caryi* (Echinodermata; Ophiuroidea) *The Biological Bulletin* 136, 241–252.

Pierce, S. D., Barth, J. A., Shearman, R. K. and Erofeev, A. Y. (2012). Declining Oxygen in the Northeast Pacific**. *Journal of Physical Oceanography* 42, 495–501

R Core Team (2016). R: A language and environment for statistical computing. R Foundation for Statistical Computing, Vienna, Austria. URL http://www.R-project.org/.

Riedel, B., Pados, T., Pretterebner, K., Schiemer, L., Steckbauer, A., Haselmair, A., Zuschin, M. and Stachowitsch, M. (2014). Effect of hypoxia and anoxia on invertebrate behavior.

Rosenberg, R., Dupont, S., Lundälv, T., Sköld, H., Norkko, A., Roth, J., Stach, T. and Thorndyke, M. (2005). Biology of the basket star Gorgonocephalus caputmedusae (L.). *Marine Biology* 148, 43–50.

Sars, M. and Kjerulf, T. (1859). *Middelhavets Lilloral-Fauna.* Christiania, Copenhagen, Denmark: Physiographic Association Christiania Printed by Brøgger & Christie.

Selvakumaraswamy, P. and Byrne, M. (2000). Reproduction, Spawning, and Development of 5 Ophiuroids from Australia and New Zealand. *Wiley on behalf of American Microscopical Society* 119, 394–402.

Smith, A. B. (1980). Stereom microstructure of the echinoid test. *The Paleontological Association* 1–81.

Smith, A. B., Paterson, G. L. J. and Lafay, B. (1995). Ophiuroid phylogeny and higher taxonomy: morphological, molecular and paleontological perspectives. *Zoological Journal of the Linnean Society* 114, 213–243.

Spicer, J. (2016). *Stressors in the marine environment: physiological and ecological responses; societal implications; Respiratory responses of marine animals to environmental hypoxia*. First edition. (ed. Solan, M.) and Whiteley, N. M.) Oxford, United Kingdom: Oxford University Press.

Stachowitsch, M., Riedel, B. and Zuschin, M. (2012). The return of shallow shelf seas as extreme environments: anoxia and macrofauna reactions in the Northern Adriatic Sea. In *Anoxia*, pp. 353–368. Springer, Dordrecht.

Stewart, B. (2000). Anatomical Features of the Euryalid Snake Star Astrobrachion constrictum (Ophiuroidea: Asteroschematidae). *Invertebrate Biology* 119, 222–233.

Stöhr, S., O'Hara, T. D. and Thuy, B. (2012). Global Diversity of Brittle Stars (Echinodermata: Ophiuroidea). *PLoS ONE* 7, e31940.

Stöhr, S., O'Hara, T. D. and Thuy, B. eds. (2018). *Ophiuroidea - The World Ophiuroidea Database*.

Thuy, B. and Stöhr, S. (2016). A New Morphological Phylogeny of the Ophiuroidea (Echinodermata) Accords with Molecular Evidence and Renders Microfossils Accessible for Cladistics. *PLOS ONE* 11, e0156140.

Thuy, B. and Stöhr, S. (2018). Unravelling the origin of the basket stars and their allies (Echinodermata, Ophiuroidea, Euryalida). *Scientific Reports* 8

Thuy, B., Kutscher, M. and Płachno, B. (2014). A new brittle star from the Early Carboniferous of Poland and its implications on Paleozoic modern-type ophiuroid systematics. *Acta Palaeontologica Polonica* 60, 923–929.

Twitchett, R. J. (2004). Experimental decay of disarticulation of Ophiura texturata: implications for the fossil record of ophiuroids. In *Proceedings of the 11th International Echinoderm Conference*, pp. 439–446. Munich, Germany.

Wakita, D. (2018). Rhythmic Movement of the Disk in the Green Brittle Star Ophiarachna incrassata.

West, G., Heard, D. and Caulkett, N. (2014). *Zoo Animal and Wildlife Immobilization and Anesthesia*. John Wiley & Sons..

Woodley, J. D. (1975). The behaviour of some amphiurid brittle-stars. *Journal of Experimental Marine Biology and Ecology* 18, 29–46.